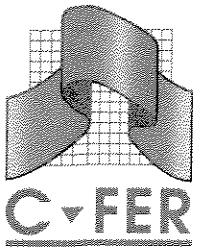

C-FER
200
Karl Clark Road
Edmonton, Alberta
Canada T6N 1H2

Tel: (403) 450-3300
Fax: (403) 450-3700

Probabilistic Assessment of Offshore Pipeline Failure Consequences

PIRAMID Technical Reference Manual No. 5.1

Confidential to C-FER's Pipeline Program Participants

Prepared by
M. J. Stephens, M.Sc.,P. Eng.
M. A. Nessim, Ph.D., P.Eng.
and
Q. Chen, Ph.D., P.Eng.

Centre For Engineering Research Inc.

November 1996
Project 95018

Probabilistic Assessment of Offshore Pipeline Failure Consequences

PIRAMID Technical Reference Manual No. 5.1

Confidential to C-FER's Pipeline Program Participants

Prepared by
M. J. Stephens, M.Sc., P.Eng.

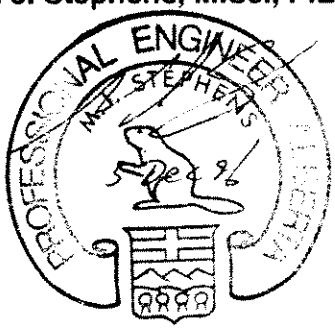

and
Q. Chen, Ph.D., P.Eng.

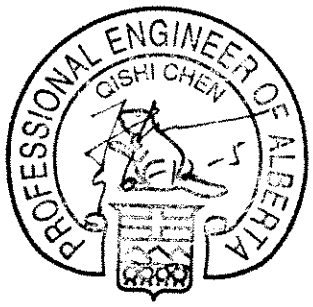

M. A. Nessim, Ph.D., P.Eng.

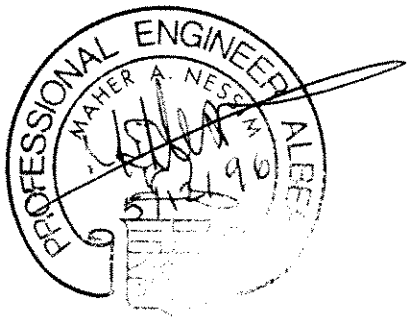

November 1996
Project 95018

PERMIT TO PRACTICE
CENTRE FOR ENGINEERING RESEARCH INC.
Signature: _____
Date: 5/12/96
PERMIT NUMBER: P4487
The Association of Professional Engineers, Geologists and Geophysicists of Alberta

NOTICE

Restriction on Disclosure

TABLE OF CONTENTS

Table of Contents

Table of Contents

Table of Contents

Table of Contents

APPENDICES

LIST OF FIGURES AND TABLES

List of Figures and Tables

List of Figures and Tables

List of Figures and Tables

EXECUTIVE SUMMARY

The Centre For Engineering Research Inc. (C-FER) is conducting a joint industry research program directed at the optimization of pipeline integrity maintenance activities using a risk-based approach. This document describes the consequence assessment model that has been developed to quantify, assess and combine the life safety, environmental, and economic consequences of offshore pipeline failure. The model is developed within the context of a decision influence diagram that incorporates integrity maintenance decisions and associated failure probabilities as well as a formal method of determining the optimal choice associated with the required decision. This influence diagram forms the basis for the initial program in the software suite *PIRAMID* (Pipeline Risk Analysis for Maintenance and Integrity Decisions).

The consequence oriented decision influence diagram described herein incorporates failure probability estimates that are based on historical pipeline incident data. This approach to probability estimation is provided as a temporary solution pending the development of more detailed failure cause specific probability estimation models in future phases of the research program. As such the decision influence diagram described herein can be used to carry out a full quantitative risk assessment for a given segment of an offshore gas or liquid pipeline. This influence diagram can also be used to optimize integrity maintenance decisions, based on user-defined failure probability estimates for each integrity maintenance action under consideration.

The consequence assessment model incorporated within the influence diagram framework addresses the financial costs associated with integrity maintenance activities and the consequence components associated with pipeline failure. The model assumes that the consequences of pipeline failure are fully represented by three parameters: the *total cost* as a measure of the economic loss, the *number of fatalities* as a measure of risk to life, and *the residual spill volume* (after clean-up and acknowledging spill decay) as a measure of the long term environmental impact. The consequence assessment approach incorporated within the influence diagram framework involves modeling the release of product from the pipeline; determination of the likely hazard types and their relative likelihood of occurrence; estimation of the hazard intensity at different locations; and finally calculation of the number of casualties, the residual spill volume impacting coastal resources, and the total cost.

The hazard types considered in the model include both the immediate hazards associated with line failure (*e.g.*, jet/pool fires, vapour cloud fires or explosions, and toxic or asphyxiating clouds), as well as the long term environmental hazards associated with persistent liquid spills that impact coastal resources. The relative likelihood of occurrence of each hazard type is determined based on product type, line failure mode (*i.e.*, leak vs. rupture) and ignition source type (*i.e.*, platform vs. vessel traffic zones). Hazard intensity models are structured to take into account the effects of pipeline geometry and operating characteristics (*e.g.*, line diameter and operating pressure), the type of line failure (*i.e.*, small leak, large leak or rupture), and the environmental conditions at the time of failure (*e.g.*, sea state, wind direction, and atmospheric stability).

Fatality estimation, based on the hazard characterization models, reflects the exposed population associated with vessel traffic and adjacent platforms and takes into account the effect of shelter and escape on survivability. Estimation of residual spill impact volume takes into account the movement and decay of spill products, the offshore and onshore clean-up potential associated with the spill and incorporates a factor that adjusts the volume measure to reflect both the environmental damage potential of the spilled product as well as the damage sensitivity of the coastal resources that are potentially impacted by the spill. The total cost estimate includes: the cost associated with the choice of integrity maintenance action (*i.e.*, the maintenance cost); the direct costs associated with line failure including the cost of lost product, line repair, and service interruption; and the hazard-dependent costs including the cost of property damage, spill clean-up, and fatality compensation. The consequence assessment model combines these three distinct consequence components into an overall measure of risk (or value).

Within the influence diagram framework the consequence assessment model is used to calculate the value associated with each candidate integrity maintenance choice, thereby providing a basis for the selection of an optimal decision. Two distinct approaches for defining value have been developed and implemented within the decision analysis framework incorporated in *PIRAMID*; one based on *utility theory*, the other based on *cost optimization* with constraints.

Using the utility theory approach, the value associated with each different choice of action is quantified to facilitate the selection of an optimal compromise between life safety, environmental impact, and economic considerations. Specifically, the theory is used to define a utility function that ranks different combinations of cost, fatalities, and spill volume according to their perceived total impact. The optimal choice of action is the one that maximizes the expected utility. The utility function described herein has been formulated to take into account both risk aversion, as it applies to financial cost and environmental damage uncertainty, and tradeoffs between losses in life, environmental damage, and cost.

Using the cost optimization approach the choice of action that produces the lowest expected total cost is considered optimal. However, if persistent liquid spill products are involved, it is assumed that an environmental impact constraint will be set by regulators or defined on the basis of precedent. In this case, the choice associated with the lowest expected total cost that does not violate the constraint will be considered optimal. The advantage of this approach is that tradeoffs between cost and environmental impact are not necessary because risk management with respect to the environmental is demonstrated by meeting established tolerable risk levels.

In summary, a quantitative risk analysis methodology for integrity maintenance planning of offshore pipelines has been developed and implemented within a decision influence diagram framework. The consequence oriented influence diagram described herein can be used to carry out a quantitative risk assessment on a given segment of offshore pipeline or as a decision making tool to determine the optimal maintenance action for a given segment, provided that representative failure probability estimates are obtained from other sources such as historical pipeline incident data.

1.0 INTRODUCTION

1.1 Background

This document constitutes one of the deliverables associated C-FER's joint industry program on risk-based optimization of pipeline integrity maintenance activities. The goal of this program is to develop models and software tools that can assist pipeline operators in making optimal decisions regarding integrity maintenance activities for a given pipeline or pipeline segment. The software resulting from this joint industry program is called PIRAMID (Pipeline Risk Analysis for Maintenance and Inspection Decisions). This document is part of the technical reference manual for the program.

Implementation of a risk-based approach, as envisioned in this program, requires quantitative estimates of both the probability of line failure and the adverse consequences associated with line failure should it occur. There is considerable uncertainty associated with the assessment of both the probability and consequences of line failure. To find the optimal set of integrity maintenance actions, in the presence of this uncertainty, a probabilistic optimization methodology based on the use of decision influence diagrams has been adopted. An introduction to this analysis approach and the reasons for its selection are given in PIRAMID Technical Reference Manual No. 1.2 (Stephens *et al.* 1995a).

Failure probability estimation, and assessment of the effect of various integrity maintenance actions on the failure probability require the development of separate influence diagrams, each tailored to address the parameters and uncertainties associated with a specific failure cause or mechanism (*e.g.*, corrosion, third party damage, or ground movement). However, central to the decision analysis approach is a probabilistic failure consequence assessment module that estimates the impact of pipeline failure, regardless of cause, on public safety, the environment, and financial cost to the operator. Therefore, as a logical first step in the implementation of the proposed methodology, a pipeline failure consequence assessment model has been developed within the context of a decision analysis influence diagram. In this consequence oriented influence diagram the probability of failure is treated as an uncertain event, for which the probability is directly quantifiable.

Based on the assumption that, failure probability estimates can be obtained from elsewhere, (*e.g.*, from historical failure rate data) the consequence oriented influence diagram can be used to perform comprehensive risk assessments and/or for decision making provided that the failure probabilities associated with candidate integrity maintenance strategies are known form previous experience.

1.2 Objective and Scope

This document describes the consequence assessment model that has been developed to quantify, assess and combine the life safety, environmental, and economic consequences of failure for offshore pipeline systems. The consequence model is developed within the context of a decision influence diagram that incorporates integrity maintenance decisions and associated failure probabilities as well as a formal method of determining the optimal choice associated with the required decision. The basic structure of the consequence oriented offshore pipeline decision influence diagram described herein is largely on the methodology described in PIRAMID Technical Reference Manual No. 1.2 (Stephens *et al.* 1995a). The present document provides a detailed technical description of the offshore pipeline influence diagram parameters and the basis for their calculation. The steps involved in solving a decision influence diagram are described in detail in PIRAMID Technical Reference Manual No. 2.1 (Nessim and Hong 1995).

2.0 THE DECISION ANALYSIS INFLUENCE DIAGRAM

2.1 Review of Diagram Representation and Terminology

A decision influence diagram is a graphical representation of a decision problem that shows the interdependence between the uncertain quantities that influence the decision(s) considered. A diagram consists of a network of *chance nodes* (circles) that represent uncertain parameters and *decision nodes* (squares) that represent choices that are to be made. A decision influence diagram will also contain a *value node* (rounded square) that represents the objective or value function that is to be maximized to reveal the optimal set of choice(s) associated with the required decision(s).

All of these nodes are interconnected by directed arcs or arrows that represent dependence relationships between node parameters. Chance nodes that receive solid line arrows are *conditional nodes* meaning that the node parameter is conditionally dependent upon the values of the nodes from which the arrows emanate (*i.e.*, direct predecessor nodes). Chance nodes that receive dashed line arrows are *functional nodes* meaning that the node parameter is defined as a deterministic function of the values of its direct predecessor nodes. The difference between these two types is that conditional node parameters must be defined explicitly for all possible combinations of the values associated with their direct conditional predecessor nodes, whereas functional node parameters are calculated directly from the values of preceding nodes. The symbolic notion adopted in the drawing of the influence diagrams presented in this report, and a summary of diagram terminology are given in Figure 2.1.

It is noted that the number and type (*i.e.*, conditional vs. functional) of chance nodes within a diagram has a significant impact on the amount of information that must be specified to solve the diagram and on the way in which the diagram is solved. A more detailed discussion of the steps involved in defining and solving decision influence diagrams, and a more thorough and rigorous set of node parameter and dependence relationship definitions is presented in PIRAMID Technical Reference Manual No. 2.1 (Nessim and Hong 1995). Subsequent discussions assume that the reader is familiar with the concepts described in that document.

2.2 The Influence Diagram

The *basic node influence diagram* for offshore pipeline consequence evaluation, as developed in this project and implemented in PIRAMID, is shown in Figure 2.2. Each node in the basic node diagram is associated with a single uncertain parameter. All nodes with the exception of the Choice node (node 1), the Pipe Performance node (node 3) and the Maintenance Cost node (node 8.1), are directly associated with the offshore pipeline failure consequence assessment model. The Pipe Performance node, which characterizes the pipeline failure probability, is included to facilitate the calculation of risk (*i.e.*, probability multiplied by consequences). The

The Decision Analysis Influence Diagram

Choices node, together with the associated Maintenance Cost node, are included to form a true decision analysis influence diagram in which the value associated with each choice can be calculated at the Value node to determine the optimal decision.

Each node in the basic node influence diagram shown in Figure 2.2 represents a single uncertain parameter (or random quantity) that is characterized by either a discrete or continuous probability distribution. This report defines each node parameter and explains the calculations that are required at the nodal level to determine the value of each basic node parameter in terms of the values associated with all immediate predecessor nodes. It is noted that to *solve* the decision analysis influence diagram to arrive at the optimal decision, the probability distributions of the node parameters must be defined for all possible combinations of direct conditional predecessor node parameters. The solution algorithm is described in PIRAMID Technical Reference Manual No. 2.1 (Nessim and Hong 1995).

The basic node diagram shows all of the uncertain parameters that have been identified as having a potentially significant impact on the decision analysis problem. The diagram consists of 33 nodes and a larger number of functional and conditional dependence arrows. At first glance the flow of information and the relationships between parameters illustrated by the basic node diagram are rather difficult to follow and understand. If, however, the various basic nodes are collected into logical groups of parameters, the resulting *compound node influence diagram* shown in Figure 2.3, is by comparison much easier to follow and provides a clearer understanding of the interdependencies between the various node parameters (or in this case parameter groups). The compound node influence diagram and the reduced set of 11 node groups identified within will form the basis for the outline of the remainder of the manual with a separate section of the document being allocated to a discussion of the parameters associated with each node group as follows:

Report Section	Node Group
3.0	Choices (node group 1)
4.0	Conditions at Failure (node group 2)
5.0	Pipe Performance (node group 3)
6.0	Release Characteristics (node group 4)
7.0	Hazard Type (node group 5)
8.0	Number of Fatalities (node group 6)
9.0	Spill Characteristics (node group 7)
10.0	Repair and Interruption Costs (node group 8)
11.0	Release and Damage Costs (node group 9)
12.0	Total Cost (node group 10)
13.0	Value (node group 11)

Figures

Node Notation

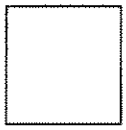

Decision node: Indicates a choice to be made

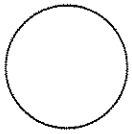

Chance node: Indicates uncertain parameter or event (discrete or continuous)

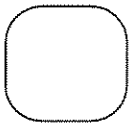

Value node: Indicates the criterion used to evaluate consequences

Arrow Notation

Solid Line Arrow: Indicates probabilistic dependence

Dashed Line Arrow: Indicates functional dependence

Other Terminology

Predecessor to node A :	Node from which a path leading to A begins
Successor to node A:	Node to which a path leading to A begins
Functional predecessor:	Predecessor node from which a functional arrow emanates
Conditional predecessor:	Predecessor node from which a conditional arrow emanates
Direct predecessor to A:	Predecessor node that immediately precedes A (i.e. the path from it to A does not contain any other nodes)
Direct successor to A:	Successor node that immediately succeeds A (i.e. the path from A to it does not contain any other nodes)
Direct conditional predecessor to A: (A must be a functional node)	A predecessor node from which the path to node A contains only one conditional arrow (may contain functional arrows)
Functional node:	A chance node that receives only functional arrows
Conditional node:	A chance node that receives only conditional arrows
Orphan node:	A node that does not have any predecessors

Figure 2.1 Influence diagram notation and terminology

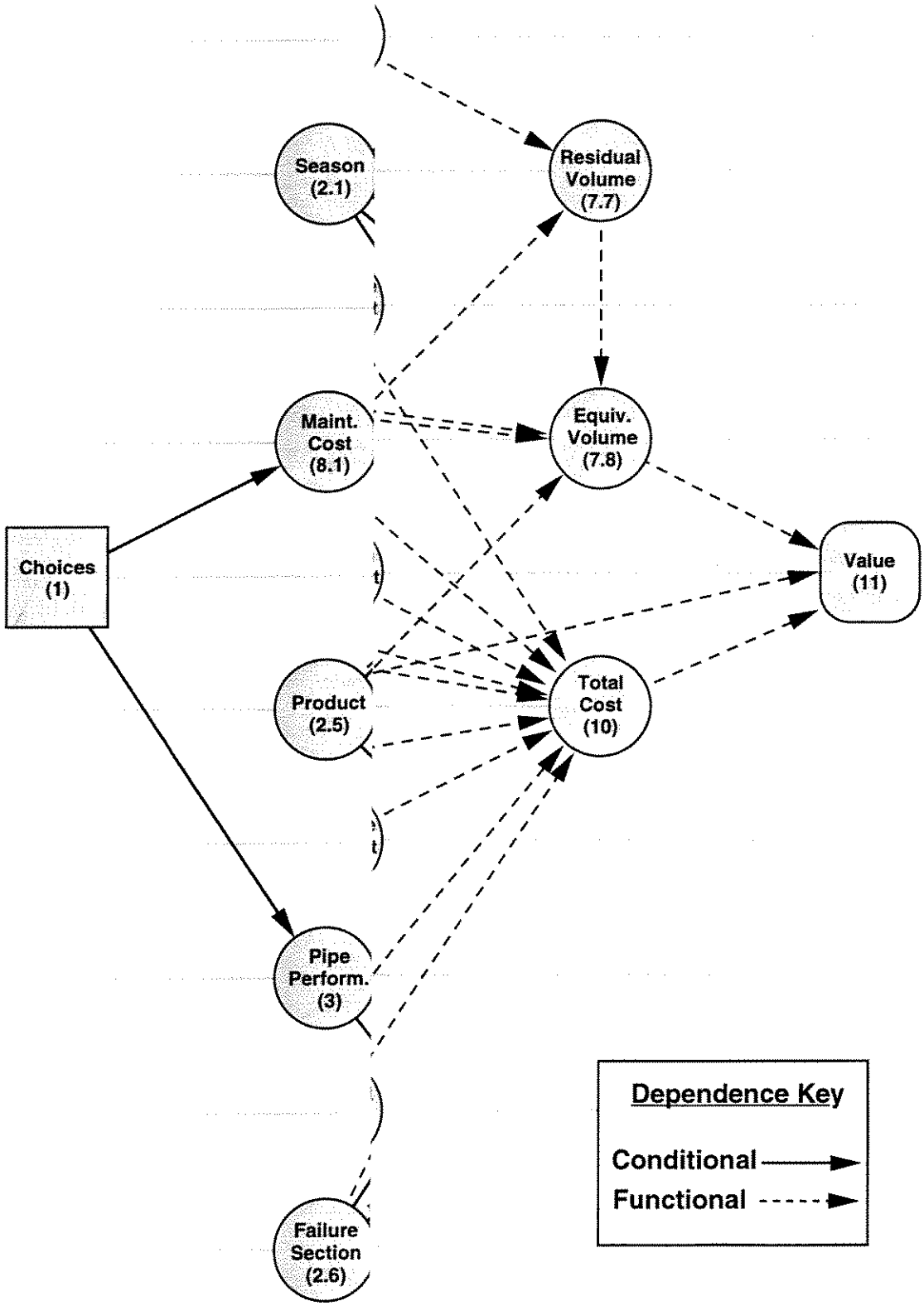
Season
(2.1)
Residual
Volume
(7.7)
Maint.
Cost
(8.1)
Equiv.
Volume
(7.8)
Choices
(1)
Value
(11)
Product
(2.5)
Total
Cost
(10)
Pipe
Perform.
(3)
Failure
Section
(2.6)
Dependence Key
Conditional
Functional

Figure

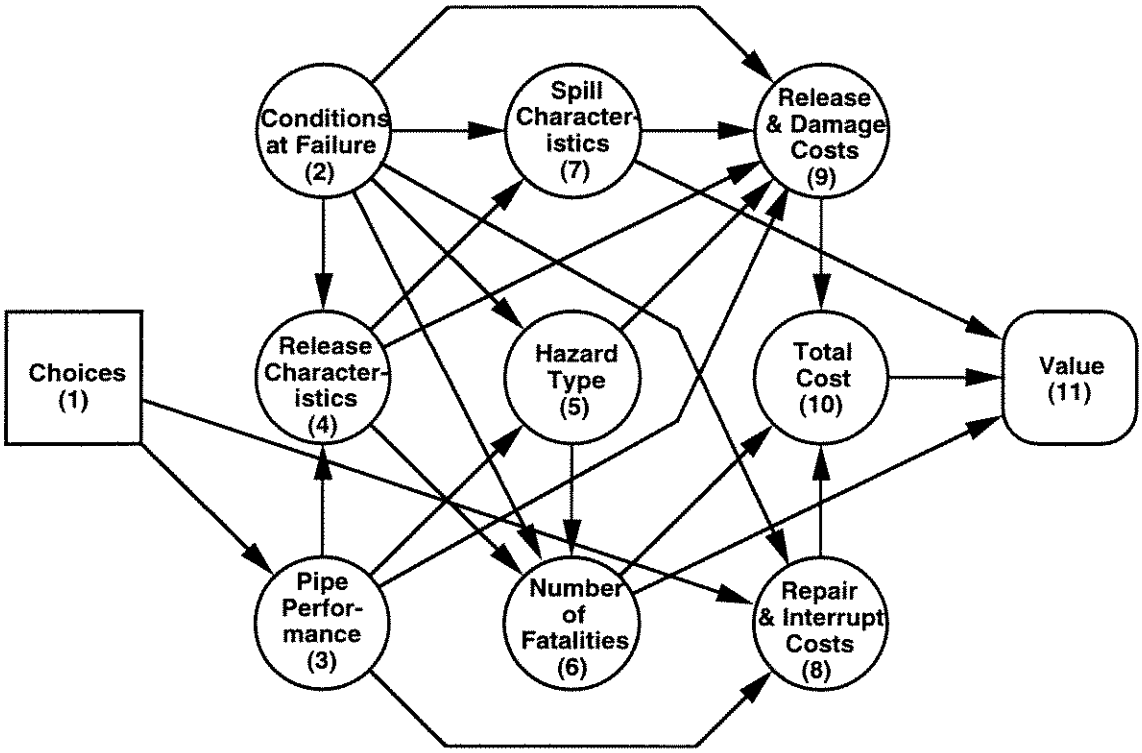

Figure 2.3 Compound node decision influence diagram for integrity maintenance optimization of offshore pipeline systems

3.0 CHOICES

The first node in the decision influence diagram is the Choices node, which constitutes the one decision node in the diagram developed for this project. It is shown in highlighted versions of the compound node influence diagram in Figures 3.1 and the basic node influence diagram in Figure 3.2. The specific Choices node parameter is the discrete set of integrity maintenance options or choices, selected by the decision maker and identified by name or number, that are to be evaluated by the influence diagram. Being the first node in the diagram, the Choices node has no predecessors (*i.e.*, it is an orphan node) which implies that the set of choices specified for consideration do not depend on any other parameters or conditions.

Figures

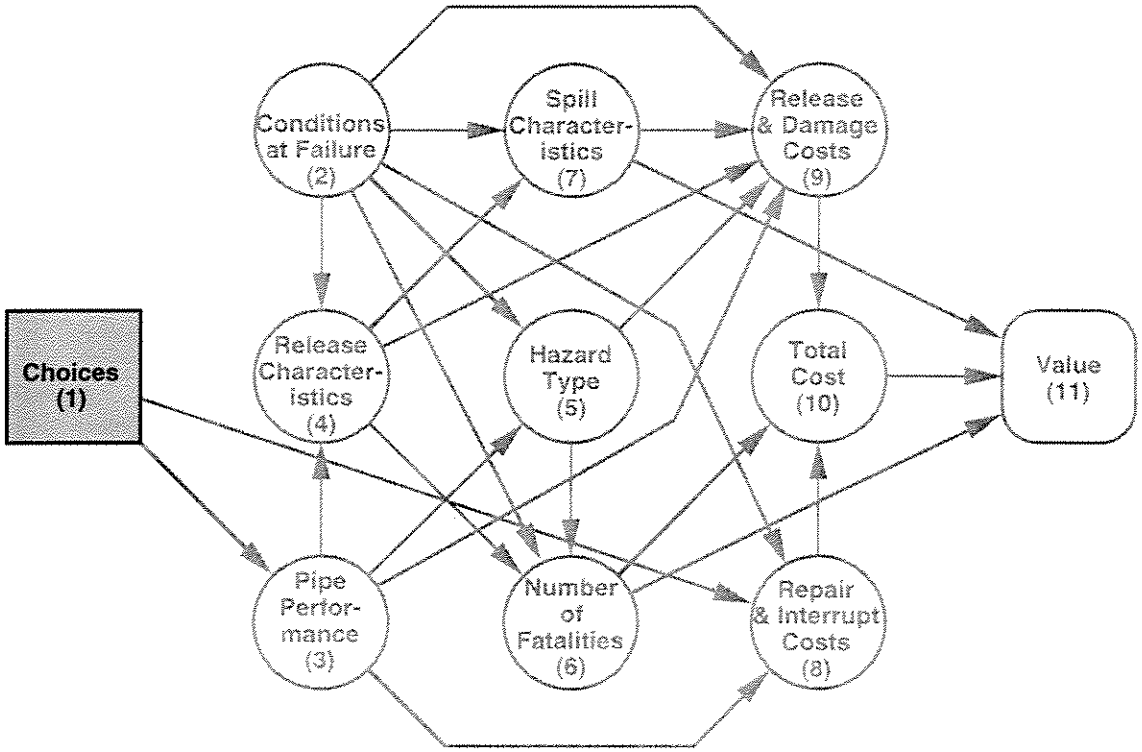

Figure 3.1 Compound node influence diagram highlighting Choices node group

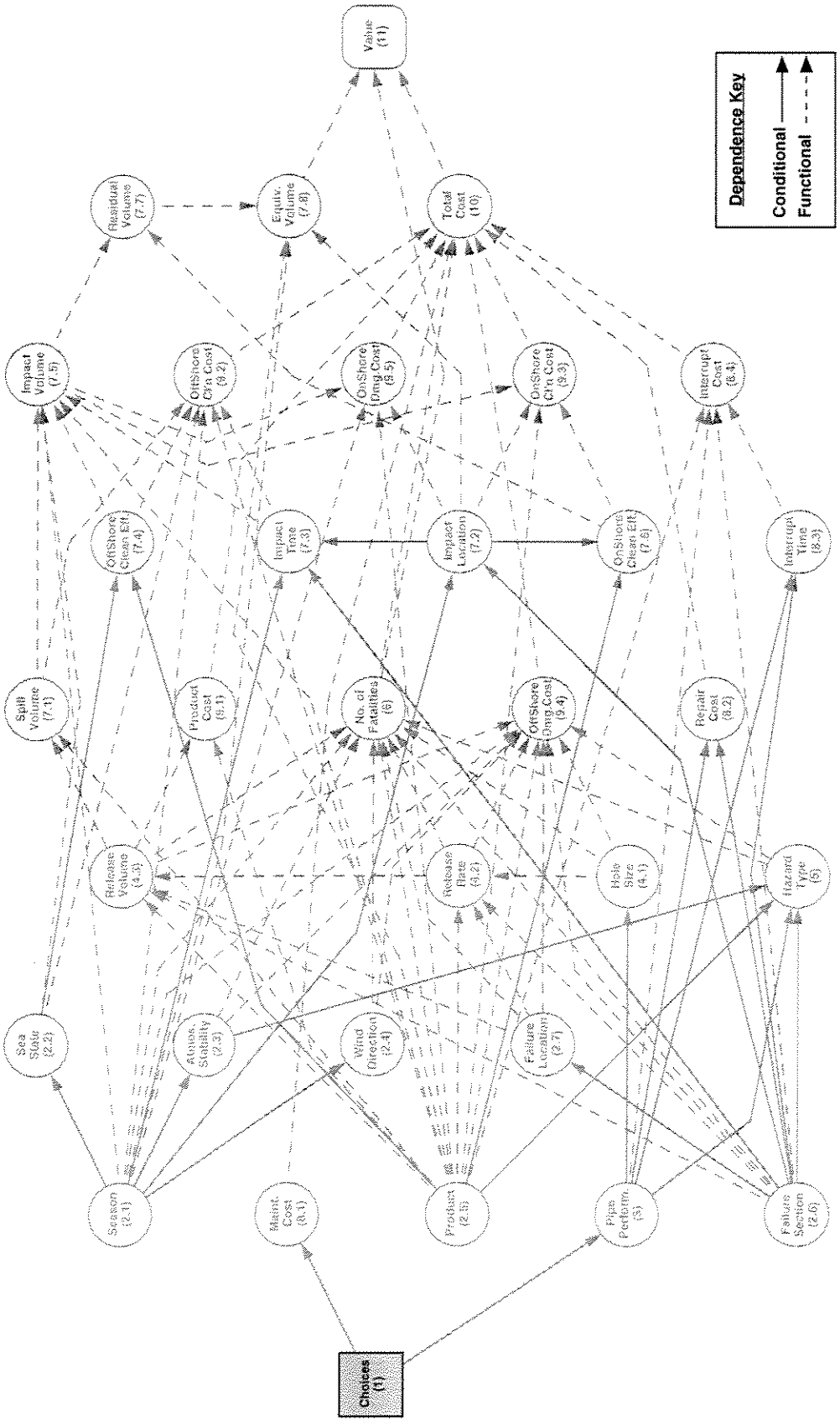

Figure 3.2 Basic node influence diagram highlighting Choices node

4.0 CONDITIONS AT FAILURE

4.1 Overview

The Conditions at Failure node group (group 2) is shown in a highlighted version of the compound node influence diagram in Figure 4.1. This node group involves parameters that are associated with conditions in the vicinity of the pipeline at the time of failure. The relevant conditions include parameters that reflect the weather (*i.e.*, season, sea state, atmospheric stability and wind direction), the product in the line, and the specific pipeline section and the location along the section where failure occurs. The individual parameters associated with the Conditions at Failure node group, as identified by the shaded nodes in a highlighted version of the basic node influence diagram shown in Figure 4.2, are discussed in the following sections.

4.2 Season

4.2.1 Node Parameter

The Season node (node 2.1) is shown in a highlighted version of the basic node influence diagram in Figure 4.2. The specific node parameter is the season and associated air temperature at time of failure (*Season*, T_a). The basic node influence diagram shows that Season has no predecessor nodes and is therefore not dependent on any other parameters or conditions. The Season node parameter set is defined by specifying the percentage of time during the year when each of two pre-defined season types (*i.e.*, summer and winter) apply and by defining the mean value of the hourly ambient air temperature associated with each season. The discrete probability distribution for Season is calculated directly from this information by assuming that failure is equally likely to occur at any time in the year. The probability of a given season at failure is therefore set equal to the percentage of time that the time the season is specified to apply.

The assumption of equal likelihood of failure throughout the year may not be strictly valid. For example, in the Gulf of Mexico failures related to mechanical damage caused by storms are expected to be more common during the summer season when tropical storms and hurricanes are more prevalent. Relaxing this assumption involves making the Pipe Performance conditional on the Season by adding a conditional arrow from the latter to the former. This aspect will be examined further when the influence diagram is expanded to estimate failure probabilities.

Note that, in the context of the offshore pipeline influence diagram, summer and winter seasons are defined as time periods which delineate significant differences in meteorological conditions (*e.g.*, air temperature, wind speed and wind direction) and oceanographic conditions (*e.g.*, water temperature, current speed and current direction). This approach to season definition was adopted primarily to accommodate the subsequent calculation of dependent node parameters

relating to liquid spill trajectory (*i.e.*, impact location and impact time) and offshore spill clean-up efficiency, both of which will affect the volume of spill impacting environmental resources, thereby influencing the environmental and financial consequences of line failure.

Note also that average hourly temperature was chosen as the most appropriate air temperature measure because product release hazards associated with pipeline failure (*e.g.*, vapour cloud formation and dispersion, jet fires, *etc.*) are typically associated with a duration measured in terms of minutes or hours.

The information required to define the node parameter is location specific. Summer and winter season durations and associated air temperatures should therefore be established on a site by site basis using historical meteorological and oceanographic information for the pipeline location in question. This information can be obtained from historical environmental data summaries (*e.g.*, Environment Canada 1984, NOAA 1975) or directly from regional or national environmental information offices.

4.2.2 Season Duration Estimates

For pipelines located in the Gulf of Mexico, an environmental impact statement prepared for proposed oil and gas lease sales (MMS 1995) describes a distinct six month summer season extending from May to October suggesting that a 50/50 summer vs. winter season split is a reasonable assumption. A review of historical weather data summarized by the National Oceanic and Atmospheric Administration (NOAA 1975) indicates that mean ambient hourly air temperatures for the corresponding summer and winter months in the central Gulf region are 27°C and 20°C, respectively. This representative season/temperature characterization is summarized in Table 4.1.

4.3 Sea State

4.3.1 Node Parameter

The Sea State node (basic node 2.2) and its direct predecessor node are shown in a highlighted version of the basic node influence diagram in Figure 4.2. The specific node parameter is the sea state that prevails in the days immediately following line failure (*Sea State*). The predecessor node arrow indicates that Sea State is a conditional node meaning that the value of the node parameter is conditionally dependent upon the value of its direct predecessor node which is Season. The Sea State node parameter must therefore be defined explicitly for all possible values associated with the Season node parameter. The node parameter is defined for each Season (*i.e.*, summer and winter) by specifying a discrete probability distribution for sea state that can take any of four specific values.

Conditions at Failure

The admissible set of parameter values is based on the traditional sea state classification system developed by mariners for estimating wind speed from the condition of the sea surface; surface conditions (mainly wave height and wave period) being important because they have a significant effect on the rate and overall extent of spill volume decay and the efficiency of offshore spill clean-up operations. The classification system involves ten sea states ('0' through '9') that correspond directly to wind speeds and indirectly to wave height and wave period. For the purposes of this project, these ten states have been reduced to four major sea state categories that are thought to effectively delineate significant changes in spill decay rates and spill clean-up efficiencies.

- Category 1 - (sea states 0 and 1) associated with calm to light winds having a speed range of 0 to 4.6 m/s (0 to 9 knots) and average significant wave heights up to 0.45 m (1.5 ft).
- Category 2 - (sea state 2) associated with gentle winds having a speed range of 4.6 to 7.1 m/s (9 to 14 knots) and average significant wave heights between 0.45 and 1.1 m (1.5 to 3.5 ft).
- Category 3 - (sea state 3) associated with moderate winds having a speed range of 7.1 to 8.7 m/s (14 to 17 knots) and average significant wave heights between 1.1 and 1.7 m (3.5 to 5.5 ft).
- Category 4 - (sea states 4+) associated with strong winds having speeds greater than 8.7 m/s (17 knots) and average significant wave heights in excess of 1.7 m (5.5 ft).

The information required to define the node parameter is location specific. The probability distribution of sea state category should therefore be established on a site by site basis using wind speed or wave height data for the pipeline location in question. This information can be obtained from historical environmental data summaries (*e.g.*, NOAA 1975) or directly from regional or national weather information offices.

4.3.2 Sea State Occurrence Probability Estimates

For pipelines located in the Gulf of Mexico, a probabilistic characterization and regression analysis was carried out on average hourly wind speed data for the central Gulf region summarized by the National Oceanic and Atmospheric Administration (NOAA 1975). The results were used to determine the relative frequency of occurrence of each sea state category for the six month summer and winter seasons identified for the Gulf in Section 4.3. The relative sea state occurrence frequencies are given in Table 4.2.

Note that the estimation of sea state occurrence frequencies based on average hourly wind speed data alone ignores the fact that the relevant sea state characteristics (*i.e.*, wave height and wave period) will also depend on other factors including the duration of wind events, fetch length and water depth, none of which are accounted for in the analysis described above. The tabulated sea state occurrence frequencies are therefore approximate values, and the implicit assumption that they can be assumed to apply for the entire duration of a given summer or winter spill event

Conditions at Failure

further emphasizes the approximate nature of the sea state characterization approach adopted herein.

4.4 Atmospheric Stability

4.4.1 Node Parameter

The Atmospheric Stability node (basic node 2.3) and its direct predecessor node are shown in a highlighted version of the basic node influence diagram in Figure 4.2. The specific node parameter is the atmospheric stability class and associated mean hourly wind speed at time of failure (S_{CLASS}, u_a). The predecessor node arrow indicates that Atmospheric Stability is a conditional node. The value of the node parameter set is therefore conditionally dependent upon the values of its direct predecessor node, Season. The node parameter set must therefore be defined explicitly for all possible values associated with the Season node parameter. The Atmospheric Stability node parameter set is defined, for each Season (*i.e.*, summer and winter), by specifying a discrete probability distribution for stability class and wind speed that can take any of six specific values.

The admissible set of parameter values is based on an atmospheric stability classification system developed by meteorologists that can be used to characterize the dilution capacity of the atmosphere; dilution capacity being important because it has a significant effect on the downwind and cross-wind extent of a gas or vapour plume resulting from product release. The system involves six stability classes ('A' through 'F') that reflect the time of day, strength of sunlight, extent of cloud cover, and wind speed.

- Classes A, B, and C are normally associated with daytime ground level heating that produces increased turbulence (unstable conditions).
- Class D is associated with high wind speed conditions that result in mechanical turbulence (neutral conditions).
- Classes E and F are associated with night-time cooling conditions that result in suppressed turbulence levels (stable conditions).

The information required to define the node parameter is location specific. The probability distribution of atmospheric stability classes and associated hourly wind speeds should therefore be established on a site by case site using historical weather data for the pipeline location in question. This information can be obtained from regional or national weather information offices.

Conditions at Failure

4.4.2 Stability Class Occurrence Probability Estimates

In the absence of location specific information, reasonable analysis results can be obtained by considering only two representative weather conditions: Stability Class D with a wind speed of 5 m/s and Stability Class F with a wind speed of 2 m/s (CCPS 1989). The former being representative of windy daytime conditions and the latter of calm nighttime conditions. In addition, based on historical atmospheric stability class data summaries compiled by the National Oceanic and Atmospheric Administration (NOAA 1976, MMS 1995), it is reasonable to assume that, for both summer and winter seasons in temperate North American climate zones including the Gulf of Mexico, the relative occurrence frequencies of Class D and Class F weather conditions are 67 percent and 33 percent, respectively. These generic modeling assumptions are summarized in Table 4.3.

4.5 Wind Direction

4.5.1 Node Parameter

The Wind Direction node and its direct predecessor node are shown in a highlighted version of the basic node influence diagram in Figure 4.2. The specific node parameter is the wind direction at time of failure (θ_w). The predecessor node arrow indicates that Wind Direction is a conditional node meaning that the parameter value is conditionally dependent upon the value of its direct predecessor node, Season. The Wind Direction node parameter must therefore be defined explicitly for all possible values associated with the Season node parameter. The node parameter is defined, for each Season (*i.e.*, summer and winter), by specifying a discrete probability distribution for wind direction that can take any of eight specific values, each corresponding to a 45 degree sector of compass direction (*i.e.*, N, NW, W, SW, S, SE, E, NE) from which the wind is assumed to blow.

The information required to define the node parameter is location specific. The probability distribution of wind direction should therefore be established on a site by site basis using historical weather data for the pipeline location in question. This information can be obtained from historical weather data summaries (*e.g.*, Environment Canada 1984, NOAA 1975) or directly from regional or national weather information offices.

4.5.2 Wind Direction Occurrence Probability Estimates

In the absence of location specific information it is reasonable to assume that the wind is equally likely to blow from any of the eight possible direction sectors. For pipelines located in the Gulf of Mexico, a review of historical meteorological data summarized by the National Oceanic and Atmospheric Administration (NOAA 1975) indicates a predominance of southeasterly and easterly winds and a moderate variation in directional frequency between summer and winter

Conditions at Failure

seasons. The calculated wind direction frequencies for the six month summer and winter seasons identified for the Gulf in Section 4.3 are given in Table 4.4.

4.6 Product

4.6.1 Node Parameter

The Product node (node 2.5) is shown in a highlighted version of the basic node influence diagram in Figure 4.2. The diagram indicates that Product has no predecessor nodes and is therefore not dependent on any other parameters or conditions. The specific Product node parameter is the product in the pipeline at time of failure (*Product*) which is defined by a discrete probability distribution that can take one of a number of values depending on the number of products carried in the pipeline.

Definition of the node parameter requires specification of the different products carried in the pipeline and the percentage of time during the year that the line is used to transport each product. The discrete probability distribution for Product at failure is calculated directly from this information by assuming that failure is equally likely to occur at any time in the year. The probability of a given product type is therefore set equal to the percentage of the time that the pipeline is specified to carry that product.

The information that must be specified to define the node parameter will obviously be pipeline specific. An example of the form and content of the required information is shown in Table 4.5.

It is noted that the adopted approach to product definition enables the decision analysis model to handle single-product as well as multiple-product pipelines. In addition, the influence diagram developed for consequence assessment has been designed to handle a broad range of petroleum hydrocarbon products. However, the emphasis in the development of product release, release hazard models, and hazard impact assessment models has been on single-phase gas and liquid products (excluding petrochemicals). Dual-phase products, specifically natural gas/condensate mixtures, are addressed in an approximate manner by assuming that the liquid fraction is fully entrained in the gas fraction as a vapour thereby justifying the use of a single-phase gas release model to calculate mixture release rates and volumes. Following gas/condensate mixture release, the gas fraction is used by the model to estimate short-term release hazards (*e.g.*, fires and explosions), and the condensate fraction is used to evaluate long-term release hazards (*i.e.*, persistent liquid product spills).

4.6.2 Deterministic Data Associated with the Product Node Parameter

Parameters associated with nodes that are dependent on the Product node will depend not just on product type but also on the specific values of the physical properties associated with each

Conditions at Failure

specified product type. The physical properties relevant to the consequence assessment model (in particular the release rate and release volume models) are listed in Table 4.6. This supplementary product data does not constitute an additional set of influence diagram parameters but rather represents a set of deterministic data that must be available to all nodes that require specific product property information to facilitate evaluation of a node parameter. The particular set of physical properties made available to the diagram for subsequent calculation will depend on the product type identified at the Product node.

Table 4.7 contains a list of petroleum gas and liquid products (or product groups) that are typically transported by offshore pipelines. For each product group a representative hydrocarbon compound (or set of compounds) is identified in the table. With regard to natural gas it is noted that sour gas (*i.e.*, natural gas containing hydrogen sulphide) has been excluded on the basis that the analysis of sour gas release consequences is beyond the scope of the current project.

For the representative hydrocarbon compound(s) associated with each of the product groups identified in Table 4.7, a product database was developed that includes relevant physical properties. The database of physical properties associated with each product group is given in Table 4.8. A discussion of the reference sources used to develop the physical property database and the approach used to select representative hydrocarbons for each product group is given in Appendix A.

4.7 Failure Section

4.7.1 Node Parameter

The Failure Section node is shown in a highlighted version of the basic node influence diagram in Figure 4.2. The diagram indicates that Failure Section has no predecessor nodes and is therefore not dependent on any other parameters or conditions. The specific Failure Section node parameter is the designation of the section within the pipeline segment considered which contains the failure location. It is defined by a discrete probability distribution that can take any number of values depending on the number of distinct sections that are defined along the length of the pipeline.

Note that a section is defined as a length of pipeline, over which the system attributes that are relevant to failure consequence assessment are constant. Definition of the node parameter therefore requires the specification of all relevant pipeline system attributes along the entire length of the pipeline. From this information the pipeline is sub-divided into distinct sections, each section being defined by a common set of attribute values. The length associated with each section is then calculated and, from this information, the discrete probability distribution for Failure Section is calculated by assuming that failure is equally likely to occur at any point along the length of the pipeline. The probability of failure associated with a given section is therefore set equal to the section length divided by the total length of the pipeline segment.

Conditions at Failure

As stated, the Failure Section node parameter is the designation of the section involved in the failure event, however, the section identification simply serves to identify which set of deterministic system attribute values are to be associated with the failure location.

4.7.2 Deterministic System Attributes Associated with the Failure Section Node Parameter

In the context of this project and the influence diagram developed herein, the attributes chosen to collectively define a pipeline section include parameters that characterize the following:

- geometric, mechanical and operational properties of the pipeline;
- proximity to offshore facilities (*i.e.*, platforms) and facility type;
- vessel traffic densities associated with the pipeline alignment; and
- pipeline location relative to the coastline as it affects the probability of spill impact.

The specific set of attributes that must be specified to define a section are listed in Tables 4.9a and 4.9b. The Table 4.9a indicates how each attribute is defined and identifies which attribute sub-sets are required for the assessment of each of the three basic consequence components addressed by the influence diagram (*i.e.*, life safety, environmental damage and financial cost). More specifically, Table 4.9b identifies the sub-set of attributes that are required to define the parameters associated with each node in the influence diagram that are dependent upon the Failure Section node.

It is noted that a significant number of the pipeline system attributes identified in Tables 4.9a and 4.9b are defined by a discrete set of predefined choices. The basis for the list of choices developed for each attribute will be explained in later sections that describe the calculation procedures for node parameters that depend on these particular attributes.

It is emphasized that, as is the case for the physical properties associated with each Product, the pipeline system attribute data described above does not constitute a set of additional influence diagram parameters. Rather, it represents an additional set of deterministic data that is available to all nodes that require specific system attribute information to facilitate calculation of a node parameter. The particular set of pipeline system attribute values made available to the diagram for subsequent calculation will depend on the section identified at the Failure Section node.

Conditions at Failure

4.8 Failure Location

4.8.1 Node Parameter

The Failure Location node and its direct predecessor node are shown in a highlighted version of the basic node influence diagram in Figure 4.2. The specific node parameter is the location of the failure point along a given section (L_s). The predecessor node arrow indicates that Failure Location is a conditional node with the parameter being dependent upon the value of its predecessor node, Failure Section. The Failure Location node parameter is characterized, for each Failure Section, by a continuous probability distribution of the distance along the length of the section to the failure point. This distance can take any value between zero and the length of the section. It is assumed that failure is equally likely to occur anywhere along the length of any given section. The continuous probability distribution of failure location along a given section is therefore taken to be uniform.

As stated, the Failure Location node parameter is the designation of the location of the failure point on a given section, however, the identification of the failure location simply serves to identify the value of certain deterministic pipeline system attributes that vary continuously along the length of the pipeline and which by their continually varying nature do not lend themselves to characterization on a section by section basis.

4.8.2 Deterministic System Attributes Associated with the Failure Location Node Parameter

In the context of this project and the influence diagram developed herein, the continuously varying pipeline system attributes that are required to complete the definition of the deterministic parameters associated with the pipeline system are:

- elevation/depth profile; and
- operating pressure profile.

These continuously varying system attributes are shown in Tables 4.9a and 4.9b together with the other system attributes that are taken to be constant along the length of each section.

Figures and Tables

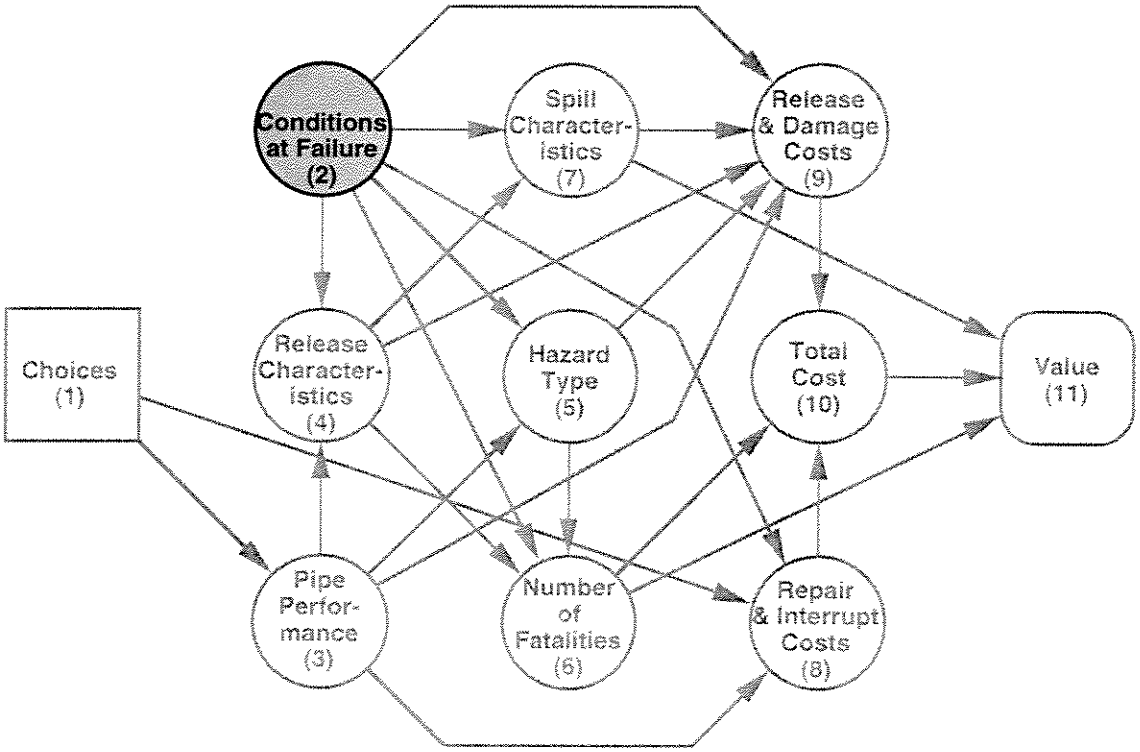

Figure 4.1 Compound node influence diagram highlighting Conditions at Failure node group

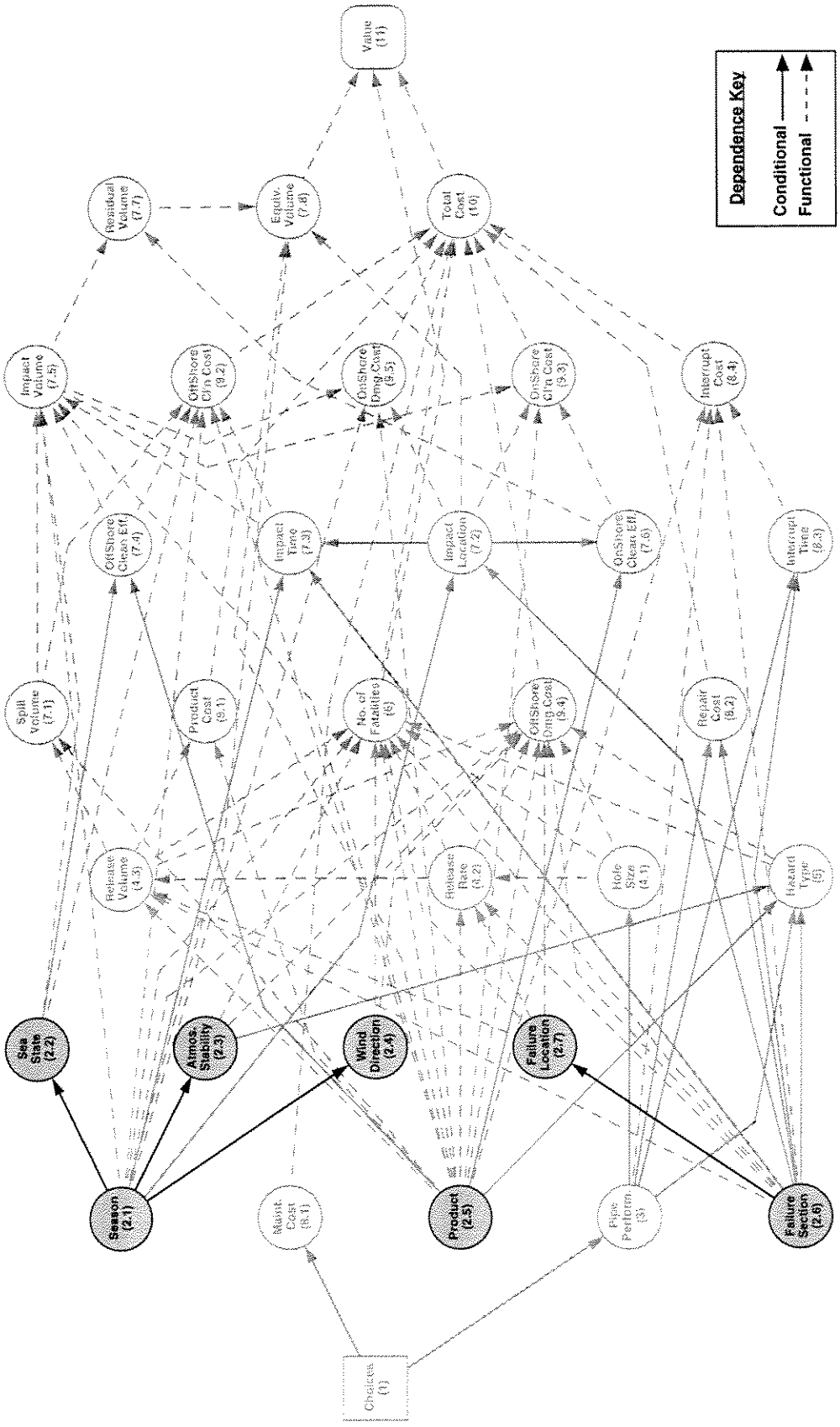

Figure 4.2 Basic node influence diagram highlighting Conditions at Failure nodes

Season	Season Duration (percent of year)	Ambient Air Temperature (°C)
Summer	50	27
Winter	50	20

Table 4.1 Representative season durations and associated average ambient air temperatures for the central Gulf of Mexico

Sea State Category	Probability of Occurrence During Summer	Probability of Occurrence During Winter
Category 1 (Sea State 0 - 1)	0.49	0.29
Category 2 (Sea State 2)	0.26	0.27
Category 3 (Sea State 3)	0.10	0.14
Category 4 (Sea State 4^{+})	0.15	0.30

Table 4.2 Representative sea state occurrence probabilities for the central Gulf of Mexico

Atmospheric Stability Class	Mean Wind speed (m/s)	Probability of Occurrence
Class A	1.0	0.0
Class B	2.0	0.0
Class C	3.0	0.0
Class D	5.0	0.67
Class E	3.0	0.0
Class F	2.0	0.33

Table 4.3 Representative atmospheric conditions for temperate climate zones including the Gulf of Mexico

Wind Direction	Probability of Occurrence During Summer	Probability of Occurrence During Winter
North	0.08	0.15
North East	0.14	0.16
East	0.23	0.18
South East	0.22	0.20
South	0.14	0.13
South West	0.07	0.05
West	0.06	0.04
North West	0.06	0.09

Table 4.4 Representative wind direction occurrence probabilities for the central Gulf of Mexico

Product	Percentage of Time
Natural Gas	80
Condensate (*i.e.*, pentanes plus)	20

Table 4.5 Example of product breakdown for an offshore gas/liquid pipeline

No.	Physical Property	Symbol	Units
1	Lower Flammability Limit	C_{LFL}	(volume conc.)
2	Heat of Combustion	H_c	J/kg
3	Heat of Vaporization	H_{vap}	J/kg
4	Molecular Weight	M_w	g/mol
5	Critical Pressure	P_c	Pa
6	Specific Gravity Ratio	SGR	
7	Specific Heat of Liquid	c_p	J/kg•°K
8	Specific Heat Ratio of Vapour	γ	
9	Normal Boiling Point	T_b	°K
10	Critical Temperature	T_c	°K
11a 11b 11c 11d	Vapour Pressure Constants	VPa VPb VPc VPd	
12	Explosive Yield Factor	Y_f	
13	Kinematic Viscosity	V_s	cs
14	Condensate / Gas Ratio	CondRatio	

Table 4.6 Physical properties of products required for consequence model evaluation

Fraction	Product Group	Carbon Range	Representative Hydrocarbon
Natural Gas	methane	C_1	CH_4 (methane)
Natural Gas Liquids	ethanes propanes butanes pentanes (condensate)	C_2 C_3 C_4 C_5 (C_3 - C_5^+)	C_2H_6 (ethane) C_3H_8 (n-propane) C_4H_{10} (n-butane) C_5H_{12} (n-pentane)
Gasolines	automotive gasoline aviation gas	C_5 - C_{10}	C_6H_{14} (n-hexane)
Kerosenes	jet fuel (JP-1) range oil (Fuel Oil - 1)	C_6 - C_{16}	$C_{12}H_{26}$ (n-dodecane)
Gas Oils	heating oil (Fuel Oil - 2) diesel oil (Fuel Oil -2D)	C_9 - C_{16}	$C_{16}H_{34}$ (n-hexadecane)
Crude Oils	_____	C_5^+	$C_{16}H_{34}$ (n-hexadecane)

Table 4.7 Representative petroleum product groups transported by pipeline

Physical Property[1]	Units	Natural Gas w/o condensate (100% methane)	Natural Gas with condensate (100% methane)	Ethanes (ethane)	Propanes (n-propane)	Butanes (n-butane)	Condensate (n-pentane)	Gasolines (n-hexane)	Kerosenes (n-dodecane)	Gas Oils (n-hexadecane)	Crude Oils (n-hexadecane)
C_{LFL}	(vol.)	0.05	0.05	0.029	0.021	0.018	0.014	0.013	0.007	0.013	0.013
H_C	J/kg	50020000	50020000	47200000	46013000	45850000	45010000	43540000	43120000	42900000	42450000
H_{vap}	J/kg	510000	510000	490000	426200	390000	357500	320000	250000	340000	340000
M_W	g/mol	16.04	16.04	30.07	44.09	58.12	72.15	86	170	226	226
P_C	Pa	4600000	4600000	4880000	4250000	3800000	3289000	3010000	182000	141000	141000
SGR		0.3	0.3	0.374	0.508	0.584	0.625	0.73	0.8	0.84	0.9
c_p	J/kg K	N/A	N/A	2450	2360	2301	2280	2260	2220	2200	2200
γ		1.306	1.306	1.191	1.13	1.094	1.076	1.054	N/A	N/A	N/A
T_b	K	111.7	111.7	184.6	231.1	272.2	270.9	343	470	560	560
T_C	K	190.4	190.4	305.4	369.8	425.5	460.8	507.5	658.2	722	722
VPa		-6.00435	-6.00435	-6.34307	-6.72219	-6.88709	-7.28936	-7.46765	77.628	89.06	89.06
VPb		1.1885	1.1885	1.0163	1.33236	1.15157	1.53679	1.44211	10012.5	12411.3	12411.3
VPc		-0.83408	-0.83408	-1.19116	-2.13868	-1.99873	-3.08367	-3.28222	-9.236	-10.58	-10.58
VPd		-1.22833	-1.22833	-2.03539	-1.38551	-3.13003	-1.02456	-2.50941	10030	15200	15200
Y_f		0.03	0.03	0.03	0.03	0.03	0.03	0.03	0.03	0.03	0.03
V_S	cs	0.0	0.0	0.11	0.21	0.29	0.38	0.5	2.0	15	10/50/200[3]
CondRatio		0.0	see note 2	N/A	N/A	N/A	N/A	N/A	N/A	N/A	N/A

Note: [1] physical properties given are based on properties of the representative hydrocarbon compound shown in parenthesis
[2] condensate ratio is the volume fraction of C_5^+ liquids in the product mixture at standard conditions
[3] product viscosity for light/medium/heavy crude oils, respectively

Table 4.8 Representative physical properties for selected petroleum hydrocarbon products and product groups

		Consequence Assessment		
		ic Conseq.		Environmental Conseq.
		nents (node 8&9)		Spill Character. (node 7)
No.	Pipeline Attribute	Liquid	Gas	Liquid
1	Pipeline Diameter	X		X
2	Pipe Wall Thickness	X		X
3	Pipeline Orientation (azimuth angle fron	X		X
4	Pipeline Elevation / Depth Profile (-ve ir	X		X
5	Operating Pressure Profile	X		X
6	Product Flow Rate between Throughpu	X		X
7	Product Temperature	X		X
8	Block Valve Spacing	X		X
9	Time to Block Valve Closure	X		X
10	Detectable Release Volume	X		X
11	Time to Leak Detection	X		X
12	Time to Leak Stoppage (from time of de	X		X
13a	Adjacent Platform Type	X		
13b	Adjacent Platform Offset	X		
14	Vessel Traffic Density	X		
15	Spill Trajectory Launch Zones	X		X
16	Water Depth Range (calculated internally from attribute No.	X		

Attribute Classes

Section type

S1 all consecutive segments defined by nu

S2 all consecutive segments defined by ar

S3 all consecutive segments defined by ar

Coordinate type

C1 numeric value of a continually varying

Platform type

P1 selected locations defined by: (a) an in

No.	Pipeline Attribute	nterrupt Time node 8.3)	Interrupt Cost (node 8.4)	Offshore Dmg. Cost (node 9.4)
1	Pipeline Diameter			
2	Pipe Wall Thickness			
3	Pipeline Orientation (azimuth angle from			
4	Pipeline Elevation / Depth Profile (-ve in			
5	Operating Pressure Profile			
6	Product Flow Rate between Throughpu		X	
7	Product Temperature			
8	Block Valve Spacing			
9	Time to Block Valve Closure			
10	Detectable Release Volume			
11	Time to Leak Detection			
12	Time to Leak Stoppage (from time of de			
13a	Adjacent Platform Type			X
13b	Adjacent Platform Offset			X
14	Vessel Traffic Density			X
15	Spill Trajectory Launch Zones			
16	Water Depth Range (calculated internally from attribute No.	X		

Attribute Classes

Section type

S1 all consecutive segments defined by nu

S2 all consecutive segments defined by an

S3 all consecutive segments defined by an

Coordinate type

C1 numeric value of a continually varying q

Platform type

P1 selected locations defined by: (a) an inc

5.0 PIPE PERFORMANCE

5.1 Node Parameter

The Pipe Performance node group (group 3) is shown in a highlighted version of the compound node influence diagram in Figure 5.1. The node group consists of a single node called Pipe Performance (node 3) which is shown together with its direct predecessor node in a highlighted version of the basic node influence diagram in Figure 5.2. The predecessor node arrow indicates that Pipe Performance is a conditional node meaning that the value of the node parameter is conditionally dependent upon the values of its direct predecessor, the Choices node. The Pipe Performance node parameter must therefore be defined explicitly for all possible integrity maintenance options identified at the Choices node. The Pipe Performance node parameter is defined by a discrete probability distribution for pipe performance that can take any of four possible states defined as:

- safe (*safe*);
- small leak (*smleak*);
- large leak (*lgleak*); and
- rupture (*rupture*).

Note that a small leak is assumed to involve a small hole and a corresponding low product release rate which does not generally result in significantly damaging release hazards or significant failure related costs. A large leak, involving a significant hole size, and a rupture, involving unconstrained product release from a hole size approaching or exceeding the line diameter, are typically associated with high release rates, particularly damaging release hazards, and significant failure costs. The distinction between large leaks and ruptures is considered necessary mainly to acknowledge the order of magnitude differences in release characteristics and their associated effects on the relative probability of occurrence of various release hazards.

Definition of the Pipe Performance node parameter requires the specification of annual failure rates (*i.e.*, annual rates of failure per unit length of pipeline for failure by small leak, large leak, and rupture) for each integrity maintenance action choice. The discrete probability distribution of pipe performance is calculated directly from this information by multiplying the specified failure rates by the length of the pipeline or pipeline segment to arrive at an annual probability of occurrence of small leaks, large leaks, and ruptures. The probability of safe performance (*i.e.*, no leaks or ruptures) is set equal to 1 minus the sum of the leak and rupture failure probabilities.

The information required to define the node parameter is obviously pipeline specific. In fact, the purpose of other projects in the current Joint Industry Program will be to develop models that facilitate the estimation of pipe performance (*i.e.*, failure rates) as a function of pipeline section attribute sets and choices regarding integrity maintenance actions. Within the context of the current document, however, failure rates are assumed to be constant along the entire length of the

pipeline under investigation (*i.e.*, constant for all sections generated by the Failure Section node), and the effect of integrity maintenance actions on failure rates are assumed to be addressed by defining appropriate failure rate estimates for each integrity maintenance option identified at the Choices node.

Note that the assumption that probability of failure is equal to failure rate times segment length is a valid approximation of the pipeline failure provided that the annual probability of more than one failure on the line segment being considered is small (*i.e.*, less than 0.1). This condition is satisfied if the product of failure rate and segment length is less than 0.5. The implications of this are that the pipeline should be analyzed in segments that meet this constraint. For example, if the annual failure rate is $1x10^{-3}$ per km·year then the segment length should not exceed 500 km ($0.5 / 1x10^{-3}$).

Note also that for pipelines in, for example the Gulf of Mexico, historical pipeline failure incident data for selected failure causes such as outside force (third party damage), suggests that line failure is more likely to occur during the summer season when tropical storms are more prevalent. This seasonal variation in failure probability is not reflected in the structure of the current influence diagram (*i.e.*, there is no conditional dependence arrow from season to pipe performance) to reduce diagram complexity and computational effort and because quantitative information on the seasonal variation in failure probability is not readily available.

5.2 Failure Rate Estimates

As part of a previous related project (Stephens *et al.* 1995b) a review of onshore pipeline incident data and statistical summary reports was carried out to facilitate the development of a set of reference failure rates that could be taken to be representative of natural gas, crude oil and petroleum product pipelines as a whole. The reference total failure rate developed from this review was 1×10^{-3} per km•yr. The review also led to the assumption that 87% of line failures corresponded to small leaks, 10% to large leaks, and 3% to full bore ruptures. A similar review of failure incident data and statistical summary reports for offshore pipelines, in particular Mare and Bakouros (1994) and Jansen (1995), supports the use of a similar reference failure rate and relative failure mode probabilities for offshore lines (excluding risers).

The set of reference failure rates developed from the literature review are given in Table 5.1. These failure rates are intended to serve as an indication of the relative likelihood of leaks and ruptures, and also as a reasonable first approximation of failure rates for typical offshore pipeline systems.

Figures and Tables

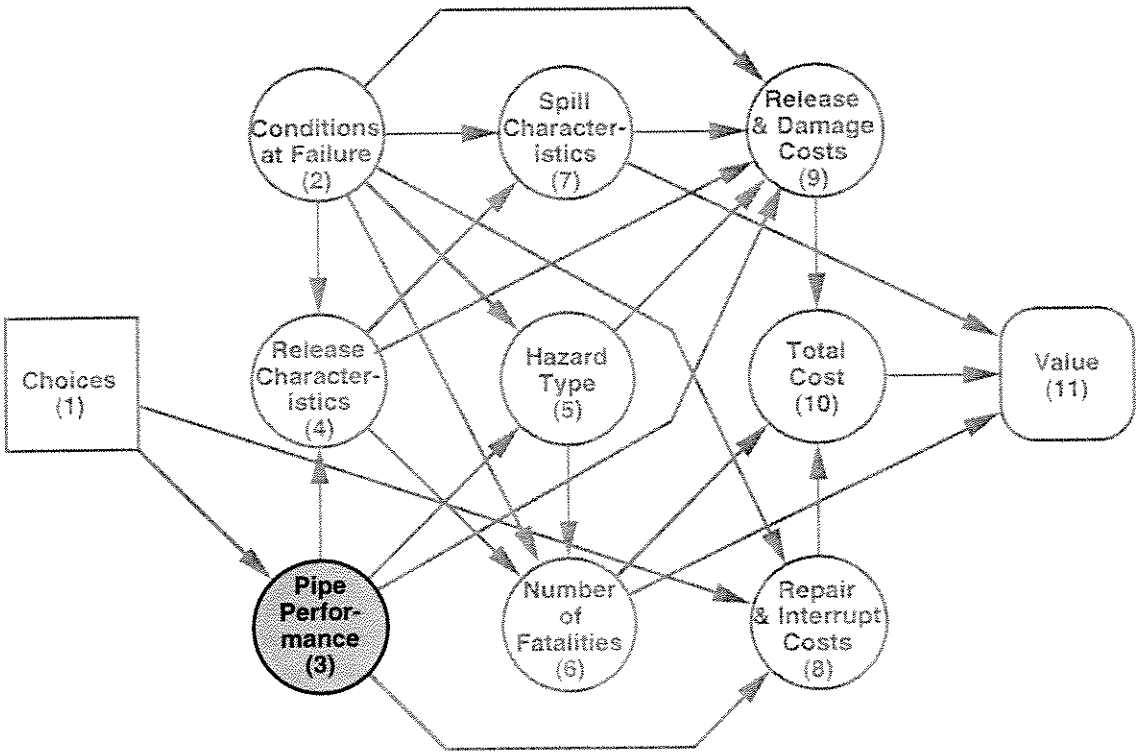

Figure 5.1 Compound node influence diagram highlighting Pipe Performance node group

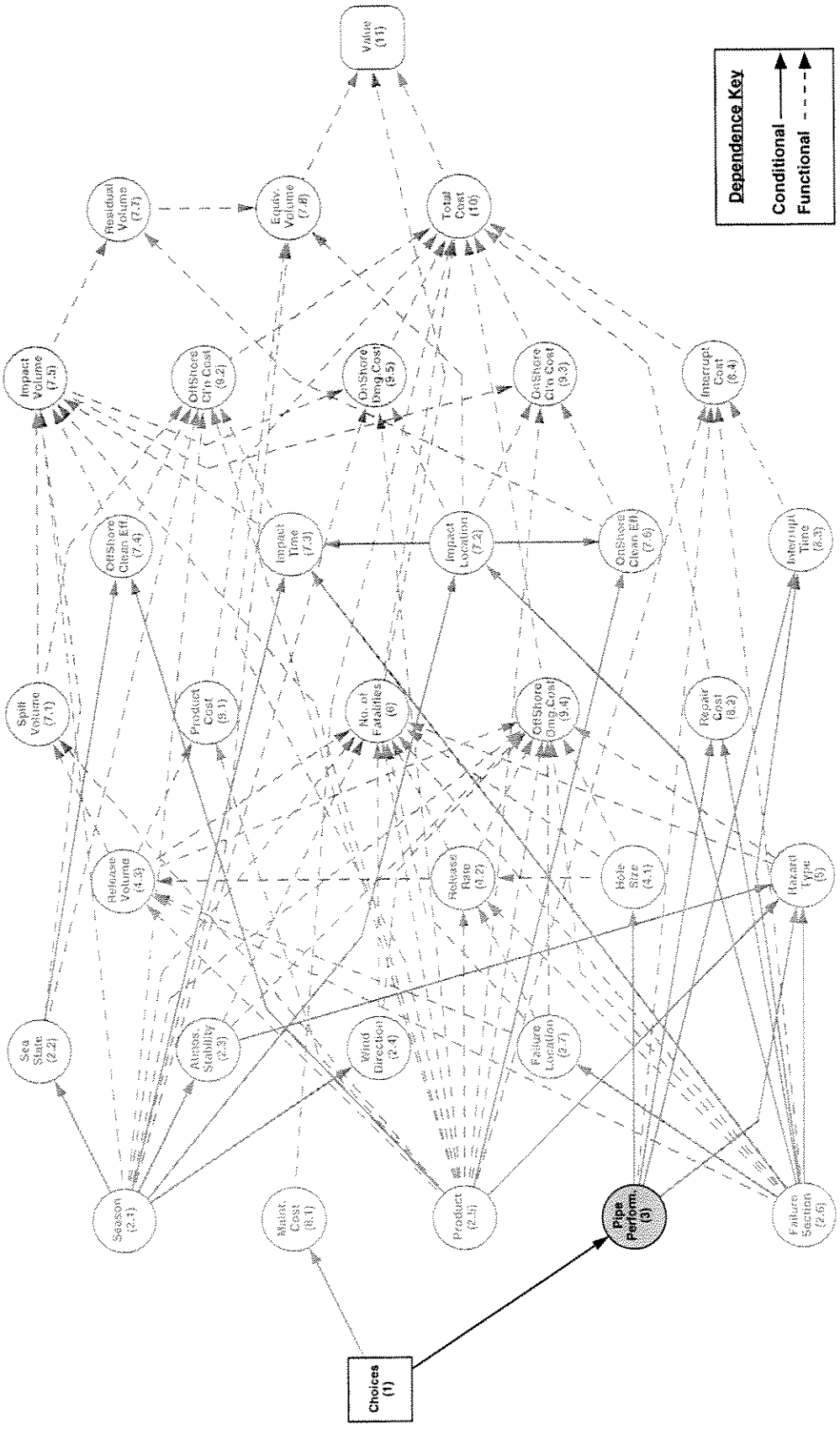

Figure 5.2 Basic node influence diagram highlighting Pipe Performance node and associated immediate predecessor node

Failure Mode	Failure Rate (per km•year)	Relative Frequency (%)
Small Leak	8.7×10^{-4}	87
Large Leak	1.0×10^{-4}	10
Rupture	0.3×10^{-3}	3
Combined Leak & Rupture	1.0×10^{-3}	100

Table 5.1 Representative failure rates for offshore petroleum gas and liquid pipelines

6.0 RELEASE CHARACTERISTICS

6.1 Overview

The Release Characteristics node group (group 4) is shown in a highlighted version of the compound node influence diagram in Figure 6.1. This node group involves parameters that are associated with the rate and volume of product that is released due to a pipeline failure. The individual parameters associated with the Release Characteristics node group, as identified by the shaded nodes in a highlighted version of the basic node influence diagram shown in Figure 6.2, are discussed in the following sections.

6.2 Hole Size

6.2.1 Node Parameter

The Hole Size node and its direct predecessor node are shown in a highlighted version of the basic node influence diagram in Figure 6.2. The specific node parameter is the effective hole diameter associated with line failure (d_h). The predecessor node arrow indicates that Hole Size is a conditional node meaning that the parameter value is conditionally dependent upon the value of its direct predecessor node, Pipe Performance. The Hole Size node parameter must therefore be defined explicitly for all possible values associated with the Pipe Performance node parameter. In the context of this project the node parameter is defined, for each Pipe Performance state (*i.e.*, safe, small leak, large leak and rupture), by specifying a continuous probability distribution for the effective hole diameter.

6.2.2 Hole Size Estimates

A review of pipeline incident data and statistical summary reports was carried out in a previous related project (Stephens *et al.* 1995b) which led to the development of a set of reference hole diameter distributions that are considered representative of onshore natural gas, crude oil and petroleum product pipelines in general. It was intended that this set of reference hole diameters would correspond to release rates that are consistent with the assumptions implicit in the definitions adopted for the various pipe performance states upon which hole diameter is dependent (*i.e.*, small leak, large leak and rupture). The corresponding information required to develop estimates of hole diameter distributions for offshore pipelines was not found in the literature. Therefore, to facilitate hole size characterization, in the absence of offshore specific data, it has been assumed that the historical data compiled on hole sizes for onshore pipelines can be used to infer hole size distributions for offshore pipelines.

Release Characteristics

6.2.2.1 Absolute Hole size

Based on hole diameter ranges reported by British Gas (Fearnehough 1985) and the correlations between hole diameter and pipe performance implicit in the reference failure rates developed herein (see Appendix B) it is assumed that a representative absolute hole diameter range is: 0 to 20 mm for small leaks, 20 mm to 80 mm for large leaks, and one or two pipe diameters for ruptures (depending on whether single- or double-ended release is involved). Due to a lack of sufficient historical data on the relative frequency of hole diameters within the indicated ranges, it is assumed that hole diameter is uniformly distributed for both small and large leaks, and equal to the line diameter for ruptures. These assumptions regarding hole size characterization are summarized in Table 6.1.

It is noted that the absolute hole diameter distributions given in Table 6.1 are based largely on incident data for gas pipelines. Given the nature of failures involving gas pipelines and the potential for effective hole diameter increase due to dynamic fracture propagation during the decompression phase of product release, it is assumed that these reference hole diameter distributions will represent a conservative approximation to the hole size distribution associated with liquid product pipelines.

6.2.2.2 Relative Hole size

As an alternative to hole size specification by absolute hole diameter, it is recognized that there are numerous literature citations for hole diameter estimates expressed as a fraction of line diameter. Typically, hole diameters for leak-type failures are estimated to be in the range of 0.01 to 0.10 times the line diameter and ruptures are usually characterized by a hole diameter equal to the line diameter. This alternate specification approach implies a direct correlation between hole size and line diameter, which is not reflected in an absolute hole size specification approach. In this regard it is noted that, except for the rupture failure mode, this implied correlation is not supported by incident data reviewed in the context of this project. (In fact, it is considered that the hole diameter associated with leak-type failure modes is more likely to be dependent on the mechanism causing line failure rather than on the diameter of the line itself.)

Given the literature precedent noted above, ignoring questions regarding the validity of a hole size specification approach that implies correlation with line diameter, it will be assumed that a representative relative hole diameter range is: 0.0 to 0.02 line diameters for small leaks; 0.05 to 0.15 line diameters for large leaks; and 1.0 line diameters for ruptures. Due to a lack of specific information it is further assumed that hole diameter is uniformly distributed for both leak-type failure modes. These assumptions regarding hole size characterization are summarized in Table 6.1.

Release Characteristics

6.3 Release Rate

The Release Rate node and its direct predecessor nodes are shown in a highlighted version of the basic node influence diagram in Figure 6.2. The predecessor node arrows indicate that Release Rate is a functional node meaning that the specific node parameter, the mass release rate at time of failure ($\dot{m}$), is calculated directly from the value of the parameters associated with its direct predecessor nodes which include: Product, Failure Section, Failure Location and Hole Size.

For gas pipelines the mass release rate $\dot{m}_{RG}$ can be calculated using an equation of the form

$$\dot{m}_{RG} = f\left(d_h, P_0, T_0, H_0, product \;\; properties\right) \qquad [6.1]$$

where d_h is the effective hole diameter, P_0 and T_0 are the line operating pressure and temperature at the failure location, and H_0 is the water depth at the location of failure. For liquid pipelines the equation for the mass release rate $\dot{m}_R$ takes the form

$$\dot{m}_R = f\left(d_h, P_0, T_0, H, H_0, product \;\; properties\right) \qquad [6.2]$$

where H is the effective hydrostatic pressure head at the failure location which depends on the elevation profile of the pipeline, the flow conditions and the product viscosity. The specific equations associated with the product release rate models adopted in this project, and the simplifying assumptions associated with their use, are described in detail in Appendix B (see Section 2.0 for gas release, and Section 3.0 for liquid release).

6.4 Release Volume

The Release Volume node and its direct predecessor nodes are shown in a highlighted version of the basic node influence diagram in Figure 6.2. The predecessor node arrows indicate that Release Volume is a functional node meaning that the specific node parameter, the total release volume at failure (V_R), is calculated directly from the value of the parameters associated with its direct predecessor nodes which include: Product, Failure Section, Failure Location and Release Rate.

For gas pipelines the total release volume V_{RG} can be calculated using an equation of the form

$$V_{RG} = \frac{\dot{m}_{RG} t_{RG}}{\rho_s} \qquad [6.3a]$$

where ρ_S is the product density under standard conditions and t_{RG} is the effective duration of the release event which in turn is given by

Release Characteristics

$$t_{RG} = f\left(\dot{m}_{RG}, \dot{m}_0, S_V, V_{dtect}, t_{dtect}, t_{close}, t_{stop}\right) \qquad [6.3b]$$

where $\dot{m}_0$ is the mass flow rate in the pipeline, S_V is the block valve spacing, V_{dtect} is the detectable release volume, t_{dtect} is the time required to detect line failure, t_{close} is the additional time required to close the block valves, and t_{stop} is the time required to reach the failure site and stop the release (which only applies to failure events involving small leaks).

For liquid pipelines the equation for the total release volume V_R takes the form

$$V_R = \frac{\dot{m}_R t_R}{\rho_s} \qquad [6.4a]$$

where t_R is the effective duration of the release event which is given by

$$t_R = f\left(\dot{m}_R, \dot{m}_0, S_V, V_0, V_{dtect}, t_{dtect}, t_{close}, t_{stop}\right) \qquad [6.4b]$$

where V_0 is the total volume of product in the line between the failure location and the surrounding valleys in the pipeline elevation profile.

The specific equations associated with the product release volume models adopted in this project, and the simplifying assumptions associated with their use, are described in detail in Appendix B (see Section 2.0 for gas release, and Section 3.0 for liquid release).

Figures and Tables

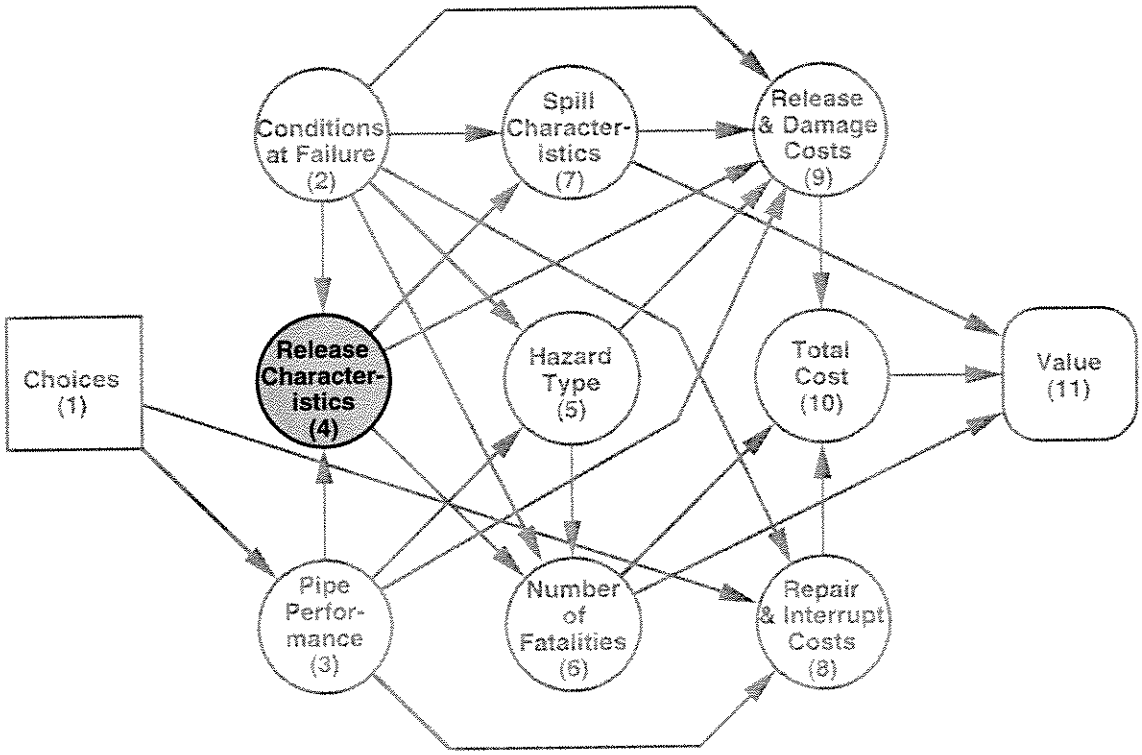

Figure 6.1 Compound node influence diagram highlighting Release Characteristics node group

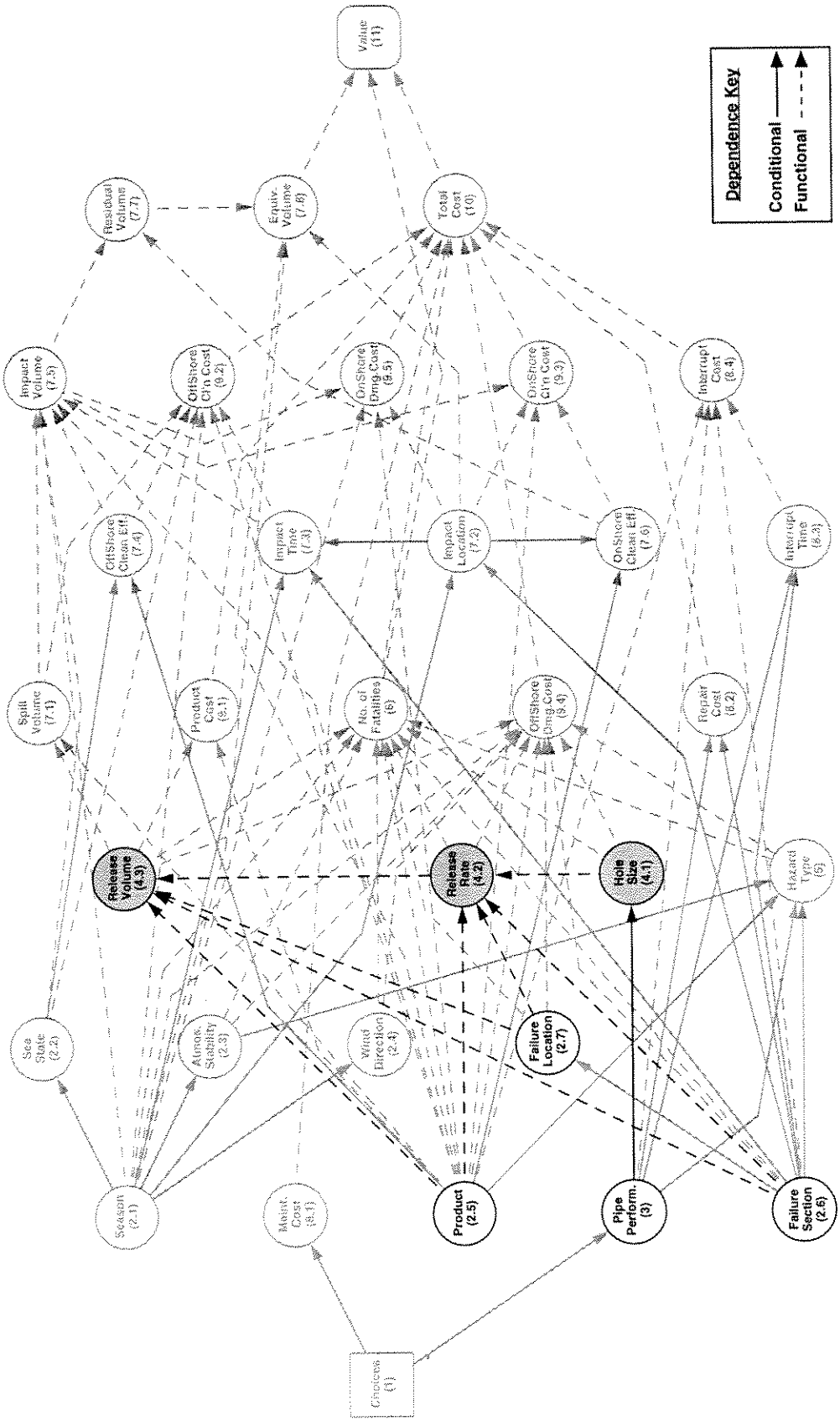

Figure 6.2 Basic node influence diagram highlighting Release Characteristics nodes and associated immediate predecessor nodes

Pipe Performance	Hole Diameter
safe	discrete value = 0.0
small leak	rectangular distribution (mean = 10 mm, std. dev. = 5.77 mm)
large leak	rectangular distribution (mean = 50 mm, std. dev. = 17.3 mm)
rupture	discrete value = 1.0 x (pipe diameter)

a) absolute hole diameter

Pipe Performance	Hole Diameter
safe	discrete value = 0.0
small leak	rectangular distribution (mean = 0.01, std. dev. = 0.00577)
large leak	rectangular distribution (mean = 0.10, std. dev. = 0.02885)
rupture	discrete value = 1.0 x (pipe diameter)

b) relative hole diameter

Table 6.1 Representative hole size distributions

7.0 HAZARD TYPE

7.1 Node Parameter

The Hazard Type node group (group 5) is shown in a highlighted version of the compound node influence diagram in Figure 7.1. The node group consists of a single node called Hazard Type (node 5) which is shown together with its direct predecessor nodes in a highlighted version of the basic node influence diagram in Figure 7.2. The specific node parameter is the hazard type associated with product release (*Hazard*). The predecessor node arrows shown in Figure 7.1 indicate that Hazard Type is a conditional node meaning that the value of the node parameter is conditionally dependent upon the values of its direct predecessor nodes which include: Product, Atmospheric Stability, Failure Section and Pipe Performance. The Hazard Type node parameter must therefore be defined explicitly for all possible combinations of the values associated with these direct conditional predecessor nodes.

The node parameter is defined by a discrete probability distribution for hazard type that can take any of five possible values. The five types of hazard considered are:

- jet fire (*JF*);
- pool fire (*PF*);
- vapour cloud fire (*VCF*);
- vapour cloud explosion (*VCE*); and
- toxic or asphyxiating vapour cloud (*TVC*).

These hazards and their associated hazard zone areas are shown schematically in Figure 7.3. Note that the offshore platform/vessel hazard associated with the zone of reduced buoyancy created above a subsea gas release has been excluded from the hazard set considered herein on the basis that it does not constitute a significant threat to life or property except in unlikely cases involving shallow water, large gas release rates, and marginal vessel stability conditions.

Definition of the Hazard Type node parameter requires the determination of the relative probabilities of occurrence of the hazard types listed above. This is achieved by first constructing hazard event trees which identify all possible immediate outcomes associated with a pipeline failure event. For use in this project, two simple event trees were developed; one for gas release (Figure 7.4a) and one for liquid product release (Figure 7.4b). These event trees were used to develop relationships which define the relative probabilities of the different possible hazard outcomes in terms of the conditional probabilities associated with the branches of the event trees. Based on the event trees shown in Figure 7.4, the relative hazard probabilities are given by the following equations.

The probability of a jet fire or pool fire ($P_{JF/PF}$) is given by

Hazard Type

$$P_{JF/PF} = P_i \qquad [7.1]$$

where P_i is the probability of immediate ignition given product release.

The probability of a vapour cloud fire (P_{VCF}) is given by

$$P_{VCF} = (1-P_i)\, P_d (1-P_e) \qquad [7.2]$$

where P_d is the probability of delayed ignition given no immediate ignition, and P_e is the probability of explosion given delayed ignition.

The probability of a vapour cloud explosion (P_{VCE}) is given by

$$P_{VCE} = (1-P_i)\, P_d P_e \qquad [7.3]$$

and the probability of a toxic or asphyxiating vapour cloud (P_{TVC}) is given by

$$P_{TVC} = (1-P_i)\,(1-P_d). \qquad [7.4]$$

It is noted that implicit in the subsequent application of the relative hazard probability obtained from Equation [7.1] are the following assumptions:

- products that are transported as a gas will produce a jet fire (as opposed to a pool fire) ;
- products that are transported as a liquid, and exist as a liquid under ambient conditions will produce a pool fire (as opposed to a jet fire); and
- products that are transported as a liquid, but exist as a gas under ambient conditions have the potential to produce both a jet fire and a pool fire.

In addition, the structure of the event trees shown in Figure 7.4 and the relative hazard probability equations developed from them also imply the following:

- hazards associated with a jet fires are more severe (*i.e.*, are more damaging) than hazards associated with pool fires;
- hazards associated with scenarios involving ignition are more severe than hazard scenarios that do not involve ignition;
- vapour cloud fires and explosions will not occur if pool or jet fires are ignited immediately; and
- vapour cloud fires and explosions are more severe hazards than the pool or jet fires that could develop following delayed ignition.

Hazard Type

Note, the last assumption listed above is justified based on the assumption that jet and pool fire hazard intensities associated with delayed ignition will be significantly lower than their corresponding immediate ignition hazard intensities due to reductions in the product release rate with time. This assumption serves to support the validity of the simplified event trees shown in Figure 7.4 which ignore the potential impact of jet and pool fires that are ignited as a direct result of the occurrence of delayed ignition hazards (*i.e.*, vapour cloud fires and explosions).

Given the stated assumptions and the equations for relative hazard probabilities, definition of the Hazard Type node parameter requires only the specification of the conditional event probabilities associated with the three event tree branches (*i.e.*, P_i, P_d and P_e) for all combinations of direct predecessor node values.

7.2 Conditional Event Probabilities

The information required to develop representative estimates of the conditional event probabilities associated with acute release hazards for offshore pipelines was not found in the literature. To facilitate hazard characterization, in the absence of offshore specific data, it has been assumed that historical data compiled on release incidents associated with onshore chemical process plants, product storage facilities, and pipelines can be used to develop reasonable event probability estimates. A review of the available literature identified specific conditions that have been shown to have a potentially significant effect on the event probabilities. The conditions identified include:

- product type (*i.e.*, gas, liquid);
- failure mode (*i.e.*, small leak, large leak, rupture);
- atmospheric stability class (*i.e.*, stable, unstable); and
- land use type (*i.e.*, industrial, urban, rural).

Based on the literature for onshore pipelines and facilities, in particular Fearnehough (1985), Crossthwaite *et al.* (1988), and EGIG (1993), representative conditional event probabilities have been established and from these event probabilities a matrix of relative hazard probabilities was developed using Equations [7.1, 7.2, 7.3 and 7.4]. These onshore hazard event probabilities were then translated into corresponding event probabilities for offshore pipelines by assuming that 'land use type' serves primarily to characterize the density of potential ignition sources. In the offshore pipeline context it is therefore assumed that ignition source density can be defined by: platform, vessel traffic, and remote (*i.e.*, negligible) ignition source density zones which are taken to be equivalent to industrial, urban and rural onshore land use types, respectively.

The conditional event probabilities so developed for offshore pipelines are summarized in Table 7.1. The hazard probabilities corresponding to each case in Table 7.1 (which effectively define the probability distribution of the Hazard Type node parameter) are given in Table 7.2. A discussion of the basis for the conditional event probabilities given in Table 7.1 is provided in Appendix C.

Hazard Type

It is noted that the use of onshore hazard event probabilities for offshore pipeline systems will result in a conservative overestimate of the likelihood of hazards involving ignited product release. This stems from the fact that the ignition of gas and liquid products will be less likely for offshore pipelines because the released product must rise to the sea surface before it can ignite and during this time water entrainment and/or product dispersion will significantly decrease the ignition potential.

Figures and Tables

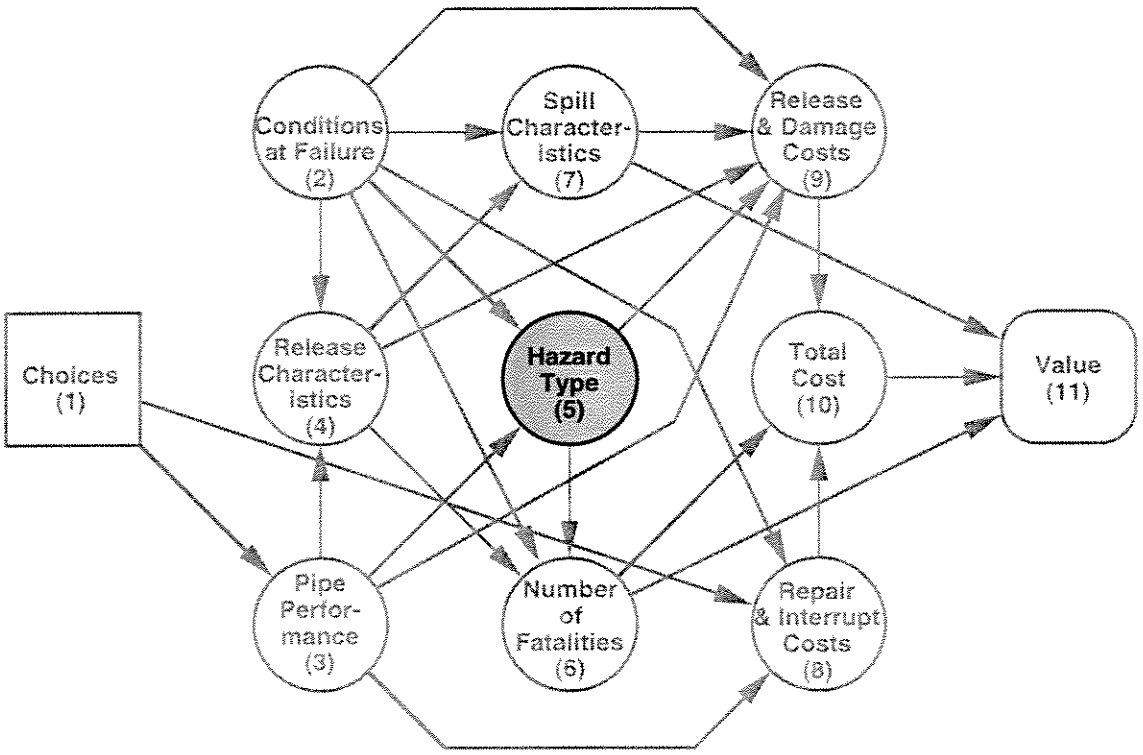

Figure 7.1 Compound node influence diagram highlighting Hazard Type node group

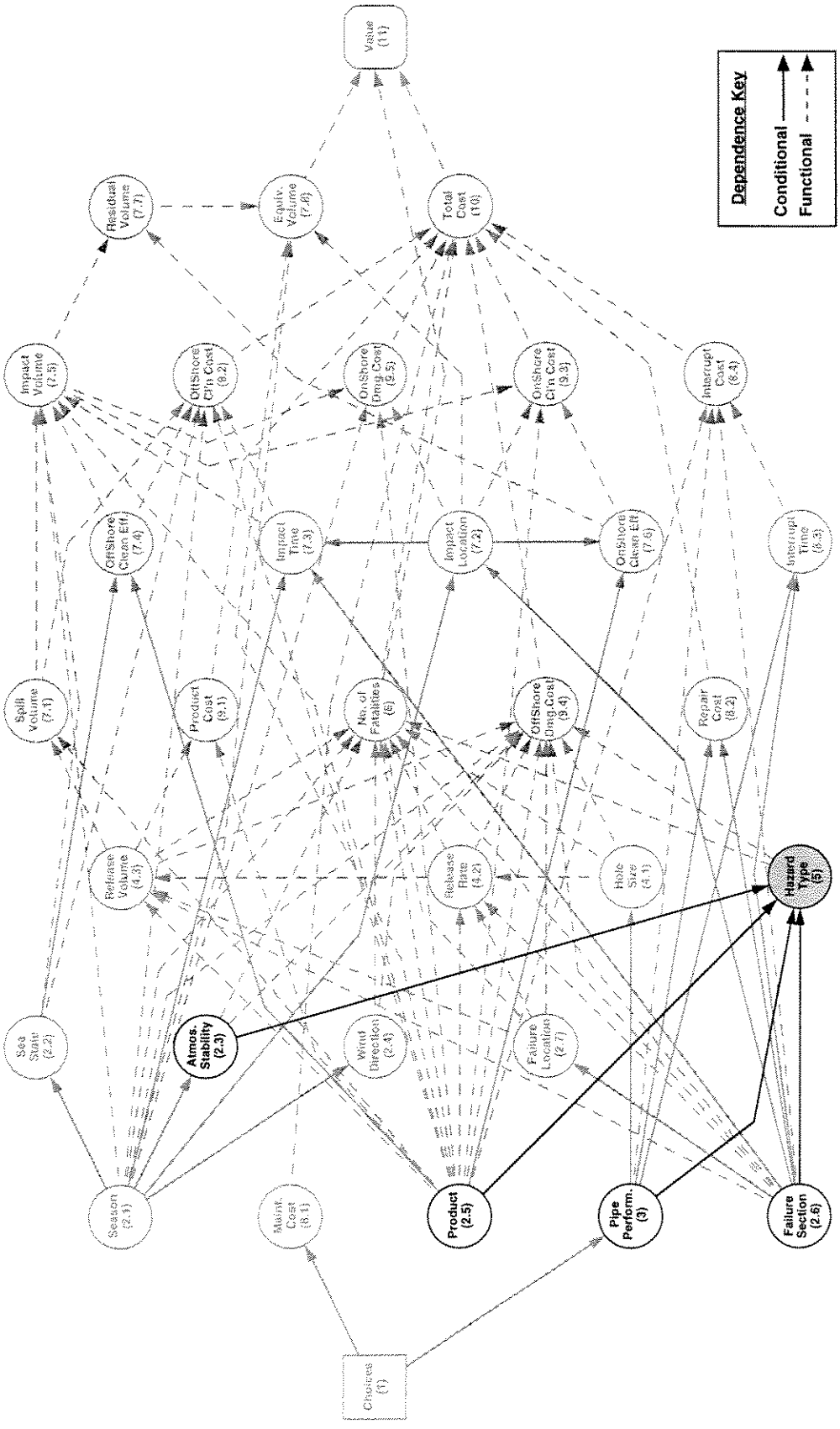

Figure 7.2 Basic node influence diagram highlighting Hazard Type node and associated immediate predecessor nodes

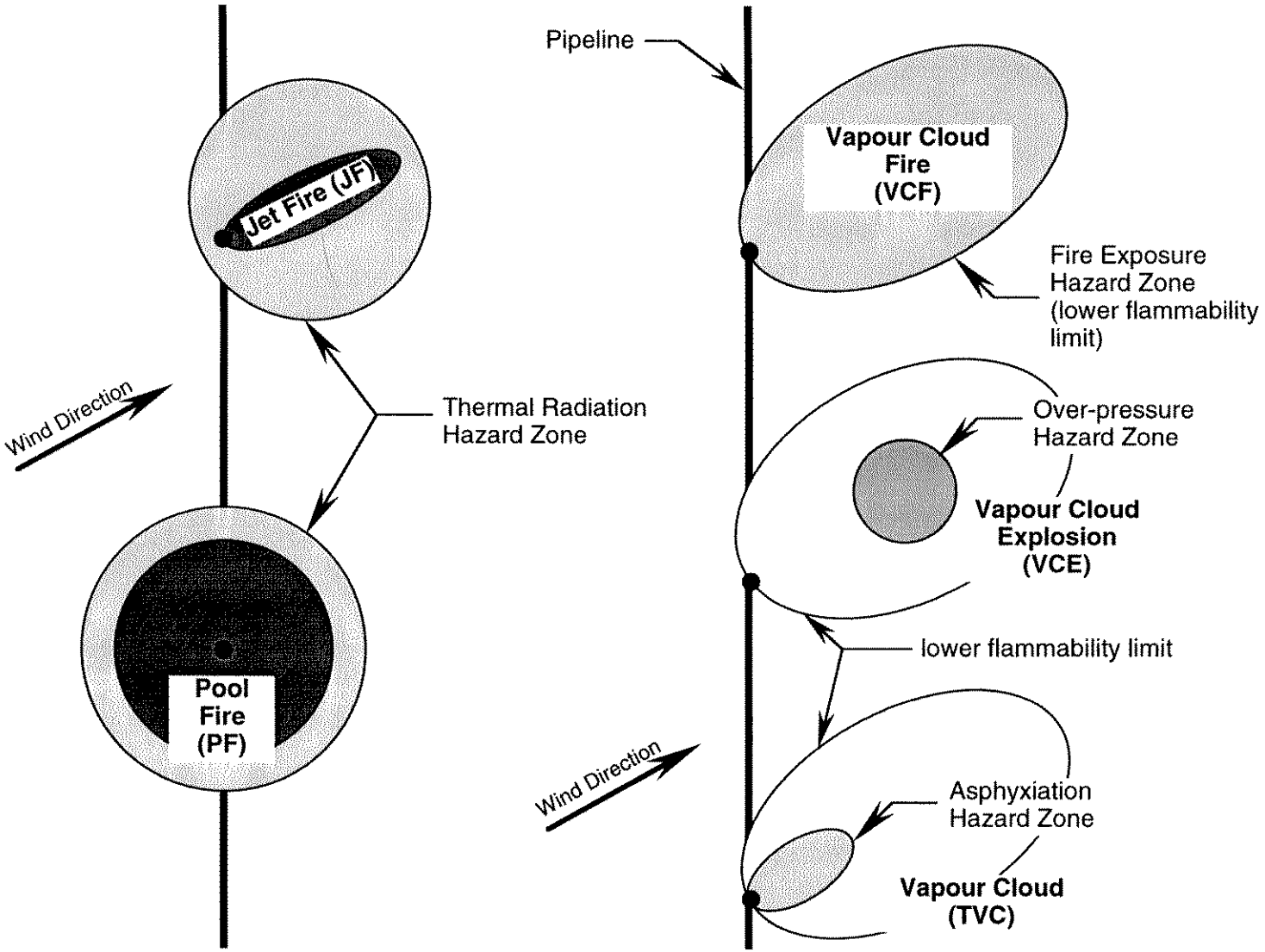

Figure 7.3 Acute release hazards and associated hazard zones for offshore pipelines

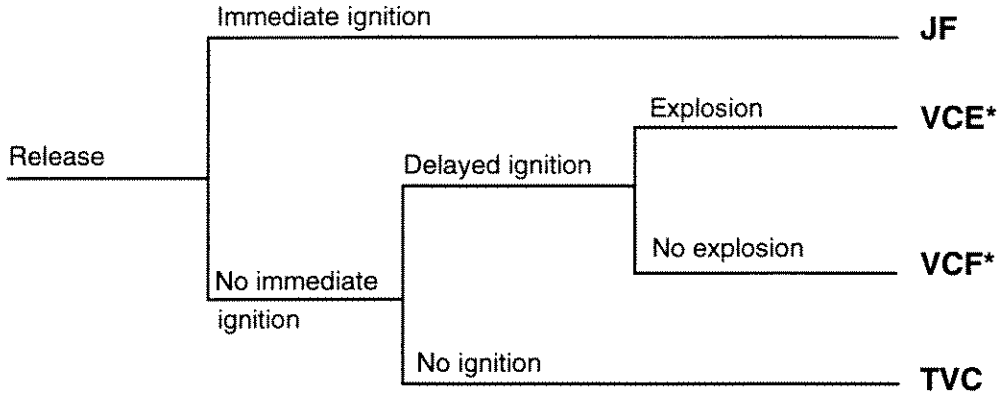

(a) Natural gas release

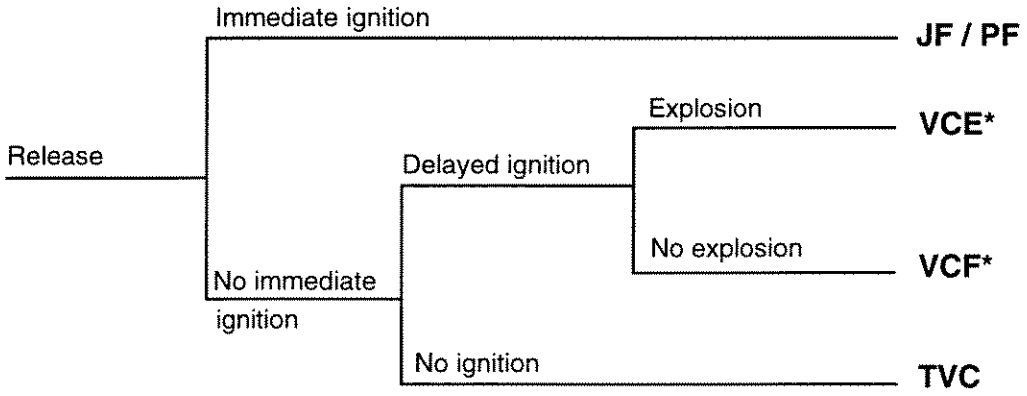

(b) Liquid release

* Note: jet fire and pool fire hazards occuring as a result of delayed ignition are ignored (see text)

Figure 7.4 Acute hazard event trees for product release from offshore pipelines

Case	Product (type)	Pipe Performance (failure mode)	Atmospheric Stability (class)	Ignition Source	Delayed Ignition Probability	Explosion Probability	Immediate Ignition Probability
1	liquid	small leak	A, B, C, D (unstable)	platform	0.3	0.33	0.05
2				vessel	0.24		
3				remote	0.012		
4			E, F (stable)	platform	0.27	0.1	
5				vessel	0.22		
6				remote	0.011		
7		large leak	A, B, C, D (unstable)	platform	0.56	0.33	0.05
8				vessel	0.45		
9				remote	0.023		
10			E, F (stable)	platform	0.51	0.1	
11				vessel	0.41		
12				remote	0.02		
13		rupture	A, B, C, D (unstable)	platform	1	0.33	0.05
14				vessel	0.8		
15				remote	0.04		
16			E, F (stable)	platform	0.9	0.1	
17				vessel	0.72		
18				remote	0.036		
19	gas	small leak	A, B, C, D (unstable)	platform	0.15	0.33	0.03
20				vessel	0.12		
21				remote	0.006		
22			E, F (stable)	platform	0.14	0.1	
23				vessel	0.11		
24				remote	0.0054		
25		large leak	A, B, C, D (unstable)	platform	0.28	0.33	0.1
26				vessel	0.23		
27				remote	0.011		
28			E, F (stable)	platform	0.25	0.1	
29				vessel	0.2		
30				remote	0.01		
31		rupture	A, B, C, D (unstable)	platform	0.5	0.33	0.25
32				vessel	0.4		
33				remote	0.02		
34			E, F (stable)	platform	0.45	0.1	
35				vessel	0.36		
36				remote	0.018		

Table 7.1 Matrix of conditional probabilities associated with acute hazard event tree branches

Case	Hazard Type			
	Jet Fire or Pool Fire	Vapour Cloud Fire	Vapour Cloud Explosion	Toxic Vapour Cloud
1	0.05	0.1910	0.0941	0.6650
2	0.05	0.1528	0.0752	0.7220
3	0.05	0.0076	0.0038	0.9386
4	0.05	0.2309	0.0257	0.6935
5	0.05	0.1881	0.0209	0.7410
6	0.05	0.0094	0.0010	0.9396
7	0.05	0.3564	0.1756	0.4180
8	0.05	0.2864	0.1411	0.5225
9	0.05	0.0146	0.0072	0.9282
10	0.05	0.4361	0.0485	0.4655
11	0.05	0.3506	0.0390	0.5605
12	0.05	0.0171	0.0019	0.9310
13	0.05	0.6365	0.3135	0.0000
14	0.05	0.5092	0.2508	0.1900
15	0.05	0.0255	0.0125	0.9120
16	0.05	0.7695	0.0855	0.0950
17	0.05	0.6156	0.0684	0.2660
18	0.05	0.0308	0.0034	0.9158
19	0.03	0.0975	0.0480	0.8245
20	0.03	0.0780	0.0384	0.8536
21	0.03	0.0039	0.0019	0.9642
22	0.03	0.1222	0.0136	0.8342
23	0.03	0.0960	0.0107	0.8633
24	0.03	0.0047	0.0005	0.9648
25	0.10	0.1688	0.0832	0.6480
26	0.10	0.1387	0.0683	0.6930
27	0.10	0.0066	0.0033	0.8901
28	0.10	0.2025	0.0225	0.6750
29	0.10	0.1620	0.0180	0.7200
30	0.10	0.0081	0.0009	0.8910
31	0.25	0.2513	0.1238	0.3750
32	0.25	0.2010	0.0990	0.4500
33	0.25	0.0101	0.0050	0.7350
34	0.25	0.3038	0.0338	0.4125
35	0.25	0.2430	0.0270	0.4800
36	0.25	0.0122	0.0014	0.7365

Table 7.2 Relative hazard event probabilities

8.0 NUMBER OF FATALITIES

8.1 Introduction

The Number of Fatalities node group (group 6) is shown in a highlighted version of the compound node influence diagram in Figure 8.1. The node group consists of a single Number of Fatalities node (node 6) which is shown together with its direct predecessor nodes in a highlighted version of the basic node influence diagram in Figure 8.2. The specific node parameter is the number of human fatalities resulting from the acute hazards associated with pipeline failure. Number of Fatalities is a functional node meaning that the value of the node parameter is calculated directly from the values of its direct predecessor node parameters which include: the product (and its characteristics), the failure location, the ambient temperature and wind conditions, and the release rate and release volume.

The node calculations model the emission of gas or liquid vapour into the atmosphere and determine the intensity of different acute hazard types (*e.g.*, heat intensity due to fires or over pressure due to explosions) at different points around the failure location. Based on this hazard characterization, and using estimates of the population density, the number of people exposed to fatal doses of these hazards can be calculated. This section describes the data and models used to calculate the number of fatalities.

8.2 Basic Calculation of the Number of Fatalities

8.2.1 Distributed Population Fatality Estimates

For distributed populations (*i.e.*, for the crew and passengers of vessels operating in the vicinity of a pipeline), the number of fatalities resulting from product release is a function of the hazard type and intensity and the tolerance threshold of humans to that hazard. Figure 8.3a gives a schematic representation of hazard intensity contours around a release source, while Figure 8.3b shows a schematic of the probability of death as a function of the hazard intensity. At the point with coordinates (x,y), the hazard intensity is $I(x,y)$ and the probability of death as a function of the hazard level is denoted $p[I(x,y)]$. Given an incident, the number of fatalities in a small area around (x,y) with dimensions Δx and Δy can be calculated by multiplying the number of people in the area by the probability of death for each person. The number of people is equal to the product of the population density $\rho(x,y)$ and the area. This can be written as:

$$n(x,y) = p[I(x,y)] \times [\rho(x,y)\ \ \Delta x \Delta y] \qquad [8.1]$$

Note that the population density is defined as the number of people who occupy the area at any given time. In the context of offshore pipelines this refers to the crew and passengers of vessels

Number of Fatalities

operating in proximity to the pipeline. The total number of fatalities for the whole area can be calculated by summing Equation [8.1] over the total area affected by the hazard. This gives:

$$n = \sum_{Area} p[I(x,y)] \times \rho(x,y)\,\Delta x\,\Delta y \qquad [8.2]$$

In Equation [8.2] $\rho(x,y)$ is calculated from the vessel traffic density for the area in question and an estimate of the average number of people occupying each vessel. $I(x,y)$ can be calculated as a function of the product type, release rate and weather conditions using a hazard model as will be discussed further in Section 8.3. The probability of death at a given hazard intensity level $p[I(x,y)]$ can be calculated from a probit analysis (*e.g.*, Lees 1980), which is essentially a method of calculating the probability that the tolerance threshold of a randomly selected individual is below the hazard dosage received. For some types of hazard (*e.g.*, thermal radiation), the dosage depends on exposure time and this is usually factored into the probit analysis, based on assumptions regarding the potential for escape within a certain period of time.

In order to simplify Equation [8.2] the following assumptions were made:

1. The population density, which is estimated from vessel traffic density, is constant for the area being considered.

2. Two hazard intensity thresholds can be defined, the first (denoted I_1) is the upper bound of human tolerance defined as the maximum intensity that has a chance of being tolerated (*i.e.*, $p(I) = 1$ for $I > I_1$), and the second (denoted I_0) defines the lower bound of human tolerance defined as the minimum intensity that has a chance of causing death (*i.e.*, $p(I) = 0$ for $I < I_0$). These thresholds take into account all aspects related to hazard dose and potential for escape.

3. The probability of death decreases linearly between the I_1 and I_0 contours.

Based on these assumptions, the number of fatalities n_1 within the upper bound tolerance threshold contour can be calculated from Equation [8.2] by using a fixed value of ρ and a value of $p[I(x,y)] = 1$. For a hazard intensity that decreases monotonically as the distance from the pipeline increases, this leads to (See Figure 8.4):

$$n_1 = \rho \sum_{A_1} \Delta x \Delta y = \rho\, A_1 \qquad [8.3]$$

where A_1 is the area within the I_1 contour. Similarly, the number of fatalities n_0 between the I_1 and I_0 contours is given by:

$$n_0 = 0.5\,\rho\,(A_0 - A_1) \qquad [8.4]$$

where A_0 is the total area within the I_0 contour. The total number of fatalities can be calculated as the sum of Equations [8.3] and [8.4], leading to

Number of Fatalities

$$n = 0.5\rho(A_0 + A_1) \qquad [8.5]$$

This approach is further illustrated in Figure 8.5, which shows a plot of the thermal radiation hazard intensity against the probability of death for a jet or pool fire. The probability of death resulting from a probit analysis that assumes a constant exposure time of 60 seconds is plotted, and compared to the assumption used in this report. In addition, a simpler assumption used in the public domain software program ARCHIE (FEMA/DOT/EPA 1989), based on a single threshold value that separates certain death from certain safety, is also shown on the plot for comparison.

Finally, distinction between 'on deck' and 'below deck' exposure is necessary because the hazard tolerance thresholds, and consequently the hazard areas used in Equation [8.5], are different for on deck and below deck locations. For example, enclosed structures provide protection from thermal radiation hazard, as long as the hazard intensity is lower than the threshold causing ignition of the structure. Taking this into account amounts to adding the number of fatalities occurring on deck and those occurring below deck based on the number of people at on deck and below deck locations at the time of the incident. This leads to:

$$n = 0.5\rho[t_i(A_0 + A_1)_i + t_o(A_0 + A_1)_o] \qquad [8.6]$$

where the subscripts i and o represent below deck and on deck, respectively. In this Equation t_i and t_o represent the ratio of time spent by vessel crew or passengers on deck or below deck.

8.2.2 Concentrated Population Fatality Estimates

For concentrated populations (*i.e.*, for the crew of permanent offshore facilities, or platforms, located near a pipeline), the number of fatalities resulting from product release is a function of the hazard type and intensity, the distance from the platform to the release source, and the hazard tolerance threshold of humans on the platform.

Given an incident, the number of fatalities on a platform can be calculated by multiplying the number of people on the platform by the probability of death for each person. The probability of death for any person on the platform is equal to the probability of an incident for which the associated hazard zone extends to involve the platform, multiplied by the probability of death for the hazard intensity associated with the hazard zone.

Calculation of the probability of an incident affecting the platform location is illustrated in Figure 8.6, which shows the hazard zone for a given release characterized by a specific set of parameters such as the release rate, weather conditions and pipeline characteristics. The figure is based on a circular hazard zone, but the same concept is applicable to elliptical hazard zones as well. Note also that the hazard zone is not centred around the failure location because of the effects of wind. Figure 8.6 shows that for the hazard zone to include the location of interest (point x), the failure must occur within a certain length along the pipeline. This length is called the interaction length for point x, and is denoted l_x. Figure 8.6 illustrates that the interaction

Number of Fatalities

length is equal to the secant of the hazard zone area passing through point x and parallel to the pipeline.

The probability of an incident affecting point x, is therefore equal to the probability of a failure occurring on the interaction length l_x. This is given by l_x/L, where L is the length of pipeline along which an incident could occur. The number of fatalities on a platform located at point x, n_x, can therefore be written as:

$$n_x = N_{px} \frac{l_x}{L} \qquad [8.7]$$

where N_{px} is the number of people on the platform.

Equation [8.7] gives the expected number of fatalities, given an incident, for one hazard contour within which the probability of death is 100%. As mentioned in Section 8.2.1, the hazard zone in this project is defined by two hazard contours: an upper limit and a lower limit tolerance threshold, with a chance of death of 100% within the upper limit contour and 50% between the two contours. Also, distinction between on deck and below deck exposure is needed here for the same reasons mentioned in connection with calculating the number of fatalities in Section 8.2.1. Considering these factors, a similar procedure to that explained in Section 8.2.1 shows that, Equation [8.7] becomes:

$$n_x = N_{px} \frac{0.5}{L} [t_i (l_{x0} + l_{x1})_i + t_o (l_{x0} + l_{x1})_o] \qquad [8.8]$$

where all the parameters are as defined before, with the subscripts i and o denoting below deck and on deck exposure, respectively.

8.3 Information Required to Evaluate the Node Parameter

8.3.1 General

To implement the models described in Sections 8.2.1 and 8.2.2 the following information is required:

- Properly calibrated upper and lower bound tolerance thresholds for different types of hazards. This information is required for both on deck and below deck exposure conditions.

- For distributed populations associated with vessel traffic:

Number of Fatalities

- models to calculate the area within the above-mentioned hazard threshold contours (these being derived from hazard models that calculate the hazard intensity as a function of the distance from the pipeline); and
- population densities and exposure times for both on deck and below deck vessel exposure.

- For concentrated populations associated with platforms:
  - models to calculate the interaction length for the above-mentioned hazard threshold contours (these also being derived from hazard models that calculate the hazard intensity as a function of the distance from the pipeline); and
  - platform populations and exposure times for both on deck and below deck platform exposure.

These items are discussed in Sections 8.3.2 and 8.3.3.

8.3.2 Hazard Tolerance Thresholds

A review of the literature was undertaken to define appropriate values of the upper and lower hazard tolerance thresholds. Table 8.1 gives a summary of the results for all acute hazard types relevant to product releases from pipelines. The main sources for this information are publications by the UK Health and Safety Executive (HSE) and by British Gas (see Appendix D).

A discussion of the rationale behind the values given in Table 8.1 is provided in Appendix D. The thresholds adopted are generally based on conservative assumptions. They also assume appropriate behaviour by those exposed to the hazard. For example, it is assumed that people in on deck locations will move away from the hazard source or seek shelter below deck. Also, in cases where being below deck provides protection from the hazard (such as for sustained jet or pool fires), it is assumed that people will remain below deck.

It is noted that exposure times are taken into account in defining the thresholds for thermal radiation and asphyxiation hazards. Time is relevant to these two types of hazards because the probability of death is a function of the total dose received, which in turn depends on the exposure time. For example, a high heat flux may be tolerated for a small period of time, whereas a lower heat flux may result in death if sustained for a long period of time. The time factor is taken into account by selecting the threshold value corresponding to a reasonable exposure time. The latter is selected on the basis of the hazard duration and the potential for escape. Details are given in Appendix D.

It is also noted that fatality thresholds are not applicable to vapour cloud fires for indoor exposure. This is because vapour cloud fires burn for very short periods of time and secondary ignition of objects within the fire zone is very unlikely. It is therefore assumed that vapour cloud fires do not represent a hazard for below deck exposure.

Number of Fatalities

8.3.3 Hazard Models

The area bound by the hazard threshold contours defined in Section 8.3.2 can be defined for each hazard type based on appropriate hazard intensity characterization models. The specific equations associated with the models adopted in this project, and the simplifying assumptions associated with their use, are described in detail in Appendix B. The following serves as a brief overview of the models used.

8.3.3.1 Jet Fire

The hazard intensity associated with a jet fire, I_{JF}, is the heat flux associated with the radiant heat source which is assumed to be located at the effective centre of the flame. The jet fire heat intensity at a given location (x,y) is given by

$$I_{JF}(x,y) = f\left(\dot{m}_{RG}, r_{xy}, x_0, y_0, product\ \ data\right) \qquad [8.9]$$

where $\dot{m}_{RG}$ is the mass flow rate associated with the gas (or vapour) fraction of released product, r_{xy} is the radius from the effective flame centre to the point of interest and x_0, y_0, are the coordinates of the horizontal projection of the flame centre relative to a point on the sea surface directly above the point of release. The location of the horizontal projection of the flame centre is given by

$$x_o, y_o = f\left(\dot{m}_{RG}, d_h, u_a, \theta_r, product\ \ properties\right) \qquad [8.10]$$

where d_h is the effective hole diameter, u_a is the wind speed, and θ_r is the wind direction relative to the bearing angle of the pipeline. (See also Appendix B, Section 5.)

8.3.3.2 Pool Fire

The hazard intensity associated with a pool fire, I_{PF}, is the heat flux associated with the radiant heat source which is assumed to be distributed over the area of the burning pool, the shape of which is approximated by a circle. The pool fire heat intensity at a given location is given by

$$I_{PF}(x,y) = f\left(\dot{m}_{RL}, r_{xy}, product\ \ data\right) \qquad [8.11]$$

where $\dot{m}_{RL}$ is the mass flow rate associated with the liquid fraction of released product and r_{xy} is the radius from the centre of the burning pool, which is assumed to be centred on the sea surface directly above the point of release, to the point of interest. (See also Appendix B, Sections 4 and 6.)

Number of Fatalities

8.3.3.3 Vapour Cloud Explosion

The hazard intensity associated with a vapour cloud explosion, I_{VCE}, is the overpressure associated with the propagating blast wave. The explosion induced overpressure at a given location is given by

$$I_{VCE}(x,y) = f\left(M_c, r_{xy}, x_1, y_1, product\ \ data\right) \qquad [8.12]$$

where M_c is the total mass of the flammable portion of the gas or vapour cloud bound by the vapour concentration associated with the lower flammability limit, r_{xy} is the radius from the effective centre of the blast to the point of interest and x_1, y_1 are the coordinates of the horizontal projection of the blast centre relative to a point on the sea surface directly above the point of release. The location of the horizontal projection of the blast centre is given by

$$x_1, y_1 = f\left(\dot{m}_{RG}, \dot{m}_V, S_{class}, u_a, \theta_r, C_{LFL}, product\ \ data\right) \qquad [8.13]$$

where $\dot{m}_{RG}$ is the mass release rate of the gas fraction, $\dot{m}_V$ is the evaporation rate from the liquid pool, C_{LFL} is the lower flammability limit, S_{class} is the atmospheric stability class and u_a is the mean wind speed. (See also Appendix B, Sections 7, 8, and 10.)

8.3.3.4 Vapour Cloud Fire

The hazard associated with a vapour cloud fire is direct exposure to the burning cloud of gas or vapour. The extent of the burning area is bound by the vapour concentration contour associated with the lower flammability limit of the product involved. The vapour concentration contour associated with C_{LFL} is given by

$$C_{C_{LFL}}(x,y) = f\left(\dot{m}_{RG}, \dot{m}_V, S_{class}, u_a, x_1, y_1, C_{LFL}, product\ \ data\right) \qquad [8.14]$$

where x_1, y_1 are the co-ordinates of the horizontal projection of the centre of the flammable vapour cloud relative to a point on the sea surface directly above the release point which is given by Equation [8.13]. (See also Appendix B, Sections 7, 8, and 9.)

8.3.3.5 Asphyxiating Cloud

The hazard associated with a toxic or asphyxiating cloud is associated with oxygen deprivation. The extent of the hazard area is bound by the vapour concentration contour associated with the vapour concentration threshold (C_{TVC}) of the product involved. The vapour concentration contour associated with C_{TVC} is given by

Number of Fatalities

$$C_{C_{TVC}}(x,y) = f\left(\dot{m}_{RG}, \dot{m}_V, S_{class}, u_a, x_2, y_2, C_{TVC}, product\ \ data\right) \quad [8.15]$$

where x_2, y_2 are the co-ordinates of the horizontal projection of the centre of the asphyxiating vapour cloud relative to a point on the sea surface directly above the release point which is given by

$$x_2, y_2 = f\left(\dot{m}_{RG}, \dot{m}_V, S_{class}, u_a, \theta_r, C_{TVC}, product\ \ data\right) \quad [8.16]$$

(see also Appendix B, Sections 7 and 8.)

8.3.4 Population and Exposure Time Estimates

For distributed populations associated with vessel traffic, the population density is dependent upon the type and density of vessel traffic in proximity to the pipeline and the number of people on each vessel. In the context of this project, it is assumed that population density is tied directly to vessel traffic density by assuming a representative vessel type and an associated average number of people on board. Vessel traffic density, and hence population density, is divided into four categories: high traffic density, moderate traffic density, low traffic density, and negligible traffic density (*i.e.*, remote locations). These categories are intended to delineate order-of-magnitude changes in population density.

For concentrated populations associated with platforms, the number of people involved is dependent upon the type, size and usage of the platform. In the context of this project, it is assumed that all platforms can be classified into one of four categories. The four categories are: major manned, minor manned, major unmanned, and minor unmanned. (Note, manned platforms are defined as structures with sleeping accommodations.) The chosen categories include unmanned platforms because the platform designation serves two purposes: 1) to define populations for fatality estimates at the Number of Fatalities node; and 2) to define platform costs for damage cost estimates at the Offshore Damage Cost node (see Section 11.5). In addition, unmanned platforms will be visited by operations and maintenance personnel on a regular basis and this intermittent platform occupancy can be reflected by an effective unmanned platform population estimate that accounts for limited exposure.

An in-depth literature survey to identify reference population densities for the various vessel traffic density categories and platform types was considered beyond the scope of this project. However, for platforms, order of magnitude population estimates can be obtained based on the following assumptions: 1) major and minor manned platforms exist in approximately equal numbers; 2) there is an order of magnitude difference in the population of major and minor manned platforms; and 3) an estimate of the average manned platform population is 14 (MMS 1995). Given the above it follows that a representative estimate of manned platform populations is 50 for major manned platforms and 5 for minor manned platforms. Assuming further that major and minor unmanned platforms are serviced three times per week and once

Number of Fatalities

every other week, respectively, and assuming that supply vessels are in the immediate vicinity of the platform for approximately four hours per visit, then the effective platform population is approximately 0.5 for major unmanned platforms and 0.05 for minor unmanned platforms. These platform population estimates are summarized in Table 8.2.

In the absence of readily citable information on vessel traffic densities and corresponding crew compliments, the following characterizations are proposed. A high density vessel traffic zone shall correspond to 10 people per km^2 (*e.g.*, a major shipping corridor with one significant vessel per square km during daylight hours, assuming a crew of 20 and 12 hours of daylight per day). A low density vessel traffic zone shall correspond to 0.1 people per km^2 (*e.g.*, an active fishing area in which a square km of area is occupied by a vessel with a crew of two to three people for a one hour period each day). A moderate density vessel traffic zone shall correspond to an intermediate population density of 1.0 person per km^2. These vessel traffic population estimates are summarized in Table 8.2.

Daily exposure time is defined as the length of time per day spent by the average person at the location in question in either an exposed (on deck) location or sheltered (below deck) location. An in-depth literature survey to identify relative exposure times for vessel and platform occupancies was beyond the scope of this project. However, since it is conservative to overestimate the duration of on deck exposure time, and because 12 hour work shifts are not uncommon in the offshore industry, it is considered reasonable to assume an equal split between on deck and below deck exposure times for people on both vessels and platforms. This exposure time assumption is summarized in Table 8.3. Note that the exposure time ratio t in Equations [8.6] and [8.8] is calculated by dividing the exposure times given in Table 8.3 by 24 hours.

Figures and Tables

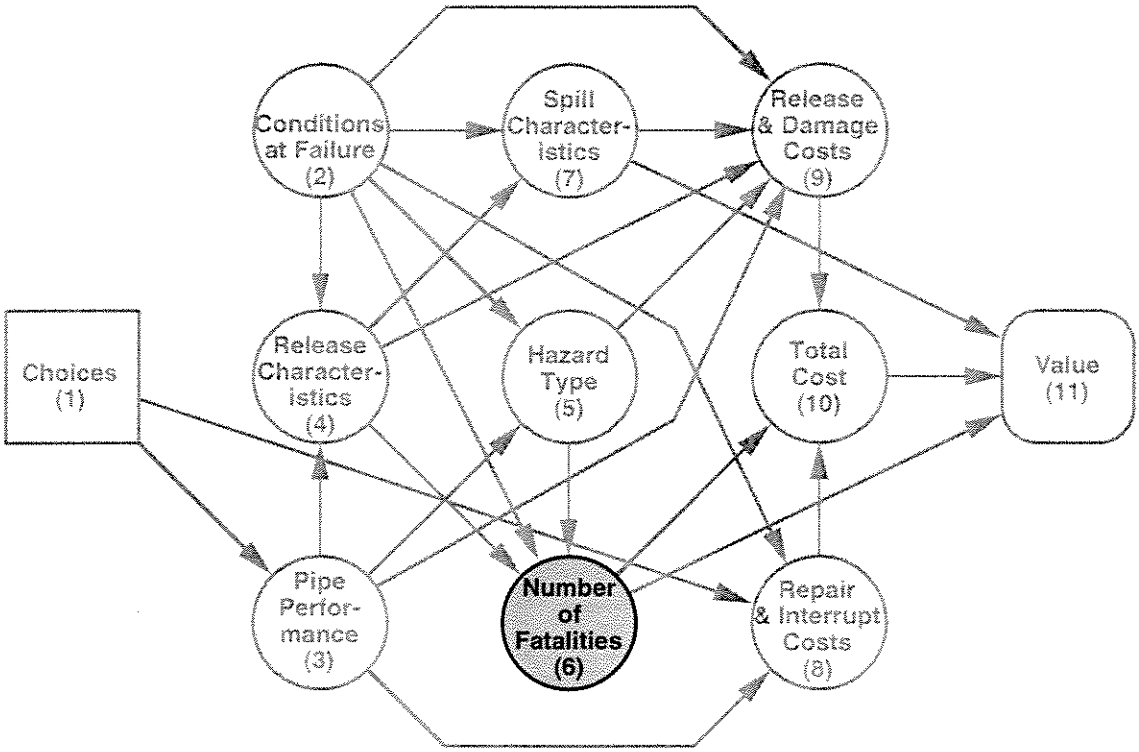

Figure 8.1 Compound node influence diagram highlighting
Number of Fatalities node group

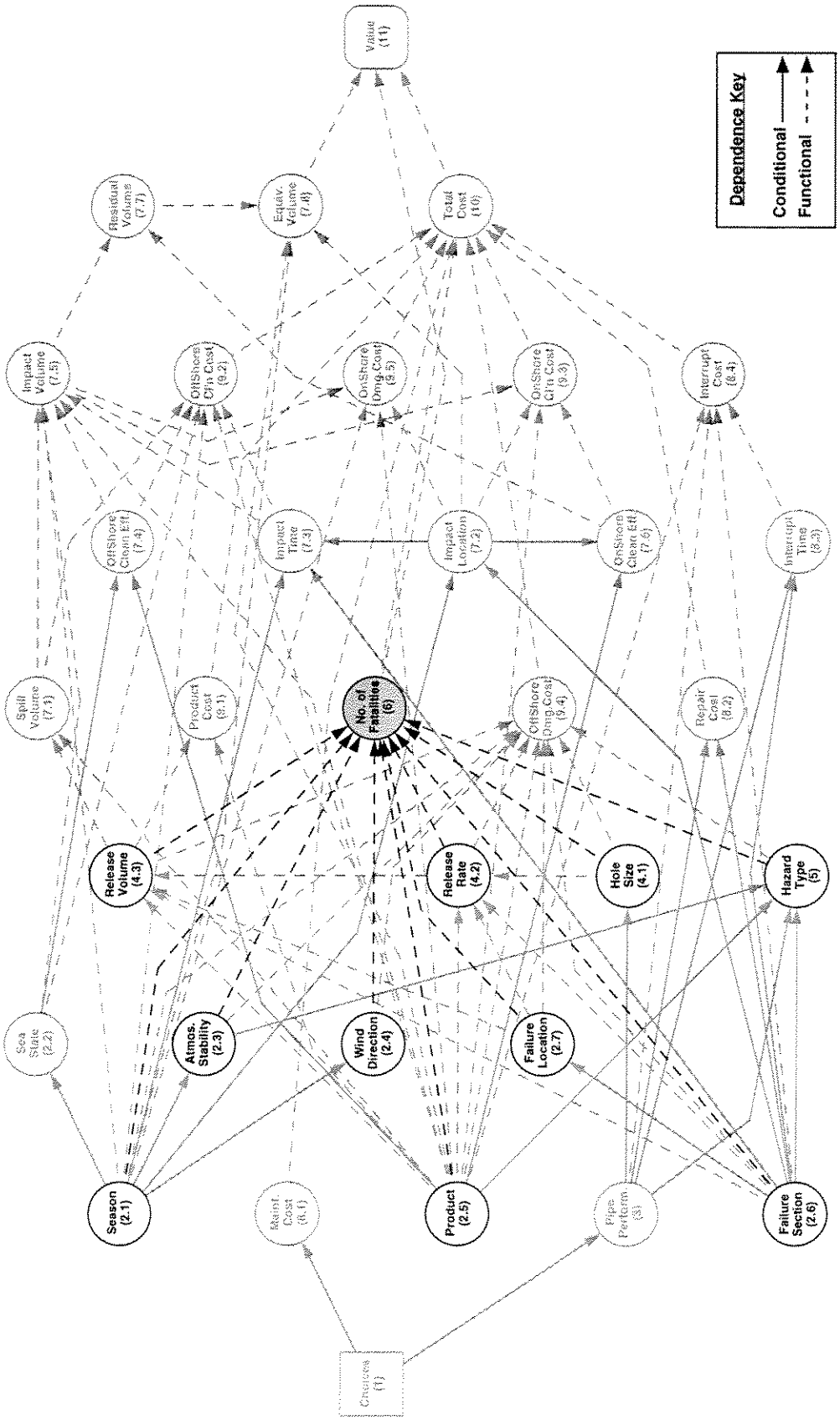

Figure 8.2 Basic node influence diagram highlighting Number of Fatalities node and associated immediate predecessor nodes

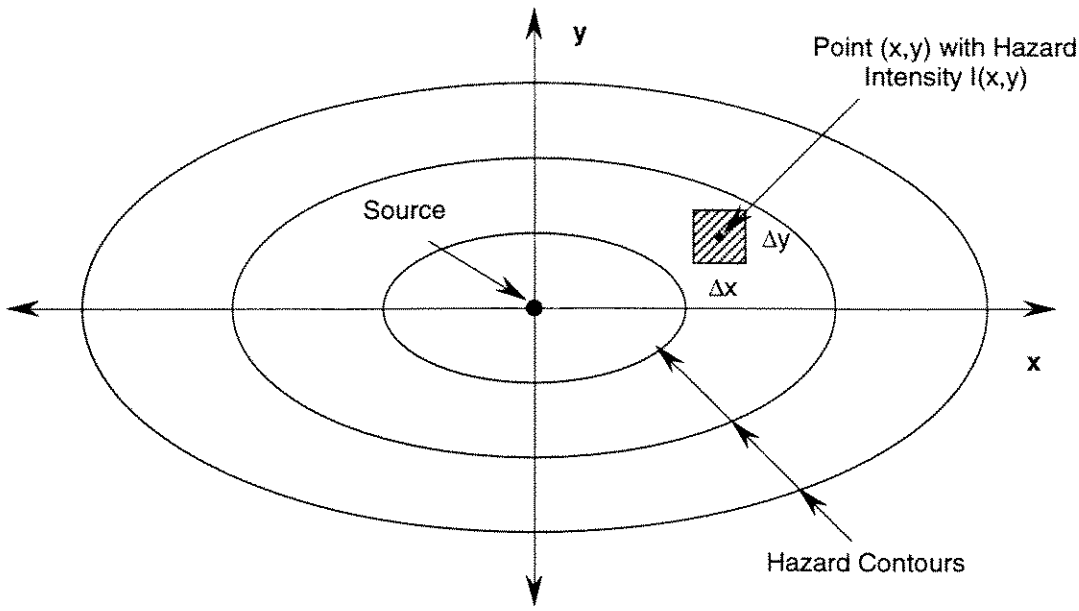

a) Hazard contours

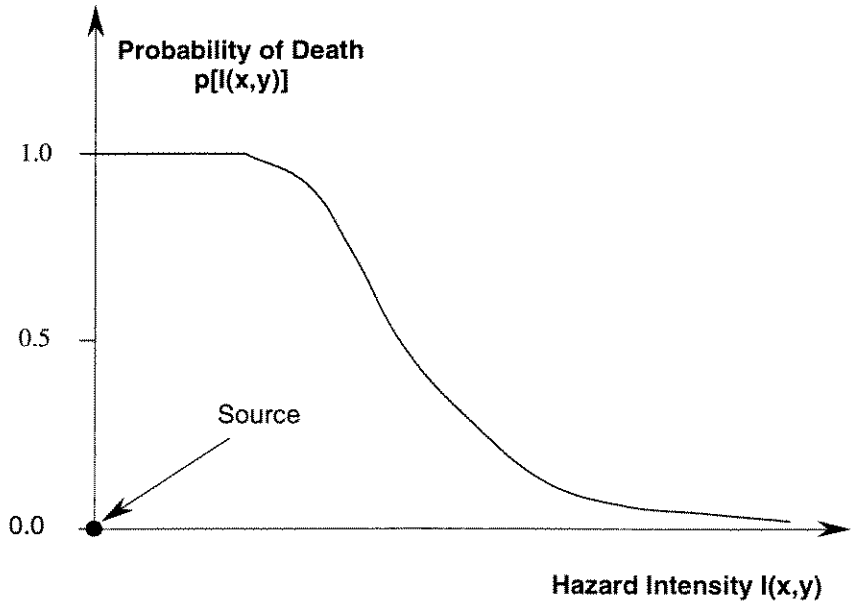

b) Probability of death as a function of hazard intensity

Figure 8.3 Illustration of the calculation of the Number of Fatalities

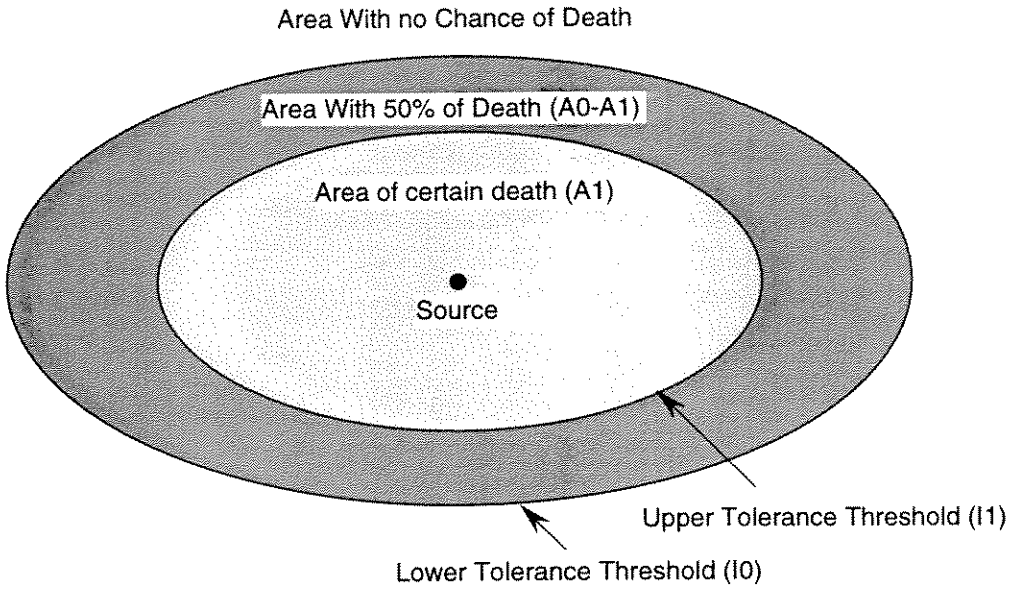

Figure 8.4 Area model used in calculating the Number of Fatalities

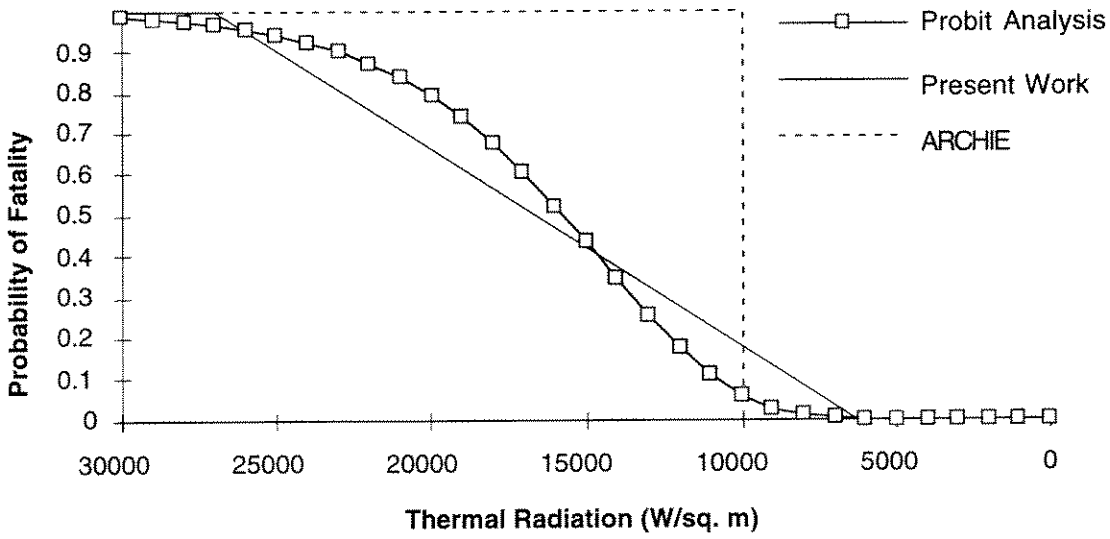

Figure 8.5 Illustration of different methods for calculating the probability of death as a function of the hazard intensity

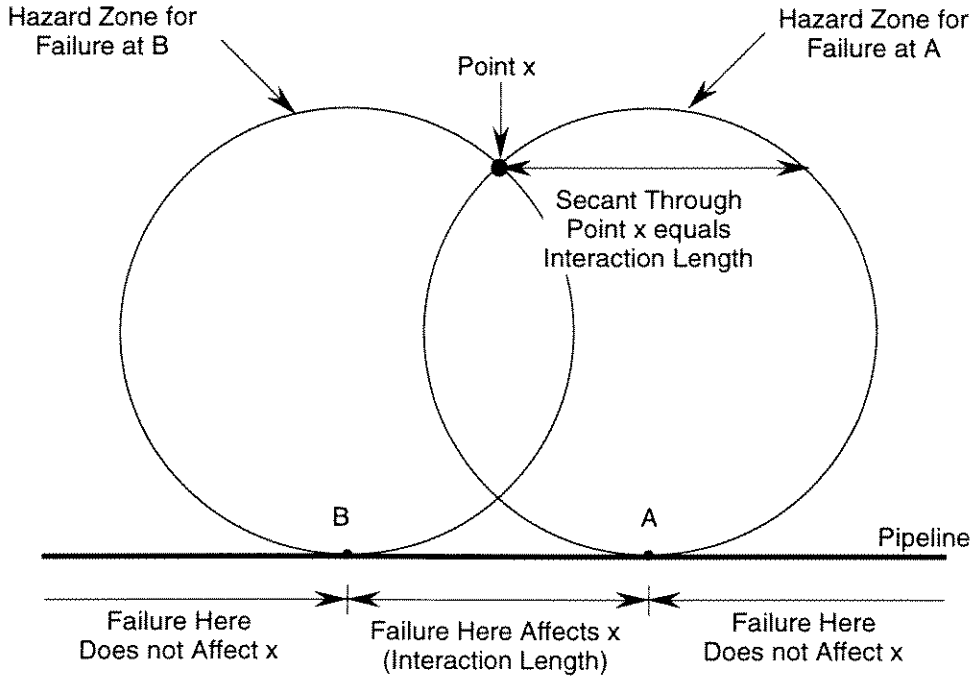

Figure 8.6 Illustration of the calculation of interaction length

Acute Hazard	Exposure	Parameter	Units	Lower Bound Tolerance Threshold	Upper Bound Tolerance Threshold
jet / pool fire	on deck	heat Intensity	kW/m^2	6.3	37.5
jet / pool fire	below deck	heat Intensity	kW/m^2	15.7	37.5
asphyxiating vapour cloud	on or below deck	volume concentration	ratio	0.306	0.713
vapour cloud fire	on deck	fraction of C_{LFL} (1)		0.5	1.0
vapour cloud fire	below deck	fraction of C_{LFL} (1)		N/A	N/A
vapour cloud explosion	on or below deck	blast pressure	kPa	15.9	69.0

(1) Lower flammability limit of product

Table 8.1 Lower and upper bound fatality thresholds for acute release hazards

Platforms	People Per Structure
Major manned	50
Minor manned	5.0
Major unmanned	0.5
Minor unmanned	0.05

Vessel Traffic Zones	People Per km^2
High density	10
Medium density	1.0
Low density	0.1
No significant traffic	0.0

Table 8.2 Representative population density estimates for platforms and vessel traffic zones

Average Daily Hours of Exposure	Working Environment	
	Platforms	Vessels
On Deck	12	12
Below Deck	12	12

Table 8.3 Number of hours of exposure by working environment classification

9.0 SPILL CHARACTERISTICS

9.1 Overview

The Spill Characteristics node group (group 7) is shown in a highlighted version of the compound node influence diagram in Figure 9.1. This node group involves parameters that are associated with released product volumes that constitute a persistent liquid spill and the potential long-term impact on human health and the environment of that portion of the liquid spill volume reaching the shoreline that is not recovered or treated during initial clean-up operations. The individual parameters associated with the Spill Characteristics node group, as identified by the shaded nodes in a highlighted version of the basic node influence diagram shown in Figure 9.2, are discussed in the following sections.

9.2 Spill Volume

The Spill Volume node (basic node 7.1) and its direct predecessor nodes are shown in a highlighted version of the basic node influence diagram in Figure 9.2. The Spill Volume node parameter, V_S, is the total volume of Low Vapour Pressure (LVP) liquid product released at the time of line failure. The predecessor node arrows indicate that Spill Volume is a functional node. The node parameter is therefore calculated directly from the value of the parameters associated with its direct predecessor nodes which include Product and Release Volume.

The total spill volume is given by the equation

$$V_S = \beta_S V_R \qquad [9.1]$$

where V_R is the total release volume and β_S is a product state factor which is equal to zero, if the product is a natural gas consisting of essentially 100% methane or a High Vapour Pressure (HVP) volatile liquid product that will rapidly boil off upon release (*e.g.*, ethanes, propanes and butanes), or 1 if it is an LVP non-volatile liquid product that will remain in the environment as liquid for a significant period of time following release (*e.g.*, condensate (or pentanes plus), gasolines, kerosenes, gas oils, and crude oils). The parameter V_R is calculated at the Release Volume node and the product state factor (β_S) is calculated directly from the physical properties associated with the product in question.

Note that for the special case of natural gas products containing a finite condensate fraction, the parameter β_S is set equal to the condensate-to-gas ratio (see the corresponding product attribute in Table 4.8). This implies that for products consisting of a gas/condensate mixture, offshore fatality and property damage estimates will be based on the hazards associated with the gas fraction (*i.e.*, methane) whereas spill characteristics and the associated costs and environmental impact will be assessed for the condensate fraction only.

9.3 Impact Location

The Impact Location node (basic node 7.2) and its direct predecessor nodes are shown in a highlighted version of the basic node influence diagram in Figure 9.2. The specific node parameter is I_L, the array of spill impact probabilities, conditional upon product release, associated with all coastal resources (*i.e.*, distinct shorelines and associated environmental resources) that could be affected by spills from the pipeline in question within the time period of interest. The predecessor node arrows indicate that Impact Location is a conditional node meaning that the value of the node parameter is conditionally dependent upon the values of its direct predecessor nodes which are Season and Failure Section. The Impact Location node parameter array must therefore be defined explicitly for both summer and winter seasons, and for each pipeline attribute defined at the Failure Section node that is considered to have a significant effect on the coastal resource impact probability.

It is assumed that the required coastal resource impact probabilities for a given pipeline segment can be obtained from the results of spill trajectory modeling. The required trajectory modeling consists of an analysis of the likely paths or trajectories of hypothetical spills, released or launched from within the specific region traversed by the chosen pipeline segment, and acted upon by the time and the spacially varying wind and ocean current fields which are assumed to drive spill movement. By considering a sufficiently large number of hypothetical spills, launched within a specific region at randomly chosen times, and acted upon by randomly sampled wind and current fields, the trajectory analysis results will approximate the statistical behaviour of spills integrated over all possible combinations of release times, winds and currents (Smith *et al.* 1982).

In the context of this project, it is assumed that based on spill trajectory analysis performed elsewhere, the node parameter can be defined for each season and distinct spill trajectory launch zone by an array of discrete conditional impact probabilities, the probability array being associated with a user defined set of susceptible coastal resources and a single 'no impact' condition which accounts for spills which do not impact any of the identified susceptible coastal resources within the time period of interest. (Note that typical time periods of interest are in the range of 30 to 60 days, depending on the spill product and spill location. It is usually assumed that beyond this time frame a spill will have decayed to the point where resource damage resulting from impact is negligible.)

Each value in the impact location probability array so developed must fall between zero and 1 with values near zero implying a very low probability of spill impact within the time period of interest, and values near 1.0 suggesting that, given product release, the spill is very likely to impact the corresponding resource within the time period of interest. In addition, to simplify interpretation of influence diagram calculation results, which depend upon the conditional impact probability estimates obtained from spill trajectory analysis, it is further assumed that the sum of all values in the probability array for a given season and launch zone must be equal to 1 (*i.e.*, the value of the 'no impact' condition is set equal to 1 minus the sum of the coastal resource impact probabilities). This implies that the trajectory model employed to develop the impact probability

array must terminate each hypothetical spill simulation when a coastal resource is first contacted. This corresponds to idealizing each spill as a point damage source which, upon contact with a particular coastal resource, concentrates all of its damage potential at that particular resource. While this ignores the potential for a spill of finite size to impact more than one coastal resource, the probabilistic nature of the final spill trajectory analysis results implicitly acknowledge the potential for multiple resource impacts.

9.4 Impact Time

The Impact Time node (basic node 7.3) and its direct predecessor nodes are shown in a highlighted version of the basic node influence diagram in Figure 9.2. The specific node parameter is t_I, the time from spill product release to impact with a given coastal resource, given that impact is assumed to occur. The predecessor node arrows indicate that Impact Time is a conditional node meaning that the value of the node parameter is conditionally dependent upon the values of its direct predecessor nodes which include Season, Failure Section and Impact Location.

Given the approach adopted for the modeling of potential spill movement and subsequent impact (see Section 9.3) the Impact Time node parameter must be defined explicitly for each user defined spill impact location as a function of season and spill launch zone (as defined at the Failure Section node). In the context of this project, given that impact time is conditional upon impact location and its associated impact probability, the node parameter must be defined for each combination by specifying a continuous probability distribution for the expected time to impact (t_I) given that impact is assumed to occur.

A probability distribution for the time to impact, conditional upon eventual coastal resource impact, can be developed for each coastal resource, season and launch zone, from the results obtained from spill trajectory modeling (see Section 9.3). The usual output generated by spill trajectory analysis includes estimates of the probabilities of resource impact given release within predefined reference impact times. (Note, typical reference impact times are 1 day, 3 days, 10 days, 30 days, and possibly 60 days.) Dividing the total impact probability estimates for each reference impact time by the total impact probability at the time corresponding to the maximum time of interest (typically 30 or 60 days) produces the required set of conditional impact probabilities (*i.e.*, the probabilities of impact within 't' days, given that impact is assumed to occur at or prior to the maximum time of interest), from which a probabilistic characterization of the conditional time to impact can be developed using standard statistical analysis techniques.

Spill Characteristics

9.5 Offshore Clean-up Efficiency

9.5.1 Node Parameter

The Offshore Clean-up Efficiency node (basic node 7.4) and its direct predecessor nodes are shown in a highlighted version of the basic node influence diagram in Figure 9.2. The specific node parameter is E_{off}, the efficiency of initial offshore clean-up operations. In the context of this project, the initial efficiency is defined as the clean-up efficiency associated with the days immediately following spill occurrence, before slick spreading and weathering begin to significantly undermine clean-up operations. The predecessor node arrows indicate that Offshore Clean-up Efficiency is a conditional node meaning that the value of the node parameter is conditionally dependent upon the values of its direct predecessor nodes which include Product and Sea State. The Clean-Up Efficiency node parameter must therefore be defined explicitly for all specified product types and for each of the four sea state categories (see Section 4.3).

In the context of this project the node parameter is defined for each product and sea state combination by specifying a continuous probability distribution for the initial clean-up efficiency (E_{off}) that can take any value between zero and 1. Efficiency values near zero are interpreted to mean that very little of the spilled product can be recovered or treated by offshore clean-up activities. Clean-up efficiency values near 1.0 are interpreted to mean that almost all of oil initially encountered by spill recovery equipment can be recovered from the sea surface, or where the use of dispersant agents is both appropriate and permitted, it means that almost all of the encountered oil can be dispersed into the water column, thereby neutralizing the damage potential of the spill product.

9.5.2 Offshore Clean-up Efficiency Estimates

The development of a comprehensive set of offshore clean-up efficiency estimates for all product types and sea state categories was beyond the scope of this project. However, based on the reported effectiveness of mechanical clean-up equipment (*i.e.,* containment booms and skimmers) on selected oil spills in various sea states, Poley (1981) developed an empirical model for oil recovery effectiveness as a function of sea state. The model is summarized in Table 9.1

The combined boom-skimmer recovery effectiveness values given in Table 9.1 are intended to reflect the percentage of oil encountered by the boom-skimmer array that is removed from the sea surface. Poley further suggests that the effectiveness estimates apply on "good" clean-up days and do not reflect factors that will reduce effectiveness such as reduced vessel and equipment handling capacity, equipment malfunction, *etc.* Based on the tabulated estimates, and introducing a subjective effectiveness reduction factor of 0.80 to account for factors besides sea state that can reduce clean-up efficiency, adjusted initial clean-up efficiency estimates (rounded to the nearest 10%) are as follows: 80%, 40%, 10% and 0% for sea states 0 - 1, 2, 3, and 4+, respectively.

Spill Characteristics

In the absence of specific information on offshore clean-up efficiency for different product types it is suggested that the above adjusted efficiency estimates be applied to all persistent liquid spill products. Finally, to acknowledge the uncertainty associated with offshore spill clean-up activities, it is suggested that the efficiency estimates be characterized by a Normal probability distribution type with a mean value equal to the reference efficiencies tabulated above and a standard deviation equal to one-quarter of the mean value (*i.e.*, assume a coefficient of variation of 25% on all efficiency estimates). The offshore spill clean-up efficiency characterization developed above is summarized in Table 9.2.

9.6 Impact Volume

9.6.1 Node Parameter

9.6.1.1 Introduction

The Impact Volume node (basic node 7.5) and its direct predecessor nodes are shown in a highlighted version of the basic node influence diagram in Figure 9.2. The specific node parameter, V_I, is the volume of persistent liquid spill product that impacts coastal resources (*i.e.*, distinct shorelines and associated environmental resources). The predecessor node arrows indicate that Impact Volume is a functional node meaning that the value of the node parameter is calculated directly from the value of the parameters associated with its direct predecessor nodes: Spill Volume, Season, Sea State, Product, Impact Time, and Offshore Clean-up Efficiency.

Specifically, the models employed to estimate impact volume assume that the spill volume reaching the coastline depends primarily on the efficiency of offshore spill clean-up operations and the weathering characteristics of the spill product. Both of these factors are influenced by the physical properties of the spill product and prevailing weather and sea conditions. In addition, the amount of product effectively eliminated from the initial spill volume by offshore clean-up and weathering action will depend upon the amount of time that elapses between spill inception and shoreline impact.

An estimate of impact volume therefore requires the characterization of offshore clean-up operations and spill weathering. Given that the amount of spill product that can be recovered depends on the rate at which the spill product spreads and decays, the two models are interrelated. In the context of this project the following models have been developed to estimate the effectiveness of offshore clean-up operations and the spill volume reduction associated with the weathering process.

Spill Characteristics

9.6.1.2 Characterization of Offshore Clean-up

The effectiveness of offshore spill clean-up operations is heavily influenced by the time required to mobilize appropriate clean-up equipment, and both the amount and efficiency of the equipment delivered to the site. The equipment efficiency will in turn be highly dependent on the product type, its weathered state at the time of encounter, and the prevailing sea state conditions. To restrict the number of uncertain parameters associated with offshore spill clean-up estimation to a manageable size, some basic modeling assumptions were made. Firstly, in estimating offshore clean-up effectiveness it is assumed that mechanical spill clean-up equipment (*e.g.*, booms, skimmers and required support equipment) will be on location at the spill site 24 hours after spill occurrence. Secondly, based on work by Schulze (1994) it is assumed that the intent of emergency spill response requirements, in effect at the time of spill occurrence, will essentially be met by providing clean-up equipment in sufficient quantity and of sufficient capacity to allow one-half of the spill area to be swept-out in the first full day of clean-up operations. (Note that product recovery from the swept-out area will depend on the efficiency of the equipment which in turn is assumed to depend on the prevailing sea state conditions.) Thirdly, it is assumed that ongoing clean-up operations will proceed with the equipment initially mobilized, such that the area swept-out by the available equipment will remain essentially constant each day. Given that the slick formed by a spill will continue to spread and break-up with time, it follows that the relative slick area encounter fraction will decrease as the slick grows larger from initially one-half of the slick area on the first clean-up day (day two relative to spill inception) to progressively lower area fractions which are inversely proportional to the effective slick area.

Ignoring spill volume loss associated with weathering, the effect on spill volume of the above assumptions can be represented by the following equation

$$f_{VR} = \frac{E_{off}}{2} \sum_{x=2}^{t} \left(\frac{1}{x-1} \right)^{a} \quad ; \qquad [9.2]$$

where f_{VR} is the volume fraction recovered by clean-up, E_{off} is the initial offshore clean-up efficiency (see Section 9.5), a is a spill encounter fraction decay exponent, and t is the time period of interest measured from the time of spill inception.

Based on statistical analysis of offshore oil spill data by Ford (1985), the average oil slick was found to grow in area at a rate that varies exponentially with time. The mean value of the area growth rate exponent was calculated by Ford to be 1.31. Since the spill encounter fraction is assumed to be inversely proportional to the slick growth rate, the exponent value of 1.31 has been incorporated into the clean-up model developed herein as a representative value for the spill encounter fraction decay exponent (a).

Spill Characteristics

9.6.1.3 Characterization of Spill Weathering

Hydrocarbon liquid products released at sea undergo physical and chemical changes collectively referred to as weathering that alter the composition and effective volume of product remaining on the sea surface. The volume remaining on the surface at any given time depends on the balance between weathering processes that reduce volume (*e.g.*, the evaporation of volatile fractions into the atmosphere, and the natural dispersion of droplets and/or dissolution of water soluble fractions into the water column), and those that promote persistence (*e.g.*, the formation of water-in-oil emulsions which resist decay). These weathering processes are highly dependent on product composition, air temperature and sea conditions.

The combined weathering process is difficult to characterize with simple models due to the many interdependent factors at play. In general, however, the lower the specific gravity of the initial spill product (*i.e.*, the lighter the product), the less persistent it will be. In addition, since most hydrocarbon products are mixtures of relatively light, volatile components and heavier, less volatile components, the lighter fractions are generally lost first leaving the progressively more persistent residual compounds behind. This type of behaviour justifies the application of the principal of half-life to the weathering of hydrocarbon spill products (Dicks 1992, ITOPF 1986) wherein half-life is taken to mean the amount of time required for half of the spill product to be removed from the sea surface by the sum of the active weathering processes. The half-life concept, when applied to oil spills, provides an estimate of the volume fraction, f_V, remaining at time t given by

$$f_V = (0.5)^{t/t_{half}} = (1-D)^t; \qquad [9.3]$$

where t_{half} is the product half-life, and D is the corresponding equivalent volume decay rate factor which, upon rearranging Equation [9.3] and solving for D, is given by

$$D = 1 - 10^{\left(-.301/t_{half}\right)}; \qquad [9.4]$$

To allow for the slowing effect of other weathering factors such as emulsification on the volume decay rate, a secondary decay rate can be introduced which can be assumed to takes effect after a decay rate transition time t_{trans}. This assumption results in a combined volume fraction estimation equation of the form

$$f_V = \left(1-D_i\right)^t \qquad \text{for } t \le t_{trans}; \text{ and} \qquad [9.5a]$$

$$f_V = \left(1-D_i\right)^{t_{trans}}\left(1-D_f\right)^{t-t_{trans}} \qquad \text{for } t > t_{trans}. \qquad [9.5b]$$

where D_i is the initial volume decay rate, prior to transition time t_{trans}, and D_f if the final decay rate following the transition time.

Spill Characteristics

It is assumed that the form of Equation [9.5] is sufficiently flexible to enable the selection of decay rate parameters that will approximate the volume decay results of many of the more sophisticated spill volume decay rate expressions available in the literature (*e.g.*, MMS 1992).

9.6.1.4 Impact Volume Model

Based on the above spill clean-up and decay characterization models, the total spill impact volume at time t_I is given by:

for $t_I \leq 1$ (*i.e.*, prior to the start of clean-up operations)

if $t_I \leq t_{trans}$ then

$$V_I = V_s\left(1-D_i\right)^{t_I}; \qquad [9.6a]$$

if $t_I > t_{trans}$ then

$$V_I = V_s\left[\left(1-D_i\right)^{t_{trans}}\left(1-D_f\right)^{\left(t_I-t_{trans}\right)}\right]; \qquad [9.6b]$$

for $t_I > 1$ (*i.e.*, after the start of clean-up operations)

if $t_I \leq t_{trans}$ then

$$V_c = V_s\left[1-\frac{E_{off}}{2}\sum_{x=2}^{t_I}\left(\frac{1}{x-1}\right)^a\right]\left(1-D_i\right)^{(t_I)}; \qquad [9.7a]$$

if $t_I > t_{trans}$ then

$$V_c = V_s\left[1-\frac{E_{off}}{2}\sum_{x=2}^{t_I}\left(\frac{1}{x-1}\right)^a\right]\left(1-D_i\right)^{t_{trans}}\left(1-D_f\right)^{\left(t_I-t_{trans}\right)}. \qquad [9.7b]$$

In the above equations V_s is the spill volume (see Section 9.2), E_{off} is the initial offshore clean-up efficiency (see Section 9.5), t_I is the time to spill impact with the shoreline (see Section 9.4), a is the spill encounter fraction decay exponent (see Section 9.6.1.2), and D_i , D_f, and t_{trans} are respectively the initial and final spill volume decay rates and the spill age corresponding to the transition from the initial to the final rate of volume decay (see Sections 9.6.1.3, and 9.6.2).

Spill Characteristics

9.6.2 Spill Volume Decay Parameter Estimates

Based on a spill volume decay model developed by the International Tanker Owners Pollution Federation (ITOPF 1986, Dicks 1992) hydrocarbon liquid spills can be divided into four broad product classes, each associated with a representative half-life range. The product classes and corresponding half-lives are:

- ***Group 1*** (light refined products, *e.g.* gasoline) specific gravity < 0.8, °API > 45
  - half-lives typically 6 to 12 hours;
- ***Group 2*** (light crude oils and fuel oils) specific gravity 0.8 to 0.85, °API 35 to 45
  - half-lives typically 24 to 72 hours;
- ***Group 3*** (medium crude oils and fuel oils) specific gravity 0.85 to 0.95, °API 17.5 to 35
  - half-lives typically about 4 days; and
- ***Group 4*** (heavy crude oils and fuel oils) specific gravity > 0.95, °API < 17.5
  - half-lives greater than 6 days
    (assume typically about 8 days).

In the absence of recognized spill volume decay parameter estimates as a function of product type, air temperature, and wind speed/sea state, the above product group half-lives can be taken as the basis for representative decay parameter estimates for all seasons and sea states. These half-life estimates can be converted to initial spill volume decay rates using Equation [9.4], and to conservatively allow for potentially significant reductions in the rate of decay caused by, for example product emulsification, it is suggested that representative final decay rate values can be taken as one-third of the initial decay rate estimates. In addition, for all product groups it can further be assumed that the transition between initial and final decay rates corresponds to the time associated with 50% volume remaining. The resulting spill volume decay parameter estimates (D_i, D_f, and t_{trans}) are summarized in Table 9.3. (Note, that the tabulated values are based on initial decay rate estimates which have been rounded to the nearest 2.5%).

9.7 Onshore Clean-up Efficiency

9.7.1 Node Parameter

The Onshore Clean-up Efficiency node (basic node 7.6) and its direct predecessor nodes are shown in a highlighted version of the basic node influence diagram in Figure 9.2. The specific node parameter is E_{on}, the efficiency of initial onshore clean-up and basic site reclamation activities. The predecessor node arrows indicate that Onshore Clean-up Efficiency is a conditional node meaning that the value of the node parameter is conditionally dependent upon the values of its direct predecessor nodes which are Impact Location and Product. The Onshore Clean-Up Efficiency node parameter must therefore be defined explicitly for all specified products and potential shoreline impact locations.

Spill Characteristics

The shoreline types chosen to delineate significant changes in the clean-up potential associated with possible spill impact locations correspond to the set of 12 shoreline types identified as a basis for ranking the environmental sensitivity of coastal resources to oil spill damage (see Section 9.9). The reference shoreline types are: Exposed Rocky Headlands, Wave-cut Platforms / Erosional Scarps, Exposed Sand Beaches, Sheltered Sand Beaches, Tidal Flats (low biomass), Sand and Gravel/Shell Beaches, Gravel Beaches, Exposed Tidal Flats (high biomass), Sheltered Rocky Areas, Sheltered Tidal Flats, Salt Marshes, and Mangrove Coasts.

In the context of this project the node parameter is defined for each product and shoreline type by specifying a continuous probability distribution for the initial clean-up efficiency (E_{on}) that can take any value between zero and 1. Efficiency values near zero are interpreted to mean either, that very little of the spilled product impacting the shoreline can be recovered using available onshore clean-up techniques, or that clean-up activities will likely do more harm than good and clean-up is therefore not undertaken (or its extent is very limited). Clean-up efficiency values near 1.0 are interpreted to mean that almost all of oil impacting the shoreline can be recovered using available technologies.

It is emphasized that the clean-up efficiency values defined at this node are intended to reflect the product recovery and/or removal potential associated with the various techniques currently available for spill containment and clean-up and for basic site reclamation operations that can be carried out in the near term. The type of operations considered in the development of the efficiency estimates include, for example: the use of absorbent pads and booms; skimming and vacuuming operations, pressure washing; and the excavation and disposal of contaminated shoreline material.

Onshore clean-up efficiency estimates are not intended to reflect the product recovery and removal potential associated with long-term shoreline remediation measures. It is assumed that the extent to which shoreline remediation techniques are employed to further reduce the residual volume of spilled product will depend on shoreline attributes that reflect the potential impact of hazardous liquid spills on long-term human health and the surrounding environment. These issues are implicitly addressed in the calculation of the parameters associated with the Equivalent Volume node (see Section 9.9) and the Value node (see Section 13.0).

9.7.2 Onshore Clean-up Efficiency Estimates

The development of a comprehensive set of deterministic onshore clean-up efficiency estimates for all shoreline and product types was beyond the scope of this project. In general, however, the literature suggests that for almost all shoreline types techniques are available that can remove substantial portions of product that comes ashore. In addition, it is usually assumed that sand beach shorelines types are generally easier to clean, and recovery efficiencies are higher, than for damage sensitive shoreline types such as sheltered rocky areas, marshes and mangroves. Finally, it is typically assumed that natural processes (*e.g.*, wave action) will remove oil impacting

exposed rocky headlands and wave-cut platforms and that these shoreline types are therefore often better left to clean themselves.

Based on the above considerations, and in the absence of specific clean-up efficiency estimates for specific products as a function of shoreline type, a reference onshore clean-up efficiency estimate of 0.5 is suggested for shoreline types of intermediate damage sensitivity and cleanability (*e.g.*, gravel and/or shell beaches and exposed tidal flats). For less sensitive, potentially easier to clean shoreline types (*e.g.*, sand beaches) a clean-up efficiency estimate of 0.67 is suggested, and for more difficult to clean, damage sensitive shorelines (*e.g.*, sheltered rocky areas and tidal flat, marshes and mangroves) a clean-up efficiency of 0.33 is suggested. For exposed rocky headlands and wave-cut platforms an efficiency estimate of zero is suggested given the clean-up potential associated with natural processes. Finally, to acknowledge the uncertainty associated with onshore spill clean-up activities, it is suggested that the efficiency estimates be characterized by a Normal probability distribution type with a mean value equal to the above reference efficiencies and a standard deviation equal to one-quarter of the mean value (*i.e.*, assume a coefficient of variation of 25% on all efficiency estimates). The onshore spill clean-up efficiency characterization developed above is summarized in Table 9.4.

9.8 Residual Volume

The Residual Volume node (basic node 7.7) and its direct predecessor nodes are shown in a highlighted version of the basic node influence diagram in Figure 9.2. The specific node parameter, V_{res}, is the volume of persistent liquid spill product remaining after onshore spill clean-up and basic shoreline reclamation operations have been undertaken The predecessor node arrows indicate that Residual Volume is a functional node meaning that the node parameter is calculated directly from the value of the parameters associated with its direct predecessor nodes; Impact Volume and Onshore Clean-up Efficiency.

The residual spill volume is given by the equation

$$V_{res} = V_I \left(1 - E_{on}\right) \qquad [9.8]$$

where V_I is the shoreline impact volume (see Section 9.6), and E_{on} is the efficiency of onshore spill clean-up operations (see Section 9.7).

As noted previously, the onshore clean-up efficiency factor represents the effectiveness of techniques that are currently available for onshore spill clean-up and basic shoreline reclamation. It does not reflect the further reduction in residual spill volume that is associated with possible long-term site remediation measures. The Residual Volume node parameter, as calculated, therefore represents an upper bound estimate (with uncertainty) of the portion of the total spill volume impacting the shoreline that will have the potential to adversely impact long-term human health and the environment.

Spill Characteristics

9.9 Equivalent Volume

9.9.1 Node Parameter

The Equivalent Volume node (basic node 7.8) and its direct predecessor nodes are shown in a highlighted version of the basic node influence diagram in Figure 9.2. The Equivalent Volume node parameter, *V*, is defined as the volume of *reference product*, impacting a *reference shoreline type*, which has an environmental damage potential equivalent to that of a given residual volume of a given product impacting a given shoreline. The predecessor node arrows indicate that Equivalent Volume is a functional node meaning that the specific node parameter is calculated directly from the value of the parameters associated with its direct predecessor nodes which include: Product, Season, Impact Location, and Residual Volume.

The node parameter calculation model takes the residual spill volume, V_{res}, that is calculated at the Residual Volume node and converts it into an equivalent volume of a reference product impacting a reference shoreline by taking into account: 1) the damage potential of the spilled product relative to that of the reference product; and 2) the environmental sensitivity of the shoreline impact location relative to that of the reference shoreline type. The model assumes that the reference product and reference shoreline type are defined by the decision-maker.

The concept of an equivalent spill volume is introduced as a means of normalizing the estimate of the environmental damage potential reflected by the residual spill volume node parameter, V_{res}, with respect to a common reference spill impact scenario. This approach provides the decision-maker with a consistent basis for the evaluation of environmental damage related consequences associated with pipeline failures involving different products that could occur at different locations along the length of the line thereby affecting different shoreline types.

Since implementation of the risk-based approach envisioned in this program, requires quantitative estimates of all of the consequences associated with pipeline failure, a quantitative approach to the assessment of potential environmental damage is necessary. However, the level of complexity associated with the current state of the art in quantitative environmental risk assessment as it applies to petroleum product spills, and the level of site specific information required to conduct such an analysis, suggests that a rigorous quantitative approach to the assessment of environmental damage potential is not feasible within the context of the current program. As an alternative, an approach originally developed by Gundlach and Hayes (1978) to characterize the oil spill damage vulnerability of major coastal environments has been adopted for the ranking of the environmental damage sensitivity of shoreline types. This ranking system yields an environmental sensitivity index for each coastal environment that can then be subjectively re-scaled based on expert opinion to yield quantitative estimates of relative environmental damage potential.

Spill Characteristics

9.9.2 Basis for an Equivalent Spill Volume

The residual spill volume normalizing approach that has been developed to estimate an equivalent spill volume is based on the following conceptual framework.

It is first assumed that, for a given shoreline spill impact scenario, a measure of the potential environmental damage, E, is given by

$$E = f\left(V_{res}, D_{prd}, S_{env}\right) \qquad [9.9]$$

where V_{res} is the residual spill volume, D_{prd} is a measure of the environmental damage potential of the spilled product, and S_{env} is a measure of the environmental damage sensitivity of the shoreline. Product damage potential is defined as a measure of the level of long-term hazard presented to human health and the environment by the contaminants present in the spilled product that washes ashore. The shoreline damage sensitivity is defined by the oil residence time and the potential extent of biological damage.

It is then assumed that for a given residual spill volume of a given product

$$E \propto f\left(S_{env}\right) = g\left(I_{shr}\right) \qquad [9.10]$$

where I_{shr} is a shoreline specific environmental sensitivity index and $g(\ )$ is a function that transforms the sensitivity index into a quantitative measure of the relative environmental damage potential associated with a unit volume of product impacting the shoreline.

It is also assumed that for a given spill impact location the overall environmental damage potential is directly proportional to the residual spill volume and the damage potential of the spilled product. This implies that

$$E \propto V_{res} D_{prd} \qquad [9.11]$$

Based on the stated assumptions it follows that, at a given spill impact location, the potential environmental damage is given by

$$E \propto V_{res} D_{prd} g\left(I_{shr}\right) \qquad [9.12]$$

If an equivalent spill volume, V, is defined as the volume of a reference product, with damage potential D_{prd}, spilled at a reference shoreline, with a sensitivity index I^{*}_{shr}, having the same environmental damage potential as that associated with a spill characterized by V_{res}, D_{prd} and I_{shr}, then in accordance with Equation [9.12]

Spill Characteristics

$$VD^{*}_{prd}\ g\left(I_{shr}{}^{*}\right) = V_{res} D_{prd}\, g\left(I_{shr}\right) \qquad [9.13]$$

By rearranging Equation [9.13] the equivalent spill volume is given by

$$V = V_{res} \frac{g(I_{shr})}{g(I^{*}_{shr})} \frac{D_{prd}}{D^{*}_{prd}} \qquad [9.14]$$

Because the above equation for equivalent volume involves product damage and shoreline sensitivity ratios, the product damage potential and the shoreline damage sensitivity need only be defined in relative terms.

The following sections develop the basis for the evaluation of a relative shoreline damage sensitivity index, I_{shr}, the sensitivity transformation function $g(\ )$, and a relative product damage potential D_{prd}.

9.9.3 Shoreline Sensitivity Index and Environmental Damage Potential Estimate

The shoreline sensitivity ranking approach adopted herein is based on the coastal resource environmental sensitivity ranking scheme originally developed by Gundlach and Hayes (1978) and later refined by Gundlach *et al.* (1981). The ranking scheme classifies shoreline types on a scale of 1 to 10 on the basis of their potential vulnerability to oil spill damage. The scale ranking of a given shoreline type reflects the degree of shoreline interaction with the physical processes that control oil spill deposition, the tendency for oil to persist in that environment, and the general extent of biological damage. A higher scale ranking implies a higher degree of environmental damage sensitivity. The twelve major shoreline types considered in this project, and the corresponding environmental sensitivity indices are summarized in Table 9.5.

To integrate the above shoreline sensitivity index scoring approach into a quantitative environmental consequence assessment model, a transformation function, $g(\ )$, is required to convert or re-scale the relative damage sensitivity ranking index, I_{shr}, into a quantitative measure of environmental damage potential. The development of this transformation function was considered beyond the scope of the current project. However, from the results of a similar quantitative re-scaling exercise, undertaken in the context of a parallel study of onshore pipeline systems (Stephens *et al.* 1995b), the transformation function developed on the basis of expert opinion yielded an environmental damage potential range of approximately one order of magnitude. Since this is consistent with the scale range associated with the shoreline sensitivity index it is suggested that, in the absence of the formal development of an offshore specific transformation function, the relative environmental damage potential of each shoreline type be set equal to the corresponding shoreline sensitivity index, or

$$g\left(I_{shr}\right) = I_{shr}\ . \qquad [9.15]$$

9.9.4 Product Damage Potential

In the context of a quantitative environmental risk assessment, the damage potential of a spill product should take into account both the acute toxicity and persistence of the product as it affects the long-term health of humans, marine organisms and plants, and the shorter-term mechanical injury potential which is associated with the ability of some products to coat and/or smoother flora and fauna.

With regard to product toxicity and persistence, both raw and refined petroleum products are extremely complex hydrocarbon compound mixtures that are highly variable in chemical content, even in their initial state, and once exposed to the environment their chemical content can change significantly over time due to weathering action that occurs as a result of various chemical, physical, and biological processes. In addition, the potential human health and environmental impact of many of the chemical compounds contained in typical petroleum products has yet to be studied to the point where reliable dose-response relationships are available for all relevant damage receptors. For these reasons, standardized methods for quantifying the level of toxicity hazard associated with broad classes of petroleum hydrocarbon mixtures (such as gasoline, fuel oil, diesel oil, and crude oil) are not currently available.

Similarly, the mechanical injury potential of hydrocarbon compound mixtures is highly dependent on chemical composition, weathering action, and time to shoreline impact. Standardized methods for characterizing the level of mechanical injury hazard associated with petroleum mixtures are also unavailable.

In the absence of the necessary quantitative data on the acute toxicity and mechanical injury potential of weathered petroleum product mixtures, it is suggested that the relative product damage potential, D_{prd}, be set equal for all petroleum products (including the reference product). A specific decision maker may, however, wish to develop damage profiles for specific product mixtures and use them to obtain more refined estimates of the relative damage potential associated with these products. These relative damage potential estimates can then be used in Equation [9.14], to produce to a more accurate assessment of the environmental impact of petroleum product spills.

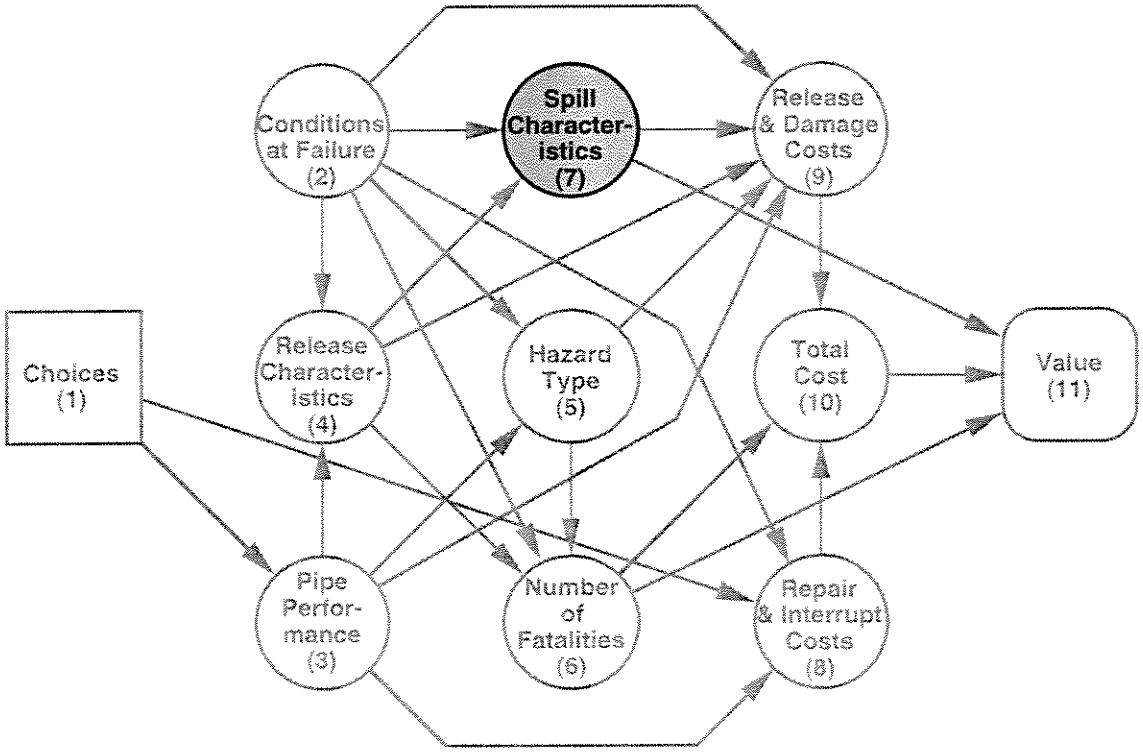

Figure 9.1 Compound node influence diagram highlighting Spill Characteristics node group

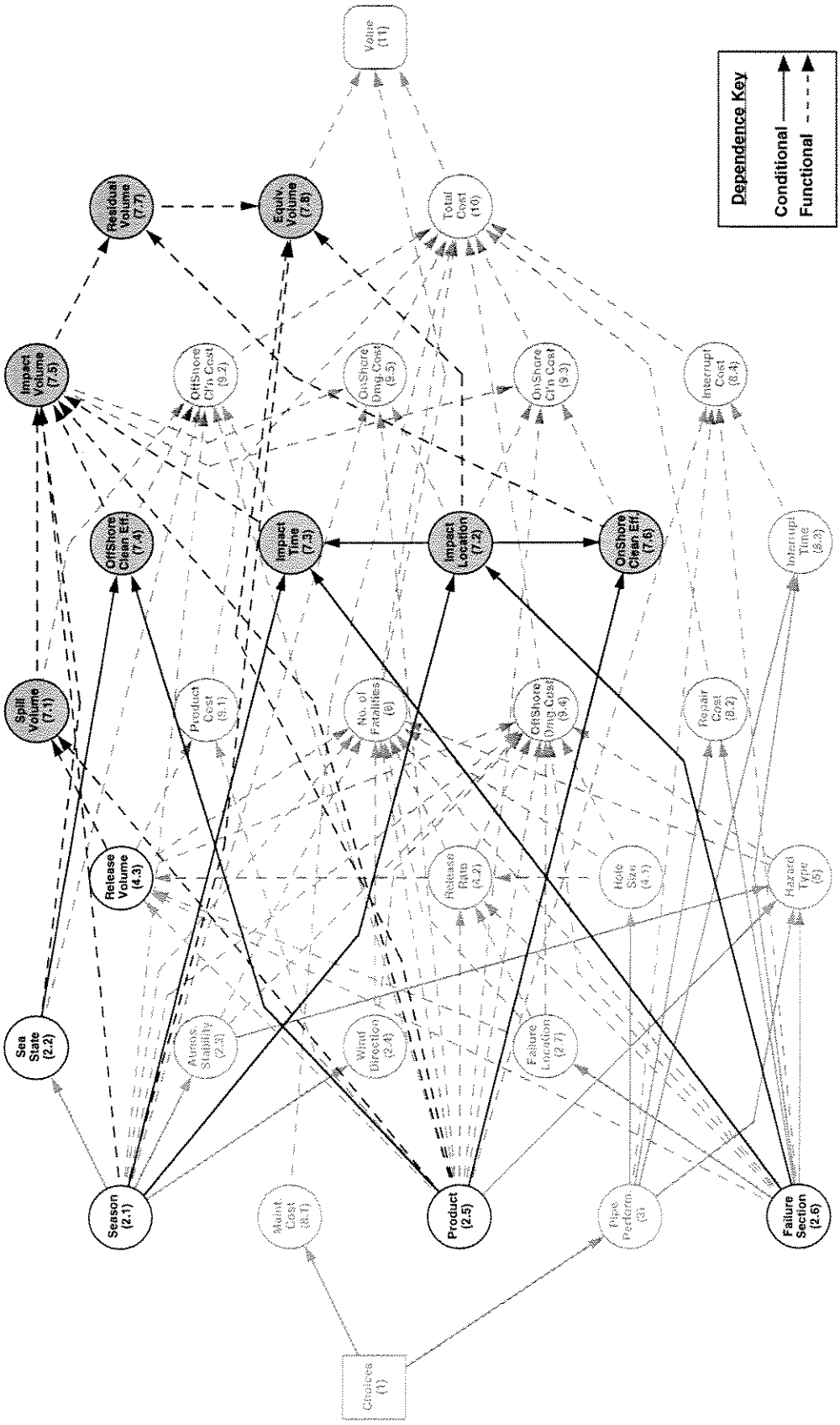

Figure 9.2 Basic node influence diagram highlighting Spill Characteristics nodes and associated immediate predecessor nodes

Sea State	Average Wind Speed	Significant Wave Height	Boom Effectiveness	Skimmer Effectiveness	Combined Effectiveness
0 - 1	0 - 4.6 m/s (0 - 9 kt)	0 - 0.46 m (0 - 1.5 ft)	100 %	100 %	100 %
2	4.6 - 7.1 m/s (9 - 14 kt)	0.46 - 1.1 m (1.5 - 3.5 ft)	67 %	67 %	45 %
3	7.1 - 8.7 m/s (14 - 17 kt)	1.1 - 1.7 m (3.5 - 5.5 ft)	33 %	33 %	11 %
4^+	> 8.7 m/s (> 17 kt)	> 1.7 m (> 5.5 ft)	0 %	0 %	0 %

Table 9.1 Estimated recovery effectiveness of boom-skimmer arrays (Poley 1981)

Sea State	Offshore Spill Clean-up Efficiency (fraction recovered or treated)
0 - 1	Normal distribution (mean = 0.8, std. dev. = 0.2)
2	Normal distribution (mean = 0.4, std. dev. = 0.1)
3	Normal distribution (mean = 0.1, std. dev. = 0.025)
4^+	0.0

Table 9.2 Representative characterization of offshore clean-up efficiency

Product Group	Initial Decay Rate D_i	Final Decay Rate D_f	Transition Time t_{trans} (days)
Group 1 (SG < 0.8, °API > 45)	0.75	0.25	0.5
Group 2 (0.8 ≤ SG ≤ 0.85, 35 < °API ≤ 45)	0.3	0.10	1.9
Group 3 (0.85 ≤ SG ≤ 0.95, 17.5 < °API ≤ 35)	0.15	0.05	4.3
Group 4 (SG > 0.95, °API < 17.5)	0.075	0.025	8.9

Table 9.3 Representative spill volume decay parameters

Shoreline Type	Onshore Spill Clean-up Efficiency (fraction removed)
Exposed rocky headlands	0.0
Wave-cut platforms	0.0
Exposed sand beaches	Normal distribution (mean = 0.67, std. dev. = 0.17)
Sheltered sand beaches	Normal distribution (mean = 0.67, std. dev. = 0.17)
Exposed tidal flats (low biomass)	Normal distribution (mean = 0.5, std. dev. = 0.125)
Sand and gravel / Shell beaches	Normal distribution (mean = 0.5, std. dev. = 0.125)
Gravel beaches	Normal distribution (mean = 0.5, std. dev. = 0.125)
Exposed tidal flats (high biomass)	Normal distribution (mean = 0.5, std. dev. = 0.125)
Sheltered rocky areas	Normal distribution (mean = 0.33, std. dev. = 0.08)
Sheltered tidal flats	Normal distribution (mean = 0.33, std. dev. = 0.08)
Salt marshes	Normal distribution (mean = 0.33, std. dev. = 0.08)
Mangrove coasts	Normal distribution (mean = 0.33, std. dev. = 0.08)

Table 9.4 Representative characterization of onshore clean-up efficiency

Shoreline Type	Coastal Resource Environmental Damage Sensitivity Index
Exposed rocky headlands	1
Wave-cut platforms / Erosional scarps	2
Exposed sand beaches	3
Sheltered sand beaches	4
Exposed tidal flats (low biomass)	5
Sand and gravel / Shell beaches	6
Gravel beaches	7
Exposed tidal flats (high biomass)	7
Sheltered rocky areas	8
Sheltered tidal flats	9
Salt marshes	10
Mangrove coasts	10

Table 9.5 Environmental damage sensitivity indices for coastal resources (adapted from Gundlach *et al.* 1981)

10.0 REPAIR AND INTERRUPTION COSTS

10.1 Overview

The Repair and Interruption Cost node group (group 8) is shown in a highlighted version of the compound node influence diagram in Figure 10.1. This node group involves parameters that represent the annual maintenance and inspection costs associated with integrity maintenance programs, the direct costs associated with pipeline repair following leak or rupture type failure, and the direct costs associated with the pipeline being out of service following failure. Because the service interruption cost is highly dependent upon the duration of the interruption period, the node group also includes a parameter that reflects service interruption time. The individual parameters associated with the Repair and Maintenance Cost node group, as identified by the shaded nodes in a highlighted version of the basic node influence diagram shown in Figure 10.2, are discussed in the following sections.

10.2 Maintenance Cost

The Maintenance Cost node (basic node 8.1) and its direct predecessor node are shown in a highlighted version of the basic node influence diagram in Figure 10.2. The specific node parameter is the annual cost of inspection and maintenance programs directed at maintaining pipeline integrity, c_{main}. The predecessor node arrow indicates that Maintenance Cost is a conditional node meaning that the value of the node parameter is conditionally dependent upon the values of its direct predecessor node which is Choices. The Maintenance Cost node parameter must therefore be defined explicitly for all inspection and maintenance options identified at the Choices node. The node parameter is defined, for each choice, by specifying a continuous probability distribution for the annual maintenance cost.

The information required to define the node parameter is highly pipeline specific. The probability distribution of annual inspection and maintenance costs for each candidate integrity maintenance program identified at the Choices node should therefore be established for a given pipeline based on operating company experience and/or budget price estimates provided by contractors that provide pipeline inspection and maintenance services.

10.3 Repair Cost

10.3.1 Node Parameter

The Repair Cost node (basic node 8.2) and its direct predecessor nodes are shown in a highlighted version of the basic node influence diagram in Figure 10.2. The specific node

parameter is the cost of repair associated with pipeline failure, c_{rpr}. The predecessor node arrows indicate that Repair Cost is a conditional node meaning that the value of the node parameter is conditionally dependent upon the values of its direct predecessor nodes which include Pipe Performance and Failure Section. The Repair Cost node parameter must therefore be defined explicitly for all possible combinations of the performance states involving failure (*i.e.*, small leak, large leak, and rupture) and for selected combinations of the pipeline system attributes associated with each section which are known to have a significant effect on repair cost. In the context of this project the node parameter is defined for each combination by specifying a continuous probability distribution for the expected repair cost that can take any value within a defined range.

With regard to the effect of performance state on repair cost, it is assumed that pipeline failure modes can be divided into two distinct categories: small leaks and large leaks or ruptures. The distinction is made on the basis that a small leak can typically be repaired using a full encirclement sleeve or repair clamp whereas a large leak or a rupture will require a more expensive cut-out type of repair.

To identify specific pipeline system attributes that have a potentially significant effect on the costs associated with pipeline repair, a literature review was carried out. Based on this review (in particular, Mohr 1992) the key system attributes identified are water depth and pipeline diameter.

In the context of this project water depth is defined by three discrete water depth ranges:

- shallow water (depths less than 10 m);
- deep water (depths between 10 and 300 m); and
- ultra-deep water (depths beyond 300 m).

The chosen depth ranges are intended to delineate significant changes in viable pipeline repair techniques, hence repair costs (since the techniques available for shallow water repairs are typically cheaper to implement than the techniques required for deep or ultra-deep water repairs). Shallow water, typically near shore, techniques (including for example the use of portable caissons) are assumed to be limited to water depths of 10 m (Å30 ft). The deep water to ultra-deep water depth transition of 300 m (Å1000 ft) was selected to correspond to the generally accepted depth limit for diver assisted repair operations (Hebert and Corder, 1995). It is assumed that pipeline repairs in water depths beyond 300 m will typically require the use of more expensive diverless repair systems such as Remote Operated Vehicles (or ROV's) and their associated support systems.

With regard to line diameter, it is assumed that larger diameter pipelines will be more expensive to repair than small diameter lines due to the need for larger equipment to handle heavier line repair components and the additional time required to manoeuvre and connect repair clamps or pipe spools. Three diameter ranges have been chosen to delineate significant repair cost increments:

Repair and Interruption Costs

- small diameter (less than 203 mm);
- medium diameter (between 203 and 406 mm); and
- large diameter (greater than 406 mm).

The performance states and the system attribute set described above define a matrix of 18 possible attribute/state combinations, each of which is potentially associated with a different repair cost. The repair cost matrix is shown in Table 10.1.

10.3.2 Repair Cost Estimates

The development of a comprehensive set of repair cost estimates for all combinations of failure modes, line diameter ranges, and water depth ranges was beyond the scope of this project. However, based on repair cost surveys compiled and summarized by Mohr (1992), small leak repairs in deep water were found to cost on average approximately $100,000 with no obvious trend in the cost data supporting an increased cost with larger line diameter (which likely reflects a lack of sufficient failure data). To account for the likely impact of water depth on repair cost, an average small leak repair cost of $50,000 is suggested for shallow water (*i.e.*, half the deep water value), and a value of $200,000 for ultra-deep water repairs (*i.e.*, twice the deep water value). For large leaks and rupture requiring cut-out repair, the historical cost data is very limited, however, repair costs on the order of $1,000,000 or more are typical. It is therefore suggested that reference large leak and rupture repair costs be set at ten times the small leak repair costs given above. Finally, to acknowledge the high degree of uncertainty associated with underwater pipeline repair costs it is suggested that the line repair cost estimates be characterized by a Normal probability distribution type with a mean value equal to the reference costs given above and a standard deviation equal to 50% of the mean value. This line repair cost characterization is summarized by the probability distributions given Table 10.1.

10.4 Interruption Time

10.4.1 Node Parameter

The Interruption Time node (basic node 8.3) and its direct predecessor nodes are shown in a highlighted version of the basic node influence diagram in Figure 10.2. The specific node parameter is the length of time during which service is interrupted in the event of pipeline failure, t_{int}. The predecessor node arrows indicate that Interruption Time is a conditional node meaning that the value of the node parameter is conditionally dependent upon the values of its direct predecessor nodes which include Pipe Performance and Failure Section. The Interruption Time node parameter must therefore be defined explicitly for all possible combinations of the pipe performance states involving failure (*i.e.*, small leak, large leak and rupture) and for selected combinations of the pipeline system attributes associated with each section which are known to have a significant effect on service interruption time. In the context of this project the node

parameter is defined for each combination by specifying a continuous probability distribution for the service interruption time that can take any value within a defined range.

It is assumed that interruption time will be proportional to the level of effort and hence proportional to the cost associated with pipeline repair. It follows then that the pipeline system attributes that affect repair cost can also be assumed to affect interruption time. The system attribute matrix developed for repair cost is therefore assumed to be directly applicable to service interruption time. The corresponding interruption time matrix is shown in Table 10.2.

It is noted that in the context of service interruption time, as opposed to repair cost, the distinction between small leaks and large leaks or ruptures is based on the assumption that small leaks will involve only partial service interruption corresponding to a pipeline pressure drop during sleeve installation, whereas large leaks and ruptures will involve complete interruption of service while the cut-out replacement is performed.

10.4.2 Interruption Time Estimates

As for repair cost, the development of a comprehensive set of interruption time estimates for all combinations of failure modes, line diameter ranges, and water depth ranges was beyond the scope of this project. However, based on repair sequence descriptions given by Mohr (1992) for various repair alternatives an average repair time of approximately 48 hours is indicated for typical repair activities. For small leaks it is therefore suggested that the average duration of service interruption associated with repair be set at 48 hours, and for large leaks and ruptures it is suggested that the average duration of service interruption time be taken as 4 days (*i.e.*, 48 hours to mobilize equipment on site and 48 hours to carry out the repair). Finally, to acknowledge the high degree of uncertainty associated with potential service interruption time it is suggested that the time estimates be characterized by a Normal probability distribution type with a mean value equal to the reference times given above and a standard deviation equal to 50% of the mean value. This interruption time characterization is summarized by the probability distributions given Table 10.2.

10.5 Interruption Cost

The Interruption Cost node (basic node 8.4) and its direct predecessor nodes are shown in a highlighted version of the basic node influence diagram in Figure 10.2. The specific node parameter is the direct cost associated with service interruption caused by pipeline failure, c_{int}. The predecessor node arrows indicate that Interruption Cost is a functional node meaning that the value of the node parameter is calculated directly from the value of the parameters associated with its direct predecessor nodes which include: Product, Failure Section, Pipe Performance and Interruption Time.

Repair and Interruption Costs

In the context of this project, it is assumed that if the volume of product delivered through a pipeline in a given month is greater than or equal to an agreed upon portion of the volume nominated or tendered by the product producer or supplier (*i.e.*, if $V_d \geq \lambda_{BAT} V_n$, where: V_d is the delivered volume, V_n is the nominated volume, and λ_{BAT} is the billing abatement threshold) then the pipeline operator will not be penalized for a delivery shortfall and the service interruption cost associated with the failure incident causing the shortfall will be zero. If, however, the delivered volume falls below the agreed upon portion of the nominated volume (*i.e.*, if $V_d < \lambda_{BAT} V_n$) then it is assumed that the operating company will be penalized such that the effective cost of service interruption associated with line failure is given by

$$c_{\text{int}} = \left(V_n - V_d\right)\ u_{trans} \qquad [10.1]$$

where u_{trans} is the unit cost to the supplier of product transportation.

The volume of product nominated or tendered by the supplier in a given month is assumed to be given by

$$V_n = \frac{\dot{m}_o}{\rho_s} t_{mth} \qquad [10.2]$$

where $\dot{m}_o$ is the product mass flow rate, ρ_s is the product density under standard conditions, and t_{mth} is the time duration of an average month.

Assuming that following line failure and subsequent repair a pipeline company will operate the line at capacity in an effort to make up for lost throughput, the volume of product delivered in a month during which line failure occurs is given by

$$V_d = V_n t_{bef}^* + V_f t_{int}^* + V_c t_{aft}^* \qquad [10.3]$$

where t_{bef} is the time prior to line failure and t_{int}^* is the duration of service interruption caused by line failure (both expressed as a fraction of the duration of an average month), and t_{aft} is the time remaining in a month following line repair which is given by

$$t_{aft}^* = 1 - t_{bef}^* - t_{int}^* . \qquad [10.4]$$

The volume of product that can be delivered in a month with the line operating at capacity, V_c, is given by

$$V_c = \frac{V_n}{f_{cap}} \qquad [10.5]$$

where f_{cap} is the volume capacity fraction, and the volume delivered in a month by the line in a 'failed' condition, V_f, is given by

$$V_f = \left(1 - r_{flow}\right) V_n ; \qquad [10.6]$$

where r_{flow} is the throughput reduction during the service interruption period caused by line failure (expressed as a fraction of the normal product flow rate).

If it is assumed that line failure is equally likely to occur at any time during a given month, it can be shown that, on average

$$t_{bef} = t_{aft} = \frac{1 - t_{int}}{2}. \qquad [10.7]$$

Substituting Equations [10.4, 10.5, 10.6, and 10.7] into Equation [10.3] gives

$$V_d = \frac{\dot{m}_o}{r_s}\left\{\left[1 + \left(1 - 2r_{flow}\right)t_{int}^*\right] + \frac{1}{f_{cap}}\left[1 - t_{int}^*\right]\right\} \qquad [10.8]$$

The service interruption cost associated with line failure can therefore be calculated using Equations [10.1, 10.2, and 10.8]. The parameters involved are largely operator and pipeline segment specific with the exception of the throughput reduction factor, r_{flow}, which can be defined in general terms as follows:

- for failures involving small leaks, which can likely be rectified using a repair sleeve, the throughput reduction during the interruption period can be assumed to be on the order of 0.2 which reflects the standard industry practice of reducing operating pressures by 20% during line repair operations; and
- for failures involving large leaks and ruptures, which will require cut-out repair, it is reasonable to assume that product flow will not be possible or will be prevented by line shut-down until repairs are made in which case the throughput reduction during the interruption period will be 1.0.

Figures and Tables

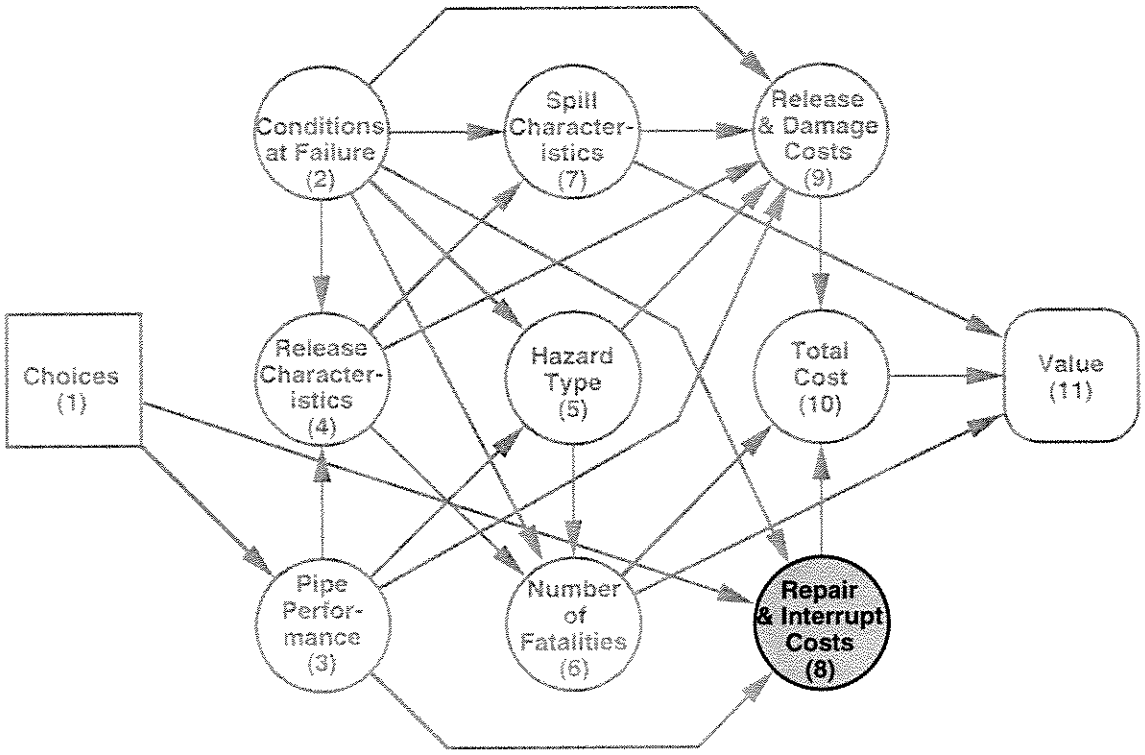

Figure 10.1 Compound node influence diagram highlighting Repair and Interrupt Costs node group

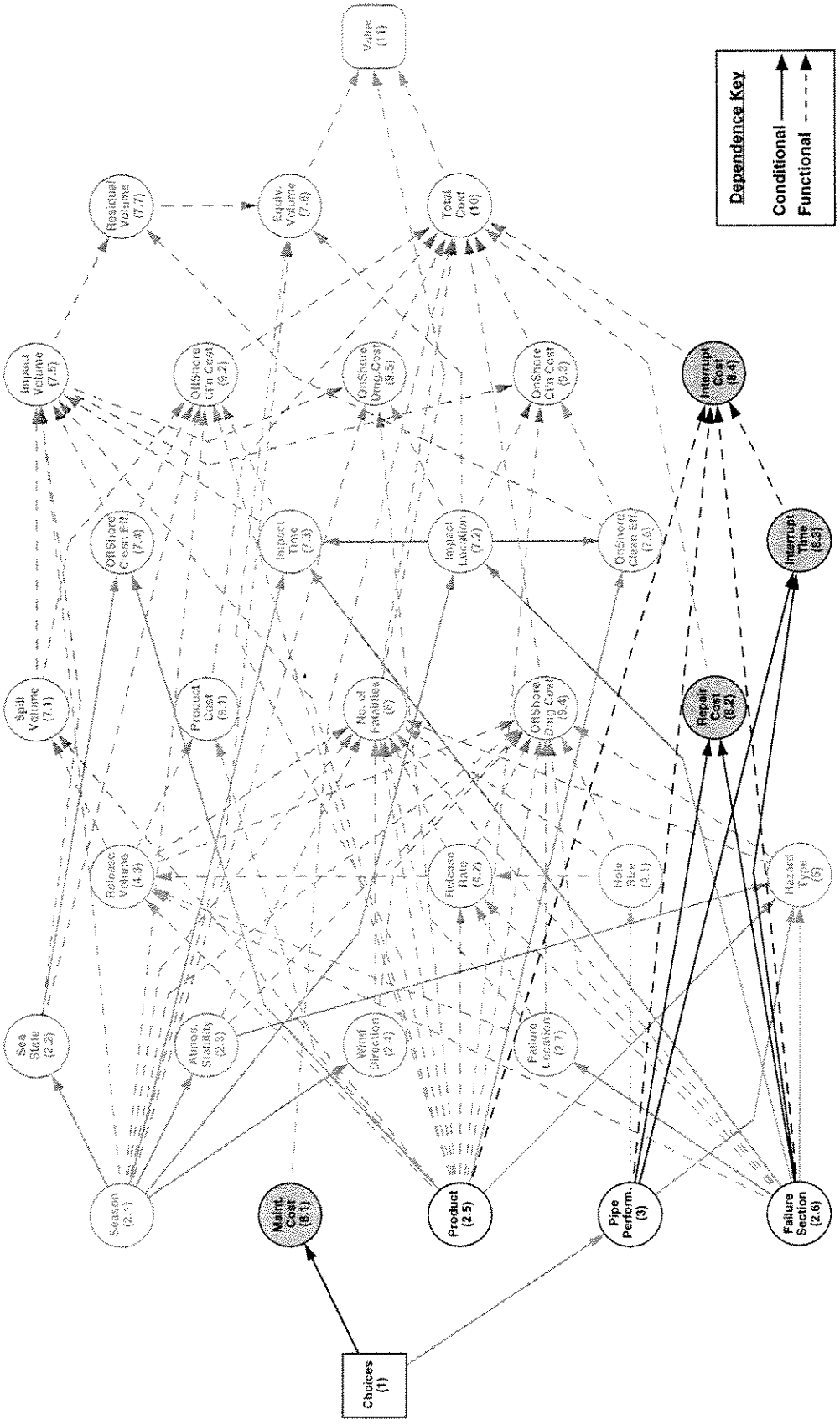

Figure 10.2 Basic node influence diagram highlighting Repair and Interrupt Costs nodes and associated immediate predecessor nodes

Water Depth Range	Pipeline Diameter Range	Repair Cost ($1000's)	
		Small Leak (*i.e.*, sleeve repair)	**Large Leak / Rupture** (*i.e.*, cut-out repair)
Shallow (less than 10 m)	small (less than 203 mm)	Normal distribution (mean = 50, std. dev = 25)	Normal distribution (mean = 500, std. dev = 250)
	medium (between 203 and 406 mm)	Normal distribution (mean = 50, std. dev = 25)	Normal distribution (mean = 500, std. dev = 250)
	large (greater than 406 mm)	Normal distribution (mean = 50, std. dev = 25)	Normal distribution (mean = 500, std. dev = 250)
Deep (between10 and 300 m)	small (less than 203 mm)	Normal distribution (mean = 100, std. dev = 50)	Normal distribution (mean = 1000, std. dev = 500)
	medium (between 203 and 406 mm)	Normal distribution (mean = 100, std. dev = 50)	Normal distribution (mean = 1000, std. dev = 500)
	large (greater than 406 mm)	Normal distribution (mean = 100, std. dev = 50)	Normal distribution (mean = 1000, std. dev = 500)
Ultra-Deep (beyond 300 m)	small (less than 203 mm)	Normal distribution (mean = 200, std. dev = 100)	Normal distribution (mean = 2000, std. dev = 1000)
	medium (between 203 and 406 mm)	Normal distribution (mean = 200, std. dev = 100)	Normal distribution (mean = 2000, std. dev = 1000)
	large (greater than 406 mm)	Normal distribution (mean = 200, std. dev = 100)	Normal distribution (mean = 2000, std. dev = 1000)

Table 10.1 Representative pipeline repair costs

Water Depth Range	Pipeline Diameter Range	Service Interruption Time (hrs)	
		Small Leak (*i.e.*, sleeve repair)	**Large Leak / Rupture** (*i.e.*, cut-out repair)
Shallow (less than 10 m)	small (less than 203 mm)	Normal distribution (mean = 48, std. dev = 24)	Normal distribution (mean = 96, std. dev = 48)
	medium (between 203 and 406 mm)	Normal distribution (mean = 48, std. dev = 24)	Normal distribution (mean = 96, std. dev = 48)
	large (greater than 406 mm)	Normal distribution (mean = 48, std. dev = 24)	Normal distribution (mean = 96, std. dev = 48)
Deep (between10 and 300 m)	small (less than 203 mm)	Normal distribution (mean = 48, std. dev = 24)	Normal distribution (mean = 96, std. dev = 48)
	medium (between 203 and 406 mm)	Normal distribution (mean = 48, std. dev = 24)	Normal distribution (mean = 96, std. dev = 48)
	large (greater than 406 mm)	Normal distribution (mean = 48, std. dev = 24)	Normal distribution (mean = 96, std. dev = 48)
Ultra-Deep (beyond 300 m)	small (less than 203 mm)	Normal distribution (mean = 48, std. dev = 24)	Normal distribution (mean = 96, std. dev = 48)
	medium (between 203 and 406 mm)	Normal distribution (mean = 48, std. dev = 24)	Normal distribution (mean = 96, std. dev = 48)
	large (greater than 406 mm)	Normal distribution (mean = 48, std. dev = 24)	Normal distribution (mean = 96, std. dev = 48)

Table 10.2 Representative duration of pipeline service interruption times

11.0 RELEASE AND DAMAGE COSTS

11.1 Overview

The Release and Damage Cost node group (group 9) is shown in a highlighted version of the compound node influence diagram in Figure 11.1. This node group involves parameters that represent the cost of lost product, liquid spill clean-up costs and the costs associated with property damage. The individual parameters associated with the Release and Damage Costs node group, as identified by the shaded nodes in a highlighted version of the basic node influence diagram shown in Figure 11.2, are discussed in the following sections.

11.2 Cost of Lost Product

11.2.1 Node Parameter

The Product Cost node (basic node 9.1) and its direct predecessor nodes are shown in a highlighted version of the basic node influence diagram in Figure 11.2. The specific node parameter is the direct cost associated with the product lost at the time of pipeline failure. The predecessor node arrows indicate that Product Cost is a functional node meaning that the value of the node parameter is calculated directly from the value of the parameters associated with its direct predecessor nodes, Product and Release Volume.

The product cost, c_{prod}, is calculated using the following equation

$$c_{prod} = u_p V_R \qquad [11.1]$$

where V_R is the total release volume and u_p is the unit product cost.

The release volume is defined at the Release Volume node leaving unit product cost (u_p) which must be defined for all products carried in the pipeline. This supplementary product data does not constitute an additional set of influence diagram parameters but rather it represents a set of deterministic data that must be available to the Product Cost node to facilitate evaluation of the node parameter.

11.2.2 Product Cost Estimates

As part of a previous related project (Stephens *et al.* 1995b) a survey of recent energy statistics was carried out to develop a representative set of unit prices for the product groups of interest.

Release and Damage Costs

Reference product cost estimates based on this information are given in Table 11.1 for each of the main product groups of interest.

11.3 Offshore Clean-up Cost

11.3.1 Node Parameter

The Offshore Clean-up Cost node (basic node 9.2) and its direct predecessor nodes are shown in a highlighted version of the basic node influence diagram in Figure 11.2. The specific node parameter is the cost of offshore spill clean-up associated with liquid product pipeline failure. The predecessor node arrows indicate that Offshore Clean-up Cost is a functional node meaning that the value of the node parameter is calculated directly from the value of the parameters associated with its direct predecessor nodes: Spill Volume, Season, Sea State, Product, Impact Time, and Offshore Clean-up Efficiency.

The total offshore spill clean-up cost, c_{offcl}, is calculated using the following equation

$$c_{offcl} = V_c u_{offcl} \qquad [11.2]$$

where u_{offcl} is the unit offshore clean-up cost (in dollars per unit of treated or recovered product) and V_c is the offshore spill volume recovered or treated. The unit offshore clean-up cost is assumed to be a deterministic function of product type and, based on the offshore spill clean-up model developed in Section 9.6, the offshore spill clean-up volume is given by the following:

for $t_I \leq 1$ (*i.e.*, prior to the start of clean-up operations)

$$V_c = 0.0; \qquad [11.3]$$

for $t_I = 2$

if $t_{trans} \geq 1$ then

$$V_c = V_s \frac{E_{off}}{2}\left(1 - D_i\right); \qquad [11.4a]$$

if $t_{trans} < 1$ then

$$V_c = V_s \frac{E_{off}}{2}\left[\left(1 - D_i\right)^{t_{trans}}\left(1 - D_f\right)^{(1-t_{trans})}\right]; \qquad [11.4b]$$

Release and Damage Costs

for $t_1 > 2$

if $t_1 \leq t_{trans} + 1$ then

$$V_c = V_s \frac{E_{off}}{2}\left[\sum_{x=2}^{t_1}\left(\frac{1}{x-1}\right)^a \left(1-D_i\right)^{(x-1)}\right]; \qquad [11.5a]$$

if $t_1 > t_{trans} + 1$ then

$$V_c = V_s \frac{E_{off}}{2}\left[\sum_{x=2}^{t_{trans}+1}\left(\frac{1}{x-1}\right)^a \left(1-D_i\right)^{x-1} + \sum_{x=t_{trans}+2}^{t_1}\left(\frac{1}{x-1}\right)^a \left(1-D_i\right)^{t_{trans}}\left(1-D_f\right)^{x-1-t_{trans}}\right] \qquad [11.5b]$$

In the above equations V_s is the spill volume (see Section 9.2), E_{off} is the initial offshore clean-up efficiency (see Section 9.5), a is the spill encounter decay exponent (see Section 9.6.1.2), and D_i, D_f, and t_{trans} are respectively the initial and final spill volume decay rates and the spill age corresponding to the transition from the initial to the final rate of volume decay (see Section 9.6.1.3).

11.3.2 Offshore Unit Clean-up Cost Estimates

The development of a comprehensive set of deterministic offshore unit clean-up costs estimates for all product types was beyond the scope of this project. However, based on a simple model developed by Holmes (1977) for the costing of oil spill clearance operations at sea, recovery costs in 1990 US dollars per unit of oil recovered or treated, are estimated to be approximately \$45/m^3 for a 50,000 m^3 spill, \$70/m^3 for a 5000 m^3 spill, and \$220/m^3 for a 500 m^3 spill. These unit cost estimates are consistent with the generic offshore unit clean-up cost estimate of approximately \$70/m^3 (in 1990 US dollars) which was incorporated into the 'Sliktrak' oil spill impact simulation model (Blaikley *et al.* 1977).

Based on the above costing information, and given that statistical analysis of pipeline oil spills in the Gulf of Mexico (MMS 1995) indicates that the median volume of significant spills (*i.e.,* spills greater than 1000 bbl) is approximately 900 m^3 (5,600 bbl), it is reasonable to assume a basic unit clean-up cost on the order of \$200/m^3 for all but the largest spills where lower unit recovery costs are indicated. Adding a 50 % surcharge to this basic unit cost estimate to cover ancillary cost components not reflected in the somewhat dated costing models sited above yields an adjusted unit clean-up cost of \$300/m^3 of oil recovered or treated. In the absence of unit recovery cost estimates for other spill products (*e.g.,* condensate and refined oil products), it is suggested that \$300/m^3 can be taken as representative unit clean-up cost for all persistent liquid spill products.

Release and Damage Costs

11.4 Onshore Clean-up Cost

11.4.1 Node Parameter

The Onshore Clean-up Cost node (basic node 9.3) and its direct predecessor nodes are shown in a highlighted version of the basic node influence diagram in Figure 11.2. The specific node parameter is the cost of spill clean-up associated with that portion of the spill that reaches the shoreline. The predecessor node arrows indicate that Onshore Clean-up Cost is a functional node meaning that the value of the node parameter is calculated directly from the value of the parameters associated with its direct predecessor nodes: Impact Volume, Impact Location, Product and Onshore Clean-up Efficiency.

The total onshore spill clean-up cost, c_{oncl}, is calculated using the following equation

$$c_{oncl} = V_I E_{on} u_{oncl} \qquad [11.6]$$

where V_I is the onshore spill impact volume (see Section 9.2), E_{on} is the onshore clean-up efficiency (see Section 9.8), and u_{oncl} is the onshore clean-up cost per unit of treated or recovered product. The unit onshore clean-up cost is assumed to be a deterministic function of shoreline type and product type.

11.4.2 Onshore Unit Clean-up Cost Estimates

The development of a comprehensive set of deterministic onshore unit clean-up costs estimates for all shoreline and product types was beyond the scope of this project. However, historical oil spill clean-up cost data summarized by Moller *et al.* (1987), suggests that unit shoreline clean-up costs can fall in the range of $600 and $6000 per cubic metre of treated or recovered oil. (A specific example of clean-up costs cited for oil recovery from sand beaches in the Arabian Gulf indicates an average unit recovery cost of approximately $1000/m^3.) This unit cost range is consistent with the generic onshore unit clean-up cost estimate of approximately $2300/m^3 (in 1990 US dollars) which was incorporated into the 'Sliktrak' oil spill impact simulation model (Blaikley *et al.* 1977).

Note that it is generally assumed that lower clean-up costs are associated with easy to clean, sand beach shorelines types and higher costs are usually associated with more difficult to clean, damage sensitive shoreline types such as sheltered rocky areas, marshes and mangroves.

Based on the above information, and in the absence of unit recovery cost estimates for specific shoreline and product types, a reference onshore spill clean-up cost of $3000 per cubic metre of recovered or treated spill product is suggested for shoreline types of intermediate damage sensitivity and cleanability (*e.g.*, gravel and/or shell beaches and exposed tidal flats). For less sensitive, potentially easier to clean shoreline types (*e.g.*, sand beaches) a clean-up cost of

$1500/m^3 is suggested (this being half of the reference cost), and for more difficult to clean, damage sensitive shorelines (*e.g.*, sheltered rocky areas and tidal flat, marshes and mangroves) a clean-up cost of $6000/m^3 is suggested (this being twice the reference cost). The onshore spill clean-up cost characterization developed above is summarized in Table 11.2.

11.5 Offshore Damage Cost

11.5.1 Introduction

The Offshore Damage Cost node (basic node 9.4) and its direct predecessor nodes are shown in a highlighted version of the basic node influence diagram in Figure 11.2. The specific node parameter is the cost of offshore property damage caused by the short term release hazards associated with product release (*i.e.*, fires and explosions). The predecessor node arrows indicate that Offshore Damage Cost is a functional node meaning that the value of the node parameter is calculated directly from the value of direct predecessor node parameters such as product type, failure location, ambient temperature and wind conditions, and release rate and release volume. The node has the same direct predecessors as the Number of Fatalities node, and uses a similar approach to calculate the node parameter. It uses release models to estimate the extent of a hazard zone, and combines this area estimate with unit costs of damaged property to calculate the total cost of damage. The methods used to calculate the cost of property damage are described in Sections 11.5.2 and 11.5.3.

11.5.2 Basic Calculation of Property Damage

For a given hazard scenario, the total property damage cost is the sum of two components: the cost of replacing or repairing damaged offshore facilities (*i.e.*, platform superstructures), and the cost of replacing or repairing damaged vessels. In both cases it is assumed that all damage is the result of an ignited product release causing a fire or explosion.

11.5.2.1 Distributed Property Damage Estimates

For distributed property (*i.e.*, for vessels operating in the vicinity of a pipeline), the damage resulting from product release is a function of the hazard type and intensity and the tolerance threshold of property to that hazard. This is directly analogous to the calculation of the number of fatalities for distributed populations (see Section 8.2.1). Based on the same set of assumptions, the total cost of offshore vessel damage, c_{vsl}, for a given hazard scenario can be calculated as follows:

$$c_{vsl} = u_{vsl} A \qquad [11.7]$$

where u_{vsl} is the vessel damage cost per unit area and A is the hazard zone area bound by the hazard intensity threshold associated with property damage. Note that in the context of this model, the unit damage cost is taken to be the average per tonne replacement cost of vessels, equipment and cargo, divided by the vessel traffic density in tonnes per unit area.

In order to implement Equation [11.7] A must be defined for different types of hazards and u_{offdmg} must be defined for each reference vessel traffic density. These parameters are addressed in Sections 11.5.3 and 11.5.4.

11.5.2.2 Concentrated Property Damage Estimates

For property concentrated at specific location (*i.e.,* for permanent offshore facilities, or platforms, located near a pipeline), the damage resulting from product release is a function of the hazard type and intensity, the distance from the property to the release source, and the hazard tolerance threshold of the property. As for distributed property, this is directly analogous to the calculation of the number of fatalities for platforms (see Section 8.2.2). Based on the same set of assumptions, the total cost of damage for a platform at offset distance x, c_{pltx}, for a given hazard scenario can be calculated as follows:

$$c_{plt_x} = Cplt_x \frac{l_x}{L} \qquad [11.8]$$

where C_{plt_x} is the cost of the platform superstructure, l_x is the interaction length for point x, and L is the length of pipeline along which an incident could occur.

To implement Equation [11.8] l_x must be defined for each hazard type and C_{plt} must be defined for each reference platform type. These parameters are addressed in Sections 11.5.3 and 11.5.4.

11.5.3 Calculation of Hazard Area and Interaction Length

The area of sea surface affected by a given hazard (A in Equation [11.7]), and the interaction length for a given hazard at offset distance x (l_x in Equation [11.8]) are calculated using the release models discussed in Appendix B. The hazards considered include thermal radiation from jet or pool fires, vapour cloud fires, and vapour cloud explosions. The hazard event tree used to determine the relative likelihood at hazard occurrence is shown in Figure 11.3. It is noted that asphyxiation which was considered a hazard to human life does not pose a risk of property damage and is therefore not considered here.

The approach used to define the extent of damage due to fires and explosions is similar to that used for calculating the number of fatalities (see Section 8.2 and Figure 8.2). Two hazard intensity thresholds are defined: an upper bound threshold defining the hazard intensity above which all property is destroyed; and a lower bound threshold below which no damage occurs.

Release and Damage Costs

Between the two thresholds the probability of damage is assumed to vary linearly between 1 and 0. Based on a similar analysis to that described in Section 8.2, it can be shown that the equivalent area A based on these assumptions is given by:

$$A = 0.5(A_1 + A_0) \qquad [11.9]$$

where A_1 is the total area within the upper bound threshold and A_0 is the total area within the lower bound threshold. Similarly, it can be shown that the equivalent interaction length is given by:

$$l_x = 0.5(l_{x0} + l_{x1}) \qquad [11.10]$$

where l_{x0} is the interaction length associated with hazard area $A_0$and l_{x1} is the interaction length associated with A_1.

The upper and lower bound thresholds used for fires and explosions are given in Table 11.3. The assumptions and justifications behind these values are discussed in Appendix D. Fire damage thresholds for vessels and platforms are based on the heat intensity that is associated with damage to process equipment. The lower bound threshold for property damage due to explosions is based on the pressure that causes distortion of steel frame structures and the upper bound threshold on the pressure that is associated with probable total building destruction and severe damage to heavy industrial equipment.

11.5.4 Offshore Unit Damage Cost Estimates

The development of a comprehensive set of deterministic offshore unit damage cost estimates for vessel traffic and platforms was beyond the scope of this project. However, based on an informal survey of offshore facility superstructure costs, the following order of magnitude cost estimates are suggested as reference values: for major and minor manned platforms $100 million and $10 million, respectively; and for major and minor unmanned platforms, $10 million and $1 million. For vessel traffic zones, a unit cost of $50 million per km^2 is suggested for high density zones (*e.g.*, a major shipping corridor with one significant vessel per km^2 during daylight hours, assuming a combined vessel and cargo value of $100 million and 12 hours of daylight per day) and $20,000 per km^2 for low density zones (*e.g.*, an active fishing area in which a square km of area is occupied by a vessel valued at $ 500,000 for a one hour period each day). The moderate density traffic zone shall correspond to an intermediate unit cost of $1 million per km^2. These reference cost estimates are summarized in Table 11.4.

Release and Damage Costs

11.6 Onshore Damage Cost

11.6.1 The Node Parameter

The Onshore Damage Cost node (basic node 9.5) and its direct predecessor nodes are shown in a highlighted version of the basic node influence diagram in Figure 11.2. The specific node parameter is the cost of long-term damage to coastal resources (*i.e.*, shorelines and environmental resources) caused by shoreline impact of persistent liquid spill products. The predecessor node arrows indicate that Onshore Damage Cost is a functional node meaning that the value of the node parameter is calculated directly from the value of direct predecessor node parameters: Impact Location, Season, Product, and Impact Volume.

As background, it is noted that an Onshore Damage Cost node is included in the model to reflect the costs associated long-term environmental damage caused by oil spills which reach the coastline. In the United States these costs are typically estimated using so-called Natural Resource Damage Assessment (NRDA) models which have been developed by various government agencies as a basis for seeking resource damage compensation on behalf of the general public to compensate for the loss of resource use, and to pay for resource restoration (Robilliard *et al.* 1993). In the context of this project, where an estimate of damage costs is required for hypothetical spills, as opposed to real spills, a simplified form of NRDA based on the use of so-called compensation formulas or compensation schedules is considered appropriate. Using the simplified compensation formula approach, for example the approach developed by Geselbracht and Logan (1993) for marine oil spills in Washington State, damage compensation estimates can be estimated as a function of parameters such as resource vulnerability (which depends on spill impact location and season), product damage potential (which depends on product type), and spill impact volume. Note that given the specified predecessor nodes in the offshore influence diagram, all of these factors are implicitly addressed by the Onshore Damage Cost node parameter calculation algorithm.

The node parameter calculation algorithm assumes that a deterministic unit damage cost estimate will be assigned to each combination of predecessor node values. In other words, unit cost estimates must be specified for all coastal resources identified at the Impact Location node, for both summer and winter seasons, for all specified product types. This node parameter input format provides maximum flexibility to the program user and allows for the specification of onshore unit damage costs that replicate the calculation approach incorporated in a variety of existing damage compensation formulas.

11.6.2 Unit Onshore Damage Cost Estimates

The development of a comprehensive set of unit onshore damage cost estimates was considered beyond the scope of this project. In general, the unit damage cost estimates are highly location specific and representative generic values are therefore difficult to establish and potentially

misleading. However, to provide an order of magnitude estimate of onshore damage costs, a review of damage cost compensation estimates generated using the Washington State NRDA compensation schedule (Geselbracht and Logan 1993) was carried out. This review indicates unit damage costs in the range of $\$260/m^3$ to $\$13,000/m^3$ ($1/USgal to $50/USgal). Based on the costing algorithm employed in the Washington model, ignoring variations in the damage potential associated with different product types, and seasonal variations in resource vulnerability, will reduce the damage cost range by a factor of 5 to 10. For a representative spill product of intermediate damage potential, the resulting unit damage cost range would therefore be on the order of $\$500/m^3$ to $\$5,000/m^3$. If the variation in onshore damage compensation cost associated with resource vulnerability is addressed in a simplistic manner by assuming that this reduced onshore damage cost range correlates directly with the coastal resource sensitivity indices developed by Gundlach *et al.* (1981) and adopted herein (see Table 9.5), then the resulting set of reference unit damage cost estimates, as a function of shoreline type, are as given in Table 11.5.

Figures and Tables

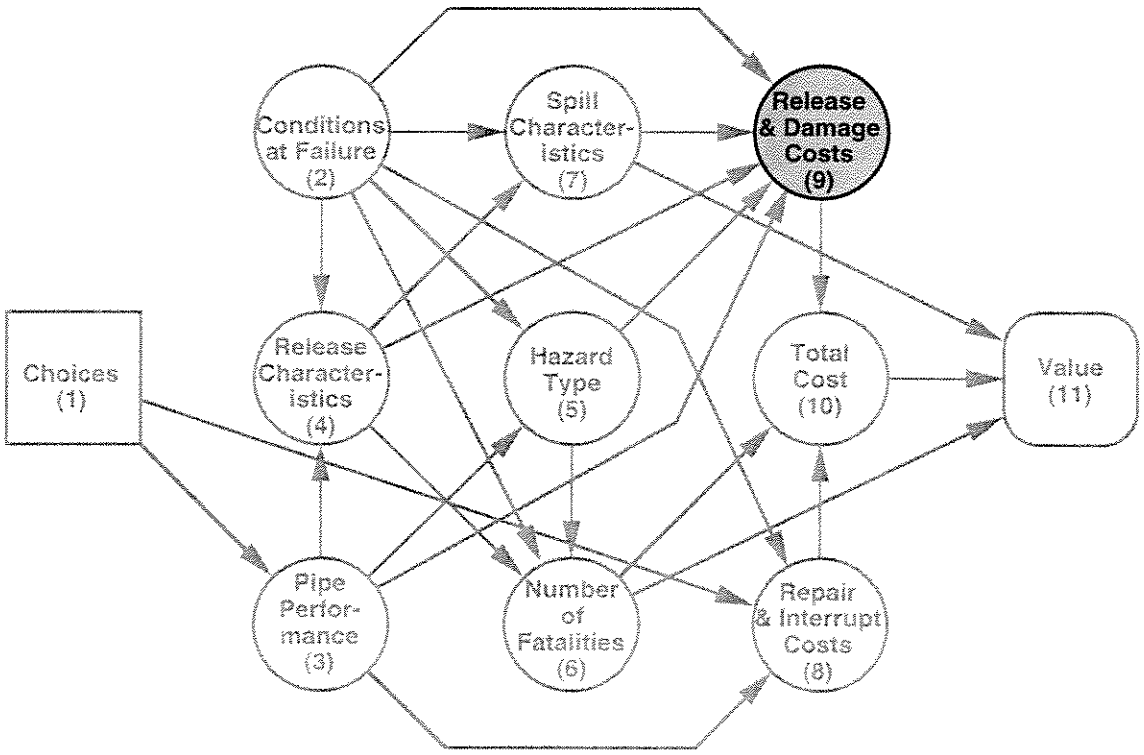

Figure 11.1 Compound node influence diagram highlighting
Release and Damage Costs node group

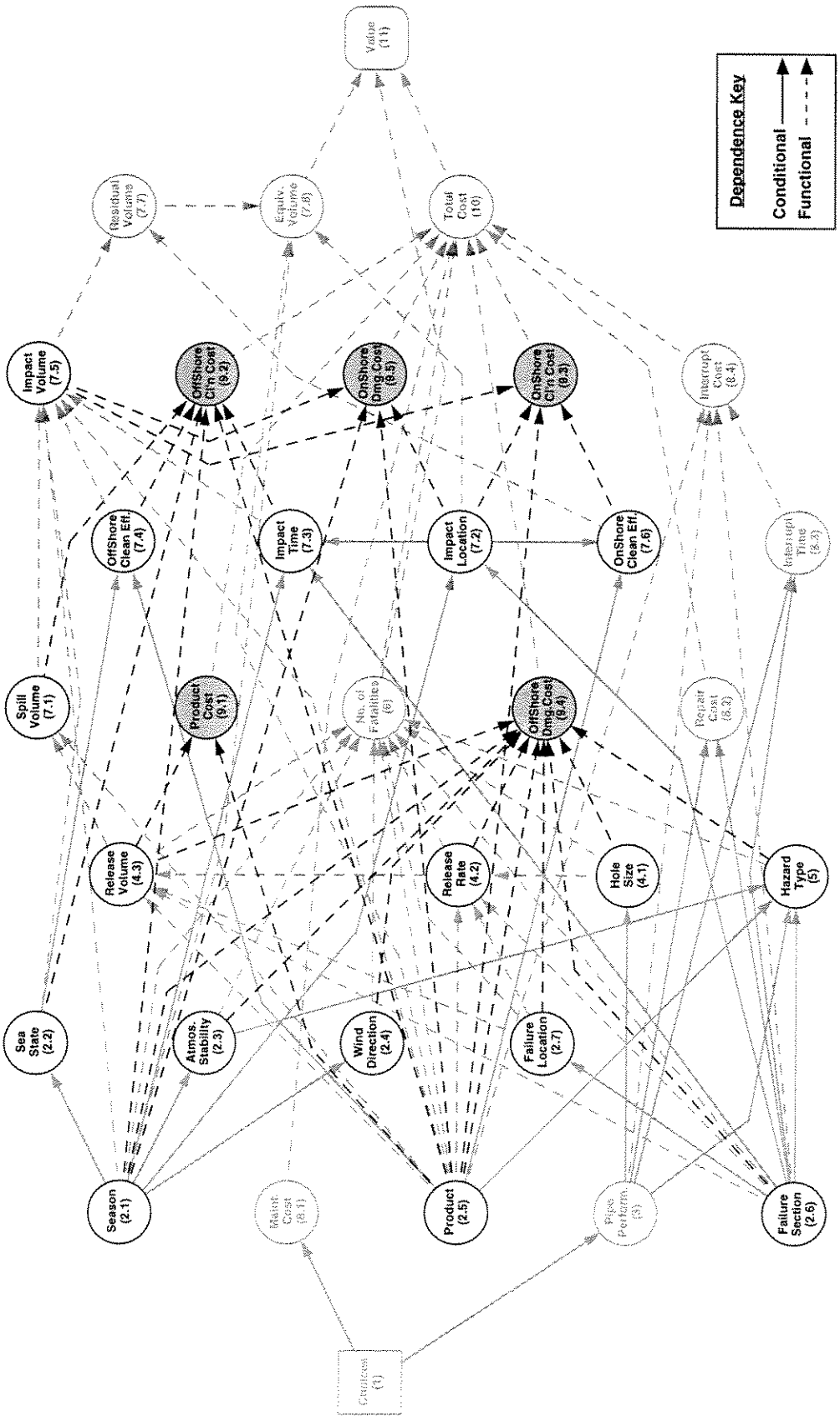

Figure 11.2 Basic node influence diagram highlighting Release and Damage Costs nodes and associated immediate predecessor nodes

Petroleum Fraction	Product Group	Cost ($/m^3)
Natural Gas	methane	0.05
Natural Gas Liquids	ethanes	60
	propanes butanes	90
	pentanes (condensate)	120
Gasolines	automotive gasoline aviation gas	200
Kerosenes	jet fuel (JP-1) range oil (Fuel Oil - 1)	
Gas Oils	heating oil (Fuel Oil - 2) diesel oil (Fuel Oil -2D)	
Crude Oils	_____	120

Table 11.1 Unit cost estimates for representative petroleum products

Shoreline Type	Unit Onshore Clean-up Cost ($ per m^3 recovered)
Exposed rocky headlands	3000
Wave-cut platforms / Erosional scarps	3000
Exposed sand beaches	1500
Sheltered sand beaches	1500
Exposed tidal flats (low biomass)	3000
Sand and gravel / Shell beaches	3000
Gravel beaches	3000
Exposed tidal flats (high biomass)	3000
Sheltered rocky areas	6000
Sheltered tidal flats	6000
Salt marshes	6000
Mangrove coasts	6000

Table 11.2 Representative unit onshore clean-up cost estimates

Hazard	Parameter	Units	Property Damage Thresholds	
			Lower Bound	Upper Bound
thermal radiation	heat intensity	kW/m^2	15.7	37.5
vapour cloud fire	fraction of C_{LFL} (1)		N/A	N/A
vapour cloud explosion	blast pressure	kPa	15.9	69.0

(1) Lower flammability limit of product.

Table 11.3 Upper and lower bound hazard thresholds for offshore property damage

Platforms	Platform Cost ($ millions)
Major manned	100
Minor manned	10
Major unmanned	10
Minor unmanned	1

Vessel Traffic Zones	Vessel Cost ($ millions / km^2)
High density	50
Medium density	1.0
Low density	0.02
No significant traffic	0.0

Table 11.4 Representative offshore damage costs for platforms and vessel traffic zones

Shoreline Type	Unit Onshore Damage Cost ($ per m^3 ashore)
Exposed rocky headlands	500
Wave-cut platforms / Erosional scarps	1000
Exposed sand beaches	1500
Sheltered sand beaches	2000
Exposed tidal flats (low biomass)	2500
Sand and gravel / Shell beaches	3000
Gravel beaches	3500
Exposed tidal flats (high biomass)	3500
Sheltered rocky areas	4000
Sheltered tidal flats	4500
Salt marshes	5000
Mangrove coasts	5000

Table 11.5 Representative onshore damage unit costs

12.0 TOTAL COST

12.1 Node Parameter

The Total Cost node group (group 10) is shown in a highlighted version of the compound node influence diagram in Figure 12.1. The node group consists of a single Total Cost node (node 10) which is shown together with its direct predecessor nodes in a highlighted version of the basic node influence diagram in Figure 12.2. The specific node parameter is the total financial cost which is taken to be the sum of the direct costs associated with pipeline inspection and maintenance and the risk related costs associated with pipeline failure including the value of compensation for property damage and human casualties. Total Cost is a functional node meaning that the value of the node parameter is calculated directly from the values of its direct predecessor nodes which include: nodes in the Repair and Interruption Cost group, the Release and Damage Cost group, and the Number of Fatalities node.

The total cost, c, is calculated from the following equation

$$c = c_{main} + c_{prod} + c_{rpr} + c_{int} + c_{offcl} + c_{oncl} + c_{vsl} + c_{plt} + a_n n \qquad [12.1]$$

where c_{main} is the direct cost associated with pipeline inspection and maintenance, c_{prod} is the value of the lost product, c_{rpr} is the cost of pipeline repair, c_{int} is the cost associated with service interruption, c_{offcl} and c_{oncl} are the costs associated with offshore and onshore spill clean-up where liquid spills are involved, c_{vsl} and c_{plt} are the costs of compensation for vessel and platform damage, and a_n is a constant that converts the number of human fatalities, n, into a financial cost.

All of the information necessary to calculate the total cost is available from preceding node parameter calculations except for the constant a_n which, in the context of the total cost node parameter, is intended to represent the cost of direct compensation to be paid for a human fatality. It is noted that the cost of compensation for loss of life (a_n) is not the same as the "value of a human life" which is intended to serve as a much broader measure of the financial impact of a human fatality on society as a whole. This societal impact of human fatality is addressed separately in the value node calculation (see Section 13).

12.2 Cost of Compensation for Human Fatality

As part of a previous project (Stephens *et al.* 1995b) a literature review was carried out and discussions were held with legal professionals working in the area of injury compensation. This review led to the basic understanding that compensation payments for loss of life are based primarily on estimates of the economic value of a human life, *EVOL*, as obtained using a 'human capital approach' wherein the compensation reflects the present capital value of the lost earnings of the person whose life has been lost. Based on employment and retirement income information

Total Cost

and statistical life tables available from Statistics Canada it was determined that the *EVOL* of the average person was approximately 40 times their annual income. (For a detailed discussion of the calculation method and the associated assumptions see Appendix H in Stephen's *et al.* 1995b).

The total compensation award package paid to dependents and other claimants also generally includes a cost allowance to account for the pain, grief and suffering experienced by the victims family, relatives and friends. Studies conducted in the UK (Marin 1986), suggest that a reasonable estimate of the "pain and suffering" allowance is on the order of 25% to 30% of the *EVOL*.

In addition, it is noted that in many countries (*e.g.*, Canada) a 20% to 25% contingency reduction is often applied by the court to compensation awards. This contingency reduction is intended to reflect factors that are not specifically addressed in the formal calculation of the *EVOL*, including for example: consideration of the fact that the deceased person may not have chosen to work continuously to the standard retirement age of 65.

Finally, the cost to the pipeline operator of compensation for human fatalities will also include legal fees for both parties because the fees for the party seeking compensation are usually built into the settlement award. The combined cost of legal fees is typically estimated to be on the order of 25% of the basic compensation award.

The above suggests that, on average, the added compensation for pain and suffering is offset by contingency reductions. The total cost of compensation for loss of life is therefore assumed to be equal to the *EVOL* plus legal fees. The equation for a_n is therefore

$$a_n = 1.25 \ EVOL \qquad [12.2]$$

In the context of this project, an average annual income range of $25,000 to $75,000 is assumed for persons likely to be affected by the hazards associated with offshore pipeline failures, with the lower end of the income range applying to vessel crew and the upper end of the range applying to platform personnel. This income range supports a representative single value income estimate of $50,000 and the *EVOL* associated with this annual income level is $2 million dollars (*i.e.*, 40 times $50,000). Based on Equation [12.2], this corresponds to an average total compensation cost, a_n, of $2.5 million dollars.

Note that there is considerable uncertainty associated with the *EVOL* due to variability in earnings and earning potential, age at time of death, and the discounting rate which depends on interest rates and the rate of inflation. The above value is, however, considered to be representative of the economic value of a statistical life for offshore workers in North America.

Figures

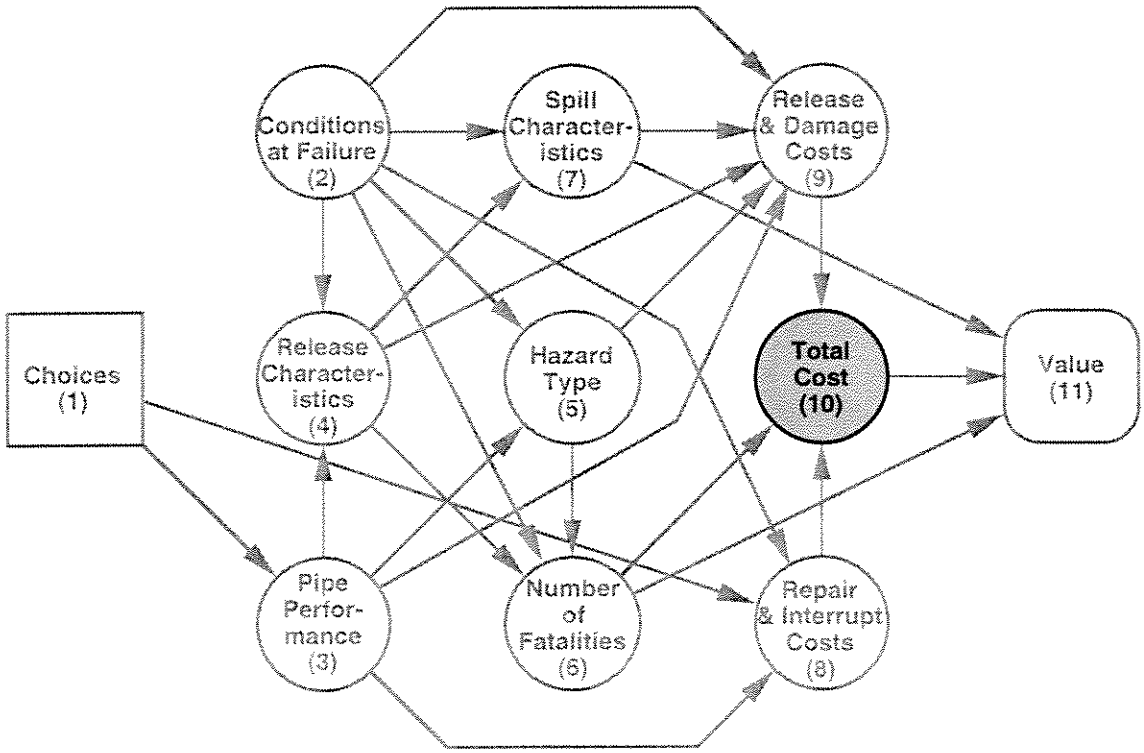

Figure 12.1 Compound node influence diagram highlighting Total Cost node group

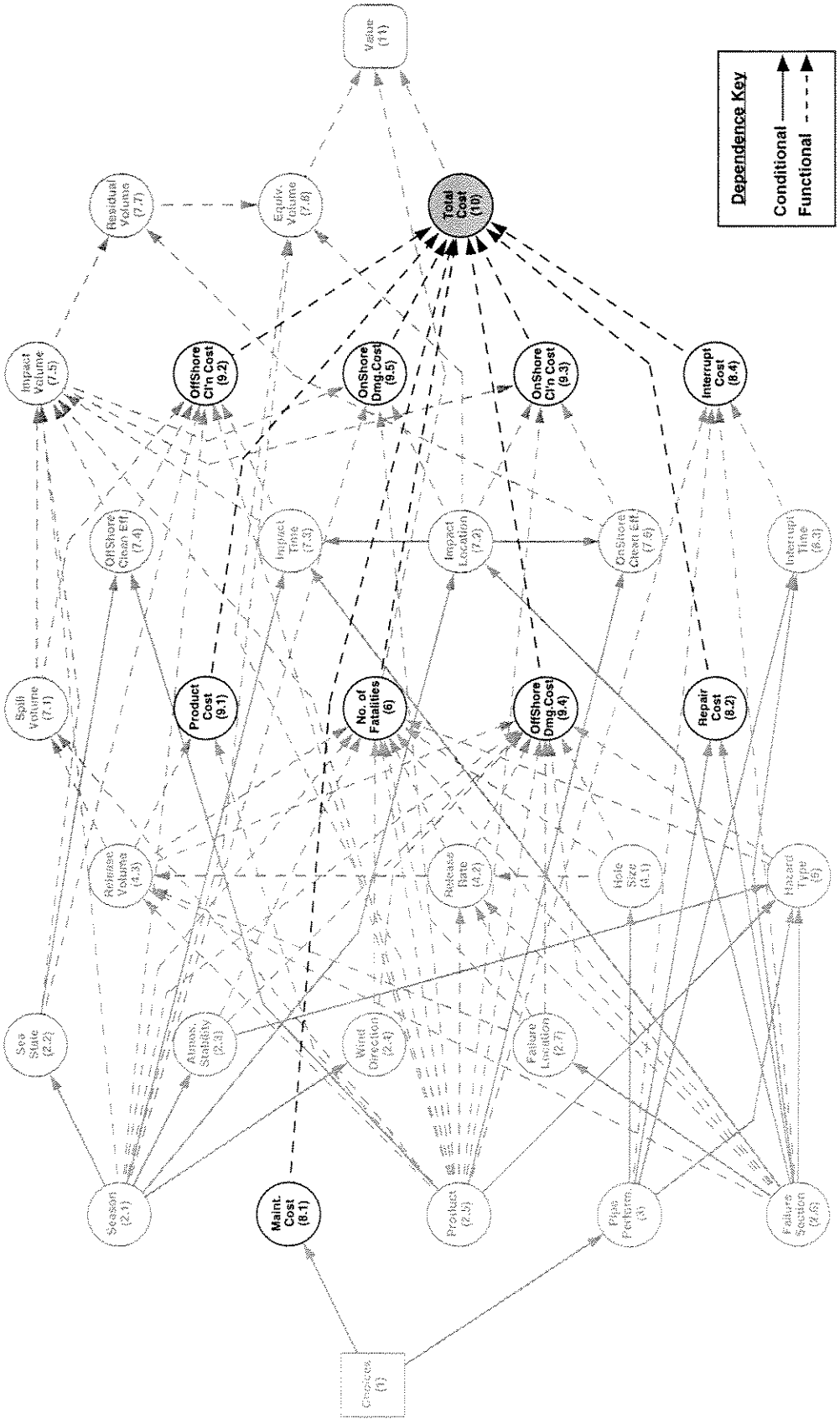

Figure 12.2 Basic node influence diagram highlighting Total Cost node and associated immediate predecessor nodes

13.0 VALUE

13.1 Introduction

The value node defines the criterion used to make the final choice on integrity maintenance action. This criterion must take into account the three major objectives associated with the decision problem, namely: 1) a high level of *safety* for those exposed to risk from the pipeline; 2) a high level of *environmental protection* from potential product spills; and 3) a low *economic* cost. Each objective is characterized by a specific parameter (called an attribute) that measures the degree to which the objective is achieved. As described in PIRAMID Technical Reference Manual No 1.2 (Stephens *et al.* 1995a), the attributes selected for the present problem are:

1. Number of Fatalities n measuring safety.
2. Equivalent spill volume v measuring environmental protection.
3. Total cost c measuring economic aspects.

Figures 13.1 and 13.2 show how this parameter relates to the influence diagram in its compact and expanded forms. Figure 13.2 shows that the value node is a functional node, with the nodes representing the above three parameters as its direct predecessors.

Two approaches for defining the value function have been developed for this program (Stephens *et al.* 1995a). These are:

- Utility Optimization. A utility measure is defined as a function of n, v and c. This function is defined such that higher expected values of the utility are preferred, and therefore the optimal choice is the one that leads to the maximum expected utility. In this approach, the value node calculates the utility u as a function of n, v, and c. Solution of the influence diagram provides the expectation of c for each choice and this information can be used to identify the choice that leads to the maximum expected utility.
- Cost optimization. Cost is optimized without constraints, for pipelines carrying non-persistent spill products, and with constraints for pipelines carrying persistent spill products that have the potential for significant environmental impact. Constrained cost optimization is achieved by first eliminating choices that do not meet the imposed environmental constraint. The optimal action is selected from among the remaining choices as the one with the lowest expected total cost.

Calculation of the value function is discussed in detail in Section 13.2 for the utility approach and in Section 13.3 for the cost optimization approach.

Value

13.2 The Utility Approach

13.2.1 Introduction

13.2.1.1 Why Utility Functions?

A commonly used basis for decision making under uncertainty is to optimize the total expected cost c_t defined as:

$$c_t = an + bv + c \qquad [13.1]$$

where the constants a and b convert losses of life and equivalent spill volumes into monetary equivalents. This approach implies that the decision maker finds any two choices with the same expected total cost equally attractive. While this appears reasonable, the presence of uncertainty causes the preferences of most people and corporations to deviate from this approach.

To illustrate this consider the choices in Figure 13.3. Choice 1 represents a 0.01 chance of paying \$20,000, whereas choice 2 represents a sure cost of \$200. The expected cost for choice 1 is 0.99 x \$0.0 + 0.01 x \$20,000 = \$200, which is equal to that of choice 2. Therefore, based on the expected cost approach the two choices would be equivalent. In reality, however, most decision makers find a payment of \$200 to be more attractive than a 1% chance of losing \$20,000. In fact most people would be willing to pay more than the expected value of \$200 to avoid the risky choice. This attitude is referred to as *risk aversion* and is widely accepted in financial risk analysis.

Another limitation of the expected total cost approach relates to tradeoffs between different attributes. This is illustrated by considering the two choices in Figure 13.4. Choice 1 represents a 0.50 chance at paying \$10 million and causing 5 fatalities, and a 0.50 chance at having no losses. Choice 2 represents a 0.50 chance at losing \$10 million (with no losses in life) and a 0.50 chance at having 5 fatalities (with no financial losses). Using Equation [13.1] (with $v = 0$ and a = \$1 million per life) the expected value of the total cost c_t can be calculated for the first choice as 0.5 x (\$10 million + \$1 million x 5 fatalities) + 0.5 x (\$0 + 0) = \$7.5 million. Similarly, choice 2 can be shown to have a total expected cost of \$7.5 million as well, so that optimization of the total expected cost would mean indifference between the two choices. It can be seen however that some decision makers may prefer choice 1 because it includes a chance of no losses, whereas choice 2 is assured to have some loss (either financial or human). This attitude relates to *tradeoffs* between costs and losses in life.

The foregoing discussion shows that the expected cost approach may lead to poor choices because it cannot reflect appropriate risk aversion and tradeoff attitudes of decision makers. Utility theory can overcome this limitation by incorporating these attitudes in the optimization

Value

process. Formal definitions of the preference attitudes alluded to in this section and the manner in which they can be represented in a utility function is addressed in Section 13.2.2.

13.2.1.2 Defining a Utility Function

The development of a utility function for a problem with multiple attributes involves two main steps.

1. Definition of individual utility functions for each attribute based on the appropriate risk attitudes.
2. Combining the individual utility functions in an overall utility function, that takes into account tradeoff attitudes between the different attributes.

Sections 13.2.2 and 13.2.3 describe the above two steps for the problem of pipeline risk-based decision making. Each section gives the basic concepts needed before describing the analysis undertaken and the conclusions reached.

13.2.2 Single Attribute Utility Functions

13.2.2.1 Risk Attitudes - Concepts and Definitions

To generalize the risk aversion concept introduced (by an example) in Section 13.2.1.1, risk aversion is said to apply for a certain attribute if the expected value of an uncertain choice (or lottery) is more attractive than the lottery itself for the whole range of attribute values. Risk aversion can be reflected in risk management choices by defining the objective function (called the utility function u) as a concave function of the attribute. This is illustrated in Figure 13.5a for the cost attribute c. The utility function $u(c)$ is a decreasing function of c and this reflects the fact that higher costs are less desirable. The figure can be used to verify that, because the function is concave, the expected utility of any option involving uncertainty is lower than the utility associated with the expect value of the option. This is illustrated in the figure by an example lottery l involving a 50-50 chance at paying the minimum cost c^* or maximum cost $c0$. Therefore, using a concave utility function over cost results in risk averse choices.

Risk proneness is the opposite of risk aversion. It is said to apply to a certain attribute if the decision maker prefers each lottery to its expected value over the whole attribute range. Risk proneness can be modeled by a convex utility function as shown in Figure 13.5b. It is noted that a linear utility function would correspond to optimizing the cost itself, and that this case is referred to as a *risk neutral* attitude.

The sure cost deemed by the decision maker to be equivalent to a certain lottery l is called the *certainty equivalent* of that particular lottery, and is denoted $\hat{c}$ (see Figure 13.5). The difference

Value

between the expected value of the lottery and its certainty equivalent, represents the amount of money which the decision-maker is willing to pay in order to avoid the risk, and is called the *risk premium* $\pi(l)$ for this particular lottery. The risk premium represents the degree of risk aversion (see Figure 13.5a). For example, if the decision maker is indifferent between a 50-50 lottery at paying \$0 or \$10,000, and a certain cost of \$6,000, then the certainty equivalent of the lottery is $\hat{c}$ = \$6,000, and the risk premium is $\pi(l)$ = \$6,000 - [0.5 (0) + 0.5 (\$10,000)] = \$1,000.

Consider a lottery represented by a 0.50 chance of paying $c - \Delta c$ and a 0.50 chance of paying $c + \Delta c$. The amount c is called the *reference amount* of the lottery, while the *range* of the lottery is $2\Delta c$. The variation of the risk premium with the reference amount for the same lottery range represents another significant attitude of risk behaviour. If the risk premium increases (decreases) monotonically with c for any fixed range $2\Delta c$, the decision maker is said to be *increasingly (decreasingly) risk averse*. Otherwise, if the risk premium is constant for all h, the decision-maker is *constantly risk averse*. Similar definitions apply to increasing, decreasing, and constant risk proneness.

Mathematical functions can be proposed to satisfy the ranking and risk characteristics that are judged to be appropriate for a certain attribute. These functions contain constants that can be determined by the decision maker's certainty equivalents for a number of lotteries equal to the number of the required constants. Examples showing the characteristics of the utility functions used for the attributes mentioned in Section 13.1 are given in Sections 13.2.2.2 and 13.2.2.4.

13.2.2.2 Utility Function for Cost

Money is the most frequently appearing attribute in utility theory applications. Hax and Wiig (1975), for example, dealt with a capital investment decision problem of bidding on a project taking into consideration the possibilities of a high or low bid, and bidding alone or with a partner. "Net present value" of the investment was taken as an attribute. Another example is a study for selecting a site for a nuclear power plant constructed by Keeney and Nair (1975). They considered the attribute "annual differential cost" for the different proposed sites. Bell (1977) analyzed the problem of dealing with forest pests in New Brunswick, based on the attribute "single year's profit". In a decision analysis study for the development of the Mexico City Airport, Keeney (1973) used "cost" as an attribute.

All the above authors and many others agree, regardless of the nature of the problem or the exact definition of the attribute, on monotonicity and risk aversion. The function is either monotonically increasing in case of gain, or monotonically decreasing in case of cost. In addition Keeney and Raiffa (1976) and Schlaifer (1969) suggest that an increasingly risk averse function (as defined in Section 13.2.2.1) would be appropriate.

In summary, the utility function over cost is: 1) monotonically decreasing; 2) risk averse; and 3) increasingly risk averse. A function that satisfies the above conditions is given plotted in Figure 13.6. Appendix E describes how the function is defined by asking the decision maker to

Value

give his or her certainty equivalent to a simple lottery. It also shows how the function is verified by using it to calculate some equivalent options and presenting them to the decision maker to ensure their consistency with his or her choices.

13.2.2.3 Utility Function for Number of Fatalities

Several authors have reported using losses in life as an attribute in decision analysis. For example, Keeney (1973) for example used the "number of people killed or seriously injured" in a study of the development of Mexico City Airport. The attribute was used in the range of 0 to 1000. A linear utility function was selected although in his discussion, Keeney suggests that a rational utility function should be risk averse.

A study of hazardous materials transportation for the Maritimes Administration by Kalelkar and Brooks (1974) used the "number of people killed" as an attribute in the range of 0 to 60. A decreasingly risk prone function was assigned to the attribute by an experienced person in the field of safety, who was asked to represent the point of view of society. The authors explained the risk proneness for small numbers of deaths by the fact that the decision maker was willing to take high chances to avoid even one certain death. So he was willing to take a 50-50 chance between 0 to 60 deaths, rather that accept 10 sure deaths. As the number of sure deaths increased, his risk proneness declined and his function became risk neutral. This explanation holds only for uncertain choices that involve a chance of no deaths, while the function still implies risk proneness for a large range of uncertain choices that do include sure deaths (*e.g.*, the certainty equivalent for a 50-50 lottery between 10 or 60 deaths is about 25). It is interesting here to note that the utility function of the same decision-maker over property damage in dollars was decreasingly risk prone. Tversky (1977) also suggested that a risk prone utility function is appropriate for losses in life.

A risk averse function was suggested by Jordaan (1982) in a study of the transportation of hazardous goods through the City of Calgary, Alberta, Canada. The function is intended to expresses the aversion of society to a catastrophe involving a large number of deaths. The function used by Jordaan was constantly risk averse (*i.e.*, the degree of risk aversion was not dependent of the number of lives lost).

The foregoing discussion shows that there is no consistency in previous work regarding risk attitudes associated with losses in life. In fact, all possible risk attitudes (risk averse, risk prone and risk neutral) have been suggested. In evaluating this information to choose an appropriate utility function, the following points were considered:

1. References that suggested a risk prone function indicate that the degree of risk proneness decreases rapidly as the number of fatalities increase, and the functions become almost risk neutral. The risk prone attitude in the low values of the attribute can be explained by the attractiveness of lotteries that involve a chance of zero deaths or injuries.

Value

2. Risk aversion was justified on the basis of society's aversion to large catastrophes. Such catastrophes are unlikely to result from a pipeline failure.

3. Any deviation from a straight line behaviour does not minimize the expected number of deaths since it means the willingness to pay a certain premium in order to avoid or seek risk. A risk averse behaviour, for example, reflects the fact that society is more shaken by 100 deaths in one accident than 10 accidents, each resulting in 10 fatalities. Most people would agree with this attitude. What is questionable, however, is the validity of accepting a higher expected number of deaths (sacrificing lives) in order to ensure that society is informed of these deaths in a more acceptable manner.

Based on this it was decided that a risk neutral (linear) utility function is most suitable. This corresponds to minimizing the expected number of fatalities directly. The utility function is given in Appendix E.

13.2.2.4 Equivalent Spill Volume

The equivalent spill volume represents the residual spill volume remaining in the environment after clean up. This volume is calculated by adjusting the actual residual volume at a given location, to a volume that is judged to have an equivalent environmental impact at a reference location of the user's choice. Details of this parameter are described in Section 9.4.

Discussions held with organizations that deal with environmental issues relating to hydrocarbon product releases (see previous study, Stephens *et al.* 1995a) indicated that decision makers typically place much more importance on the prevention of spills than on limiting the spill size if one should occur. In other words, the utility drops at a high rate for low spill volumes and this rate decreases as the spill volume increases. This trend implies that the utility function is convex or risk prone.

The function used is plotted in Figure 13.7. Details of the derivation and verification of the function are given in Appendix E.

13.2.3 Multi-attribute Utility Function

13.2.3.1 Tradeoff Attitudes - Concepts and Definitions

A multi-attribute utility function is defined as a function of the individual utility functions for each attribute, and a number of constants representing tradeoffs between the individual attributes. The multi-attribute utility function can represent different assumptions regarding how the attributes interact. Interaction between attributes relates to such questions as: do preferences over lotteries involving cost c depend on the number of fatalities n or the volume of spill v?, or do tradeoffs between c and n depend on the values of v. If all such dependencies are permitted, the form of the multi-attribute utility function becomes very complex. With some constraints,

Value

however, significant simplifications to the function can be made. Two types of constraints are discussed in the following paragraphs.

The first constraint relates to *preferential independence*, which means that preferences over a given subset of the attributes are independent of the values of the remaining attributes. For example, if tradeoffs between the cost c and number of fatalities n are unaffected by the equivalent spill volume v, then if can be stated that the subset $\{c,n\}$ is preferentially independent of v. It is noted that preferential independence relates to tradeoffs under certainty and therefore it can be established without consideration of any uncertain choices.

The other constraint that can be exploited to simplify the utility function is called *utility independence*. A given attribute is utility independent of another attribute if preferences under uncertainty for the former are not affected by the value of the latter. For example, cost c is utility independent of the number of fatalities n if preferences regarding cost lotteries (such as the one in Figure 13.3) are not affected by the number of fatalities.

The utilization of these independence characteristics to select an appropriate form of the multi-attribute utility function in discussed in Section 13.2.3.2.

13.2.3.2 The Multi-attribute Utility Function

Figure 13.8a shows two equivalent choices involving cost c. Since this equivalence does not take into consideration the number of fatalities n, it is valid for $n = 0$, and the equivalence in Figure 13.8b holds. Now, if the value of n is changed from zero to 5 say, would this change the above equivalence in c ? In other words, does the indifference relation in Figure 13.8a imply the one in Figure 13.8d for any value of n ? It is reasonable to answer the above questions positively, and this implies that c is Utility Independent (UI) of n A similar argument can be developed to show that it is reasonable to assume that c is UI of v. Therefore it can be stated that c is UI of $\{n, v\}$.

Now consider tradeoffs between c and n for a certain value of v. Assume that the consequence $\{c = \$50$ million, $n = 0$ fatalities, $v = 0$ m$^3\}$ is equivalent to $\{c = \$0$, $n = 5$ fatalities, $v = 0$ m$^3\}$. This means that a loss of \$50 million is equivalent to 5 fatalities provided that $v = 0$ m^3 (*i.e.*, there is no spill). Assume that the value of v is changed to 1000 m^3, would this affect the values of c and n in the above equivalence relationship? In other words, does the tradeoff between c and n depend on the value of v? A negative answer is reasonable, implying that $\{c, n\}$ is preferentially independent on v, denoted $\{c, n\}$ is PI of v. A similar argument can be used to show that $\{c, v\}$ is PI of n.

The above-mentioned conditions are sufficient to justify a simplified form of the utility function called the multiplicative form. This function and the input required to define and verify it is given in Appendix E. It is noted that, as is shown in the Appendix, defining the multi-attribute

Value

utility function involves indirect definition of the monetary equivalents of losses in life and spills.

13.3 Cost Optimization

As discussed earlier, the cost optimization approach is based on selecting the lowest expected cost option. If constraints are imposed, the optimal choice will be the lowest expected cost option that meets the pre-defined constraints. For pipelines carrying products with significant environmental impact potential, the constraint is associated with a minimum level of environmental protection. This approach eliminates the need to consider the tradeoffs discussed in Section 13.2, which may be considered an advantage by some decision makers who find it difficult to explicitly consider such issues as the monetary value of environmental protection. It must be mentioned, however, that such values are implied by the decision made regardless of the method used. For example, the value of environmental protection implied by a given choice can be calculated using the decision influence diagram. Therefore, it can be argued that since these issues cannot be avoided it is better to consider them explicitly in order to ensure consistency and understand the implications of a given decision.

The constrained expected cost optimization approach is best suited to cases where policy or regulations are in place that dictate certain levels of environmental protection. In such cases, this approach allows meeting these regulations at the lowest possible cost.

Calculation of the total cost is addressed in Section 12.0, and need not be repeated in this section. The environmental constraint is defined in terms of an expected annual equivalent volume per km length of the pipeline. Recall that the equivalent spill volume is a measure of the environmental impact of the residual spill volume remaining following offshore clean-up and initial onshore clean-up activities (see Section 9.9 for details of how this parameter is calculated). Use of the total expected value of the equivalent spill volume per km of the pipeline results in a measure of the total expected environmental impact due to a unit length of the pipeline. Any choice that leads to an average per km equivalent spill volume greater than the tolerable value is considered inadmissible.

Figures

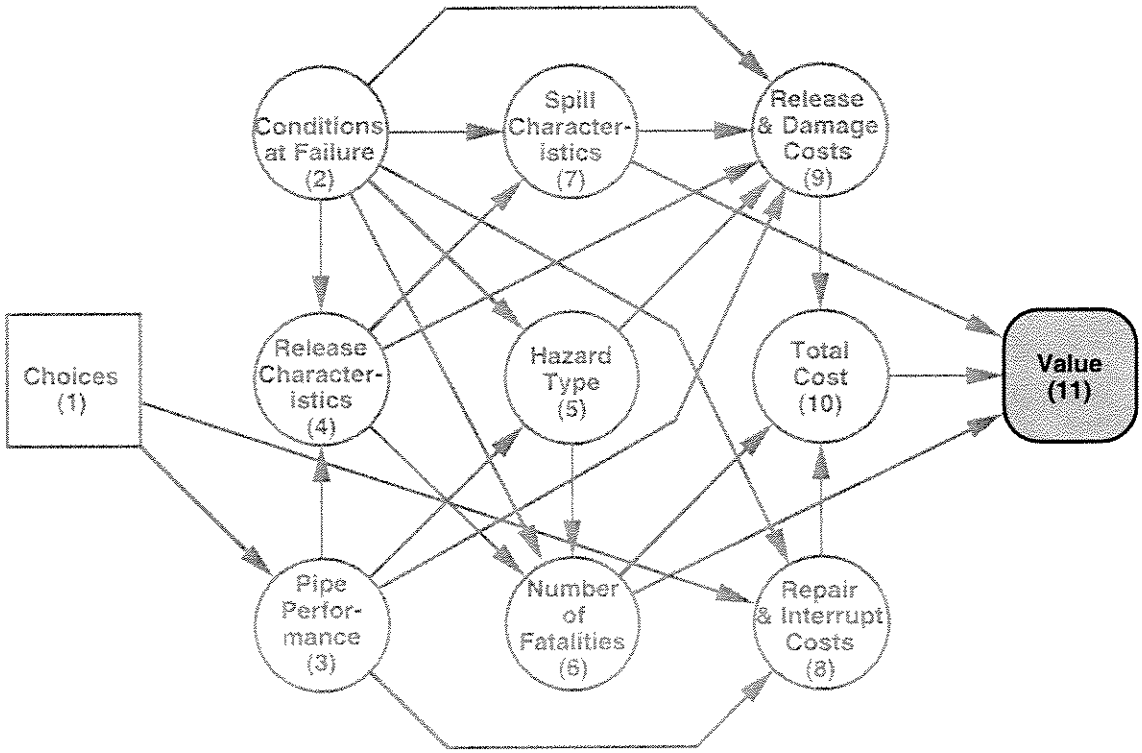

Figure 13.1 Compound node influence diagram highlighting Value node group

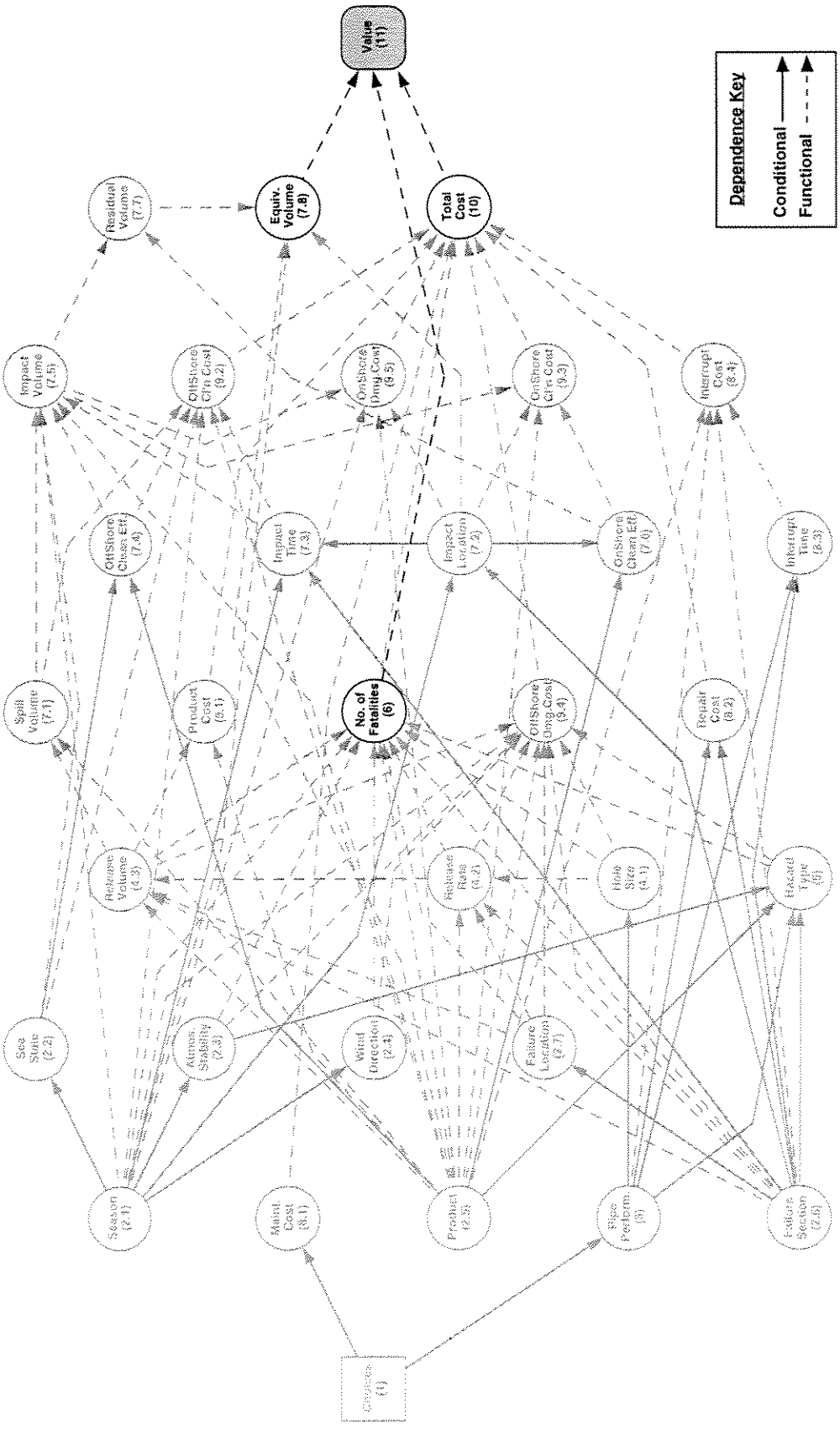

Figure 13.2 Basic node influence diagram highlighting Value node and associated immediate predecessor nodes

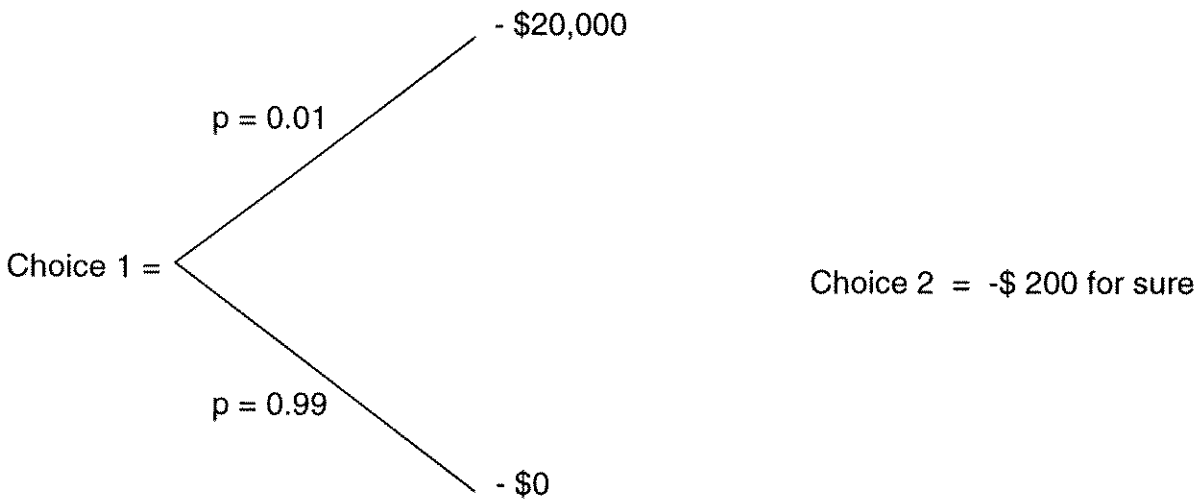

E (C) = 0.01 x -$20,000 + 0.99 x 0. = -$200

Figure 13.3 Choices with equivalent expected costs and different risk levels

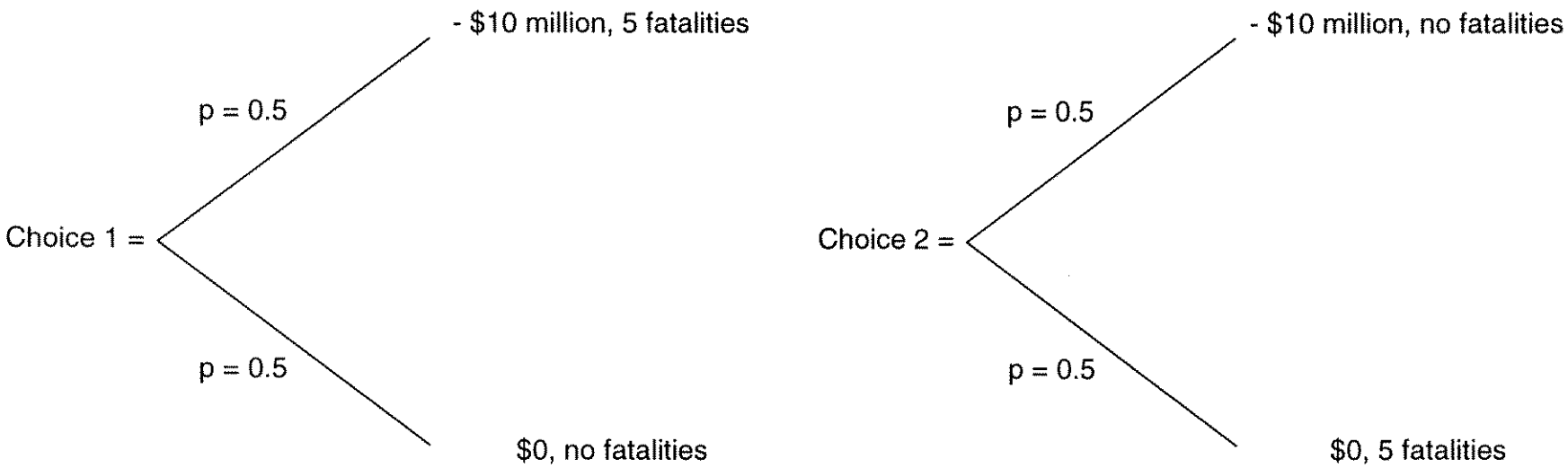

Figure 13.4 Uncertain choices involving combinations of costs and fatalities

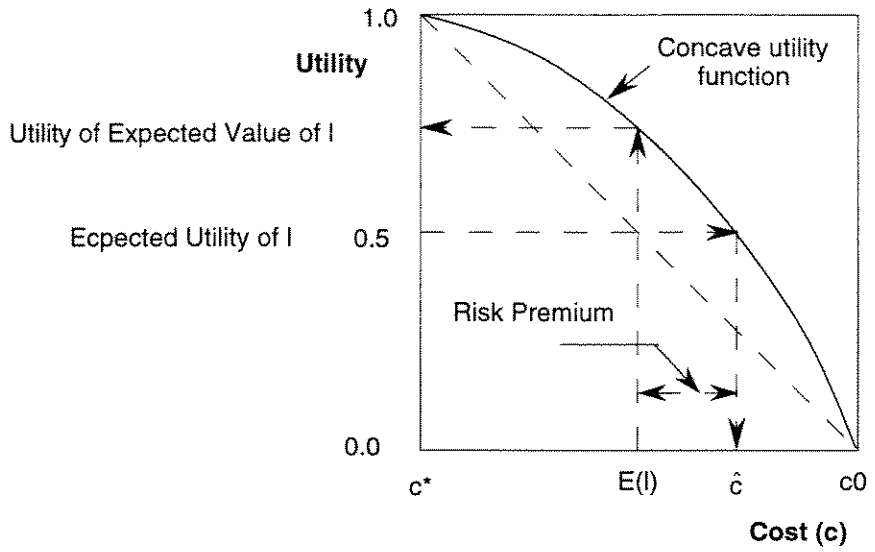

a) Risk Averse: Utility of the expected value > expected utility of lottery

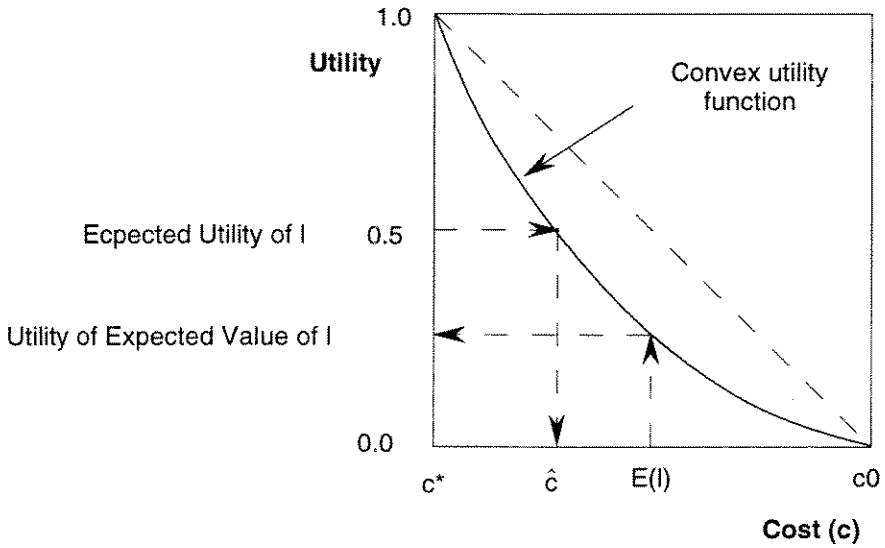

b) Risk Prone: Utility of the expected value < expected utility of lottery

c*	= Minimum cost
c0	= Maximum cost
I	= a 50-50 chance of c* or c0
E(I)	= Expected value of lottery = (c*+c0)/2
E[u(I)]	= Expected utility of the lottery = [u(c*)+u(c0)]/2 = 0.50
ĉ	= Certainty Equivalent of I

Figure 13.5 Illustration of risk averse and risk prone utility functions

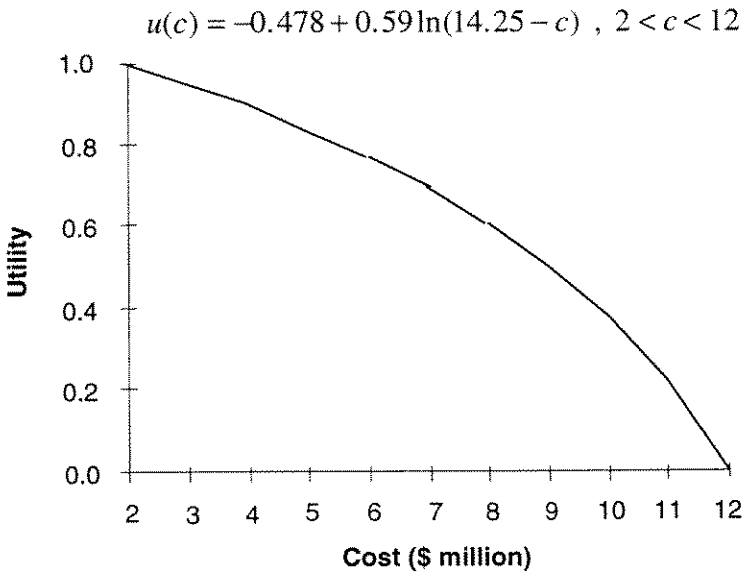

Figure 13.6 Example of an increasingly risk averse utility function over cost

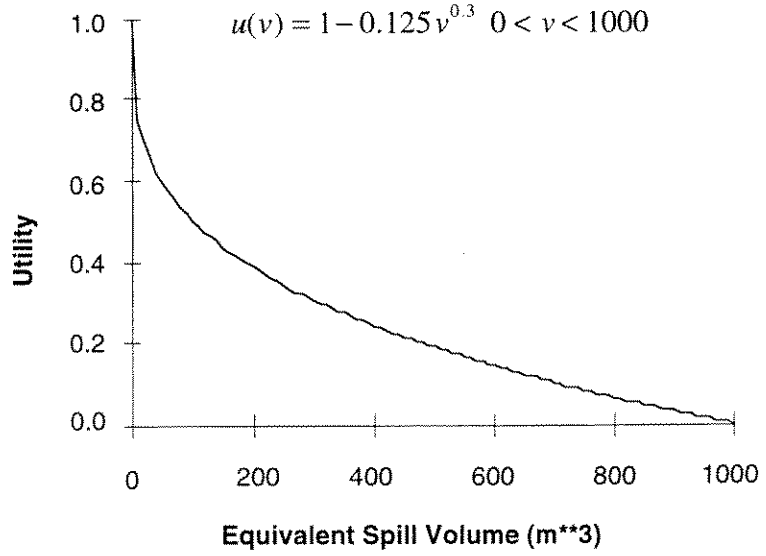

Figure 13.7 Example of a risk prone utility function over equivalent spill volume

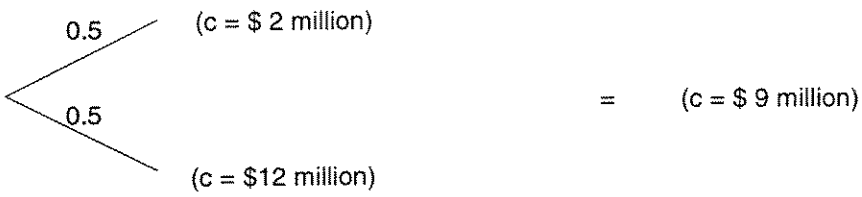

a)

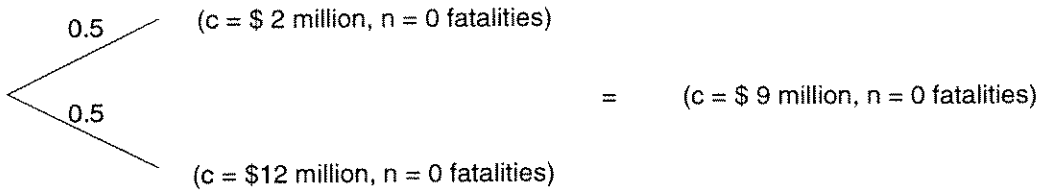

b)

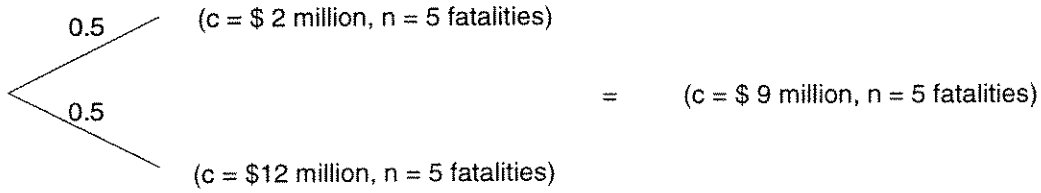

c)

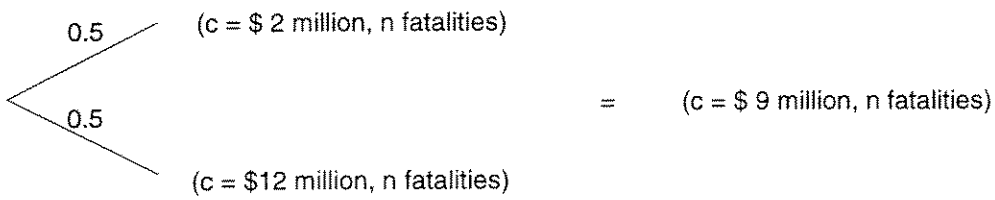

d)

Figure 13.8 Illustration of the conditions necessary to justify preferential independence

14.0 APPLICATION TO DECISION MAKING

14.1 Introduction

Sections 3.0 to 13.0 of this document give a description of the data and models used to define each influence diagram node. Once this information is defined, the influence diagram can be solved to produce the decision making aids that are required to make an optimal choice. The solution methodology and resulting outputs are described in PIRAMID Technical Reference Manual (Nessim and Hong 1995). This section gives a description of the main outputs for the consequence analysis problem and discusses their use in decision making.

14.2 The Main Decision Making Tools

The main decision making tool obtained by solving the influence diagram is the expectation of the value node for each choice. As discussed in Section 13.0, three different methods for defining the value node are available. Each of these methods corresponds to a different decision making criterion. These are as follows:

- *Utility optimization.* The result of this method is illustrated in Figure 14.1, in which the expected utility is plotted for each choice. Since the utility function is defined in such a way as to incorporate all of the decision maker's preferences, risk attitudes and tradeoffs between different attributes, the optimal choice in this case is the one that achieves the maximum expected utility.

- *Cost optimization.* Figure 14.2a illustrates the format of the results for unconstrained cost optimization (applicable to pipelines carrying products with no significant environmental impact potential). This plot shows the total expect cost for each choice. The optimal choice is the one that achieves the minimum expected cost. The format of the results for constrained cost optimization (applicable to pipelines carrying products with significant environmental impact potential) is shown in Figure 14.2b. This plot shows the expected cost versus the criterion used to define the constraint for each choice. In this case, the expected total cost is plotted against the equivalent spill volume associated with the choice. The constraint, defined by the maximum allowable equivalent volume, is also plotted on the figure. A strict application of the constrained cost optimization would mean that all choices that do not meet the constraint should be eliminated. Among the choices that meet the constraint, the one with the lowest expected cost is optimal. In practical terms, Figure 14.2b can be used in a more flexible sense to compare different options with respect to their expected total cost and their deviation from the constraint. For example, if the absolute lowest cost option does not meet the constraint, the expected cost associated with meeting the constraint can be defined as the difference between the absolute lowest cost and the lowest cost for an option that meets the constraint. The figure can also be used to determine how far the lowest cost option is from meeting the constraint. Subjective assessment can then be made regarding which option should be selected.

Application to Decision Making

In addition, the influence diagram can be used for *sensitivity analyses*. By changing the value of a given parameter and repeating the calculation, the impact of this parameter on the final choice can be determined. This type of sensitivity analysis can be performed for input parameters that are not well defined. It can increase the confidence of the decision maker that the best decision has been made. For example, if a parameter that cannot be defined with accuracy is changed within a reasonable range without affecting the optimal choice, confidence in the appropriateness of this choice is increased. Similarly, sensitivity analysis can be used to determine the ranges of a given parameter for which different choices are optimal. The optimal choice in this case can be obtained by placing the parameter in a given range instead of giving it a precise value or probability distribution, which is an easier way of characterizing parameters with high uncertainty. The user of the methodology can develop many similar applications of sensitivity analysis, producing valuable information to understand and substantiate the final choice.

14.3 Information on Other Parameters

In addition to the main decision aids described in Section 14.2, probabilistic descriptions can be obtained for any node parameter in the diagram. Such information can be useful in assessing the contributions of different factors to the overall risk and understanding all the implications of a certain choice. This information includes:

1. *Expected values of node parameters for all choices.* Any node in the influence diagram can be treated as the final (or pseudo-value) node, creating a truncated diagram that includes only the predecessors of that node. Analysis of this new diagram allows the user to calculate the expected value of the node parameter in question for the different choices. For example, by treating the number of fatalities node as the final node (see Figure 14.2b), the total expected number of fatalities for each decision can be obtained. Similarly, the total expected spill impact volume can be calculated for each decision by treating it as the final node. This information gives insight into the actual consequences contributing to the total risk as characterized by the value node.

2. *Conditional probability distributions of functional node parameters.* For any intermediate node, the probability distribution of the node parameter for any combination of the direct conditional predecessors of the node can be obtained. For example, the probability distributions of the hazard type and the number of fatalities can be obtained for any selected combination of season, failure section, product and failure mode. This information is useful in understanding the relative contributions of different factors to the risk to human life (*e.g.*, the risk may be dominated by one product).

14.4 Risk Assessment Applications

It must be recognized that although this approach is geared toward decision problems in which different choices are being evaluated, the methodology can also be used for *risk assessment*. In this type of analysis, a quantitative estimate of the risk associated with an existing pipeline is required, without consideration of any specific maintenance choices. In this case, the influence

diagram can be developed with only one choice (representing the status quo), and the results would represent the financial, environmental, life and overall risks associated with the pipeline. For example, the total cost and residual spill volume nodes can be used to assess the expected level of financial and environmental risks posed by a certain pipeline segment.

Figures

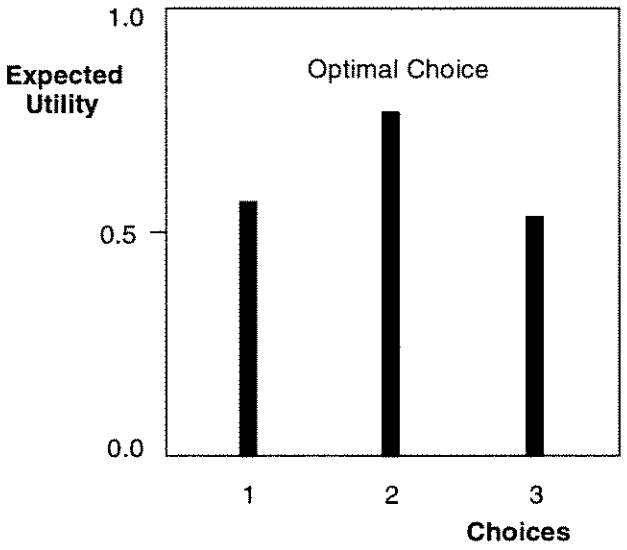

Figure 14.1 Expected utility plot for different choices

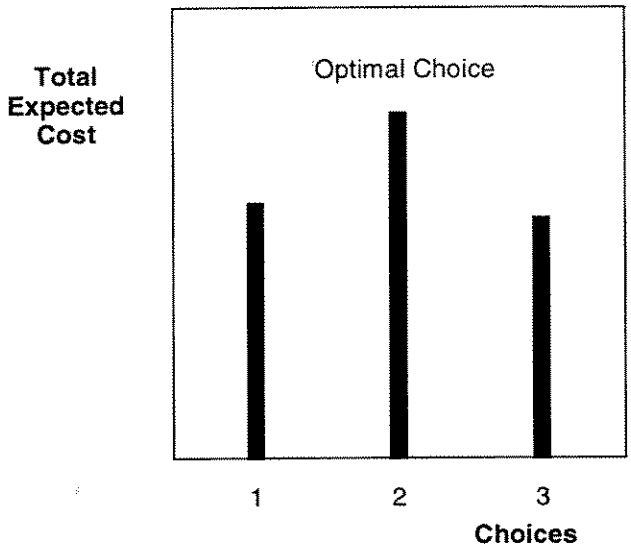

a) cost optimization without constraint

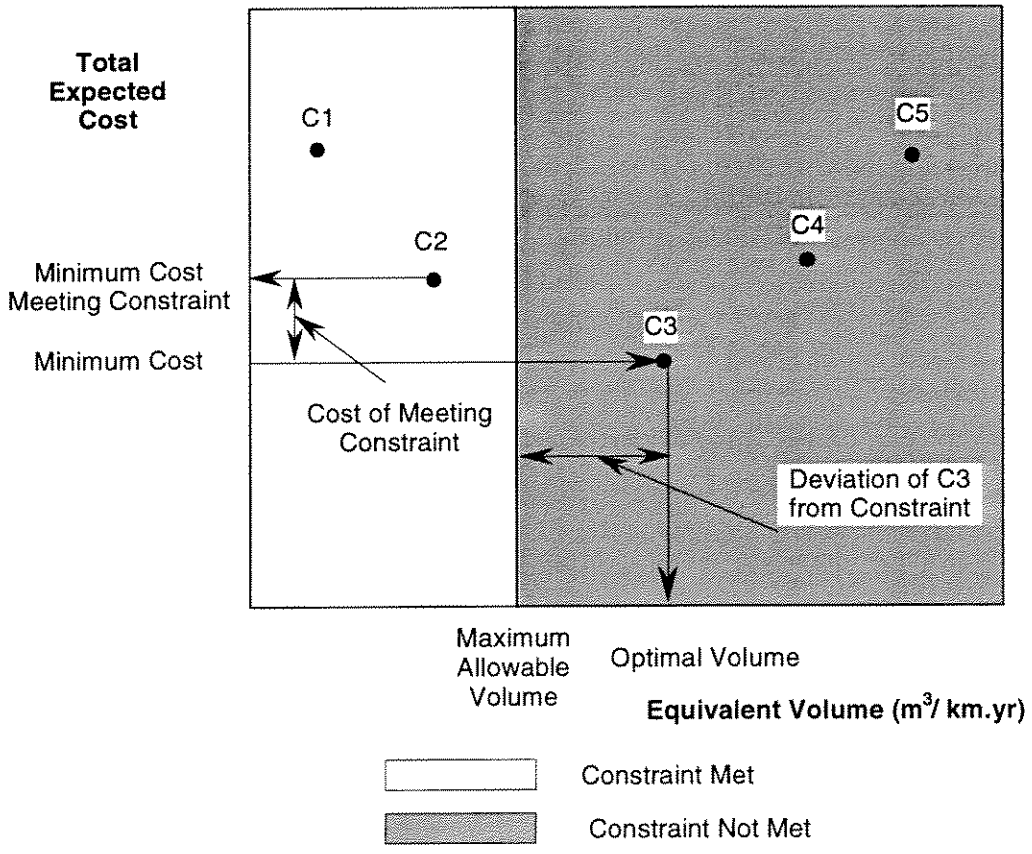

b) cost optimization with constraint

Figure 14.2 Illustration of the output for the cost optimization approach

15.0 REFERENCES

Stephens, M. J., Nessim, M. A. and Chen, Q. 1995a. A Methodology for Risk-Based Optimization of Pipeline Integrity Maintenance Activities - PIRAMID Technical Reference Manual No. 1.2. Confidential to C-FER's Pipeline Program Participants, C-FER Report 94006, October.

Nessim, M. A. and Hong, H. P. 1995. Probabilistic Decision Analysis Using Influence Diagrams: PIRAMID Technical Reference Manual No. 2.1. Confidential to C-FER's Pipeline Program Participants, C-FER Report 94022, October.

Weather Conditions

CCPS 1989. Guidelines for Chemical Process Quantitative Risk Analysis. Center for Chemical Process Safety of the American Institute for Chemical Engineers, New York, N. Y.

Environment Canada 1984. Canadian Climate Normals 1951 - 1980, Minister of Supply and Services Canada, Ottawa.

MMS 1995. Gulf of Mexico Sales 157 and 161: Central and Western Planning Areas, Draft Environmental Impact Statement. Minerals Management Service Gulf of Mexico OCS Region, U.S. Department of the Interior, New Orleans.

NOAA 1975. Summary of Synoptic Meteorological Observations, North American Coastal Marine Areas - Revised Atlantic and Gulf Coasts, Volume 4, Areas 22 - 29. Environmental Data Service, National Oceanic and Atmospheric Administration of the U. S. Department of Commerce.

NOAA 1976. A Climatological Analysis of Pasquill Stability Categories Based on 'STAR' Summaries. National Climatic Center, National Oceanic and Atmospheric Administration of the U. S. Department of Commerce.

Pipe Performance

Jansen, H. J. M. 1995. Pipeline Integrity. Proceedings of the EPRG/PRC Tenth Biennial Joint Technical Meeting on Line Pipe Research, Cambridge, UK, 1-1 to 1-11.

Mare, R. F. and Bakouros, Y. L. 1994. Predicting Pipeline Reliability Using Descriminant Analysis: A Comparison Between North Sea and Gulf of Mexico Performance. Proceedings of the Fourth International Offshore and Polar Engineering Conference, Osaka, Japan, 460-466.

Stephens, M. J., Nessim, M. A. and Chen. Q. 1995b. Probabilistic Assessment of Onshore Pipeline Failure Consequences: PIRAMID Technical Reference Manual No. 3.1. Confidential to C-FER's Pipeline Program Participants, C-FER Report 94035, October.

References

Release Characteristics

Fearnehough, G. D. 1985. The Control of Risk in Gas Transmission Pipeline. Institute of Chemical Engineers, Symposium Series No. 93, 25-44.

Stephens, M. J., Nessim, M. A. and Chen. Q. 1995b. Probabilistic Assessment of Onshore Pipeline Failure Consequences: PIRAMID Technical Reference Manual No. 3.1. Confidential to C-FER's Pipeline Program Participants, C-FER Report 94035, October.

Hazard Type

Crossthwaite, P. J., Fitzpatrick, R. D. and Hurst, N. W. 1988. Risk Assessment for the Siting of Developments Near Liquefied Petroleum Gas Installations. Institute of Chemical Engineers, Symposium Series No. 110, 373-400.

Fearnehough, G. D. 1985. The Control of Risk in Gas Transmission Pipeline. Institute of Chemical Engineers, Symposium, No. 93, 25-44.

EGIG 1993. Gas pipeline incidents, Report 1970-1992, European Gas Pipeline Incident Data Group.

Number of Fatalities

FEMA/DOT/EPA 1989. Handbook of Chemical Hazard Analysis Procedures, U.S. Federal Emergency Management Agency, U.S. Department of Transportation, U.S. Environmental Protection Agency, Washington.

Lees 1980. Loss Prevention in the Process Industries. Butterworth, London.

MMS 1995. Gulf of Mexico Sales 157 and 161: Central and Western Planning Areas, Draft Environmental Impact Statement. Minerals Management Service Gulf of Mexico OCS Region, U.S. Department of the Interior, New Orleans.

Nessim, M. A. and Hong, H. P. 1995. Probabilistic Decision Analysis Using Influence Diagrams: PIRAMID Technical Reference Manual No. 2.1. Confidential to C-FER's Pipeline Program Participants, C-FER Report 94022, October.

Spill Characteristics

Dicks, B. 1992. The Behaviour of Spilled Oil and Consequences for Clean-up. Proceedings of the CONCAWE/DGMK Scientific Seminar, "Remediation of Oil Spills", Hamburg, May.

Ford, R. G. 1985. Oil Slick Sizes and Length of Coastline Affected: A Literature Survey and Statistical Analysis. Final Report prepared for U. S. Department of the Interior, Minerals Management Service, Pacific OCS Region, Contract No. 14-12-0001-30224, MMS85-0105, October.

References

Gundlach, E. R., Finkelstein, K. J. and Sadd, J. L. 1981. Impact and Persistence of IXTOC I Oil on the South Texas Coast. Proceedings of the 1981 Oil Spill Conference (Prevention, Behavior, Control, Clean-up), Atlanta, March.

Gundlach, E. R. and Hayes, M. O. 1978. Vulnerability of Coastal Environments to Oil Spill Impacts. Marine Technical Society Journal, Vol. 12, No. 4.

ITOPF 1986. Fate of Marine Oil Spills. Technical Information Paper No. 11. ITOPF, London.

MMS 1992. Adaptation of the Minerals Management Service's Oil-Weathering Model for Use in the Gulf of Mexico Region. Minerals Management Service Gulf of Mexico OCS Region, U.S. Department of the Interior, OCS Study MMS 92-0034, New Orleans, June.

Poley, J. Ph. 1981. Tailored Oilspill Contingency Planning for Offshore Blowouts - A Tale of Lessons-Learned. Proceedings of the 1981 Oil Spill Conference (Prevention, Behavior, Control, Clean-up), Atlanta, March.

Schulze, R. 1994. Use of Spill Encounter Rate to Establish Regulatory Requirements for Advancing Skimmers. Proceedings of the Seventeenth Arctic and Marine Oilspill Program Technical Seminar, Vancouver, June.

Smith, R. A., Slack, J. R., Wynat, T. and Lanfear, K. J. 1982. The Oil Spill Risk Analysis Model of the U. S. Geological Survey. U. S. Geol. Surv. Prof. Paper., 1227. 40 pp.

Stephens, M. J., Nessim, M. A. and Chen. Q. 1995b. Probabilistic Assessment of Onshore Pipeline Failure Consequences: PIRAMID Technical Reference Manual No. 3.1. Confidential to C-FER's Pipeline Program Participants, C-FER Report 94035, October.

Repair and Interruption Costs

Herbert, C. and Corder, J. 1995. Repair Considerations, Working Group Report 4. Proceedings of the International Workshop on Damage to Underwater Pipelines, New Orleans, February.

Mohr Research and Engineering, Inc. 1992. Diver Assisted Pipeline Repair Manual, PR-209-9122. Prepared for the Offshore Supervisory Committee of the Pipeline Research Committee, American Gas Association, December.

Release and Damage Costs

Blaikley, D. R., Dietzel, G. F. L., Glass, A. W. and van Kleef, P. J. 1977. "Sliktrak" - A Computer Simulation of Offshore Oil Spills, Cleanup, Effects and Associated Costs. Proceedings of the 1977 Oil Spill Conference, 45-52.

References

Geselbracht, L. and Logan, R. 1993. Washington's Marine Oil Spill Compensation Schedule - Simplified Resource Damage Assessment. Proceedings of the 1993 International Oil Spill Conference (Prevention, Preparedness, Response), Tampa, March-April.

Gundlach, E. R., Finkelstein, K. J. and Sadd, J. L. 1981. Impact and Persistence of IXTOC I Oil on the South Texas Coast. Proceedings of the 1981 Oil Spill Conference (Prevention, Behavior, Control, Clean-up), Atlanta, March.

Holmes, P. D. 1977. A Model for the Costing of Oil Spill Clearance Operations at Sea. Proceedings of the 1977 Oil Spill Conference, 39-43.

MMS 1995. Gulf of Mexico Sales 157 and 161: Central and Western Planning Areas, Draft Environmental Impact Statement. Minerals Management Service Gulf of Mexico OCS Region, U.S. Department of the Interior, New Orleans.

Moller, T. H., Parker, H. D. and Nichols, J. A. 1987. Comparative Costs of Oil Spill Cleanup Techniques. Proceedings of the 1987 Oil Spill Conference (Prevention, Behavior, Control, Cleanup), Baltimore, April.

Robilliard, G. A., Fischel, M., Desvousges, W. H., Dunford, R. W. and Mathews, K. 1993. Evaluation of Compensation Formulae to Measure Natural Resource Damages. Proceedings of the 1993 International Oil Spill Conference (Prevention, Preparedness, Response), Tampa, March-April.

Stephens, M. J., Nessim, M. A. and Chen. Q. 1995b. Probabilistic Assessment of Onshore Pipeline Failure Consequences: PIRAMID Technical Reference Manual No. 3.1. Confidential to C-FER's Pipeline Program Participants, C-FER Report 94035, October.

Total Cost

Marin, A. 1986. "Evaluating the nation's risk assessors: nuclear power and the value of life". Public Money, 6(1), 41-45.

Stephens, M. J., Nessim, M. A. and Chen. Q. 1995b. Probabilistic Assessment of Onshore Pipeline Failure Consequences: PIRAMID Technical Reference Manual No. 3.1. Confidential to C-FER's Pipeline Program Participants, C-FER Report 94035, October.

Value

Bell, D. W. 1977. A Decision Analysis of Objectives for a Forest Pest Problem. Conflicting Objectives in Decisions, edited by Bell, Keeney and Raiffa. John Wiley & Sons, pp. 389 - 421.

Farmer, F. R. 1967. Siting Criteria - A New Approach. Nuclear Safety, 8, pp. 539 - 548.

References

Hax, A. C. and Wiig, K. M. 1977. The Use of Decision Analysis in Capital Investment Problems. Conflicting Objectives in Decisions, edited by Bell, Keeney and Raiffa. John Wiley & Sons, pp. 277 - 297.

HSE 1988. The Tolerability Risk from Nuclear Power Stations, Health and Safety Executive, London, U.K.

HSE 1989. Risk Criteria for Land-Use Planning in the Vicinity of Major Industrial Hazards, Health and Safety Executive, London, U.K.

Jordaan, I. J. 1982. Private Communication.

Kalelkar, A. S. Partridge, L. J. and Brooks, R. E. 1974. Decision Analysis in Hazardous Material Transportation. Proceedings, The 1974 International Conference on Control of Hazardous Material Spills. American Institute of Chemical Engineers, San Francisco, California, pp. 336 - 344.

Keeney, R. L. 1973. A Decision Analysis with Multiple Objectives: The Mexico City Airport. Bell Journal of Economics and Management Science, 4, pp. 101 - 117.

Keeney, R. L. and Nair, K. 1975. Decision Analysis for the Siting of Nuclear Power Plants--The Relevance of Multiattribute Utility Theory. Proceedings, IEEE, 63, pp. 494 - 501.

Keeney, R. L. and Raiffa, H. 1976. Decisions with Multiple Objectives: Preferences and Value Tradeoffs. John Wiley & Sons.

MIACC 1993. Land Use Guidelines for Pipeline Corridors, Major Industrial Accidents Council of Canada, Ottawa, Ontario.

Ramsay, S. and Hilbert, M. 1994. Consequence Modelling for Transportation Risks Associated with the ASWMS. Final Report prepared for the Institute for Risk Research, University of Waterloo.

Schlaifer, R. 1969. Analysis of Decisions Under Uncertainty. McGraw Hill Book Co.

Statistics Canada 1990. Canada Year Book, Ottawa, Ontario.

Stephens, M. J., Nessim, M. A. and Chen, Q. 1995a. A Methodology for Risk-Based Optimization of Pipeline Integrity Maintenance Activities - PIRAMID Technical Reference Manual No. 1.2. Confidential to C-FER's Pipeline Program Participants, C-FER Report 94006, October.

APPENDIX A

PHYSICAL PROPERTIES OF REPRESENTATIVE PRODUCT GROUPS

The following describes the information sources and calculation methods employed to define representative petroleum products for each product group identified in Table 4.7, and to develop the physical properties data base given in Table 2.8.

(1) For all product groups the following properties are based on Weiss (1980):

- lower flammability limit (C_{LFL});
- heat of combustion (H_c);
- heat of vaporization (H_{vap});
- normal boiling point (T_b);
- specific gravity ratio (SGR); and
- specific heat ratio of vapour (γ).

For gasolines, kerosenes and gas oils, the normal boiling point is taken as the lower value of the given range. Since crude oil has a particularly broad range of boiling points, its mid-point value of 290 °C (IARC 1989) is used as a representative value.

(2) For product groups involving compounds with a single carbon number (*e.g.*, methane, ethane, propane, butane and pentane), molecular weight (M_w), specific heat of liquid (c_p), and the parameters used for vapour pressure calculation are taken from Reid *et al.* (1987).

The vapour pressure parameters include:

- critical temperature (T_c);
- critical pressure (P_c); and
- constants *VPa*, *VPb*, *VPc* and *VPd*.

The equation for vapour pressure (P_v) is

$$\ln(P_v/P_c) = (1-x)^{-1} [(VPa)\, x + (VPb)\, x^{1.5} + (VPc)\, x^3 + (VPd)\, x^6)] \qquad [A.1]$$

where: $x = T/T_c$, T and T_c are in °K, and P_v and P_c are in bars.

The properties given for propanes are based on n-propane (C_2H_6), properties for butanes are based on n-butane (C_4H_{10}), and those for pentane are based on n-pentane (C_5H_{12}). Since

pentane is the major constituent of condensate, the properties of pentane may be used to represent condensate.

(4) Selected properties for petroleum products involving a mixture of hydrocarbon compounds with varying carbon numbers (*e.g.*, crude oils, gasolines, kerosenes and gas oils) can be determined in a rigorous manner if an accurate analytical report of product composition is available (*e.g.*, Reid *et al.* 1987). However, a simplified approximate approach was adopted in developing the product database for the following reasons: the exact composition of a given product type or product group will exhibit considerable variation; and, variations in the properties of interest, such as vapour pressure and liquid specific heat will not critically affect the outcome of acute hazard analysis for these low vapour pressure (LVP) products.

For each product mixture, a representative n-alkane was selected by examining the normal boiling point and the major hydrocarbon compounds present in the mixture. The following n-alkanes were selected because their boiling points are considered representative of the mixture as a whole (*i.e.*, boiling points are approximately in the middle of the range for the dominant hydrocarbon compounds):

- n-hexane (C_6H_{14}) for gasolines;
- n-dodecane ($C_{12}H_{26}$) for kerosenes; and
- hexadecane ($C_{16}H_{34}$) for gas oils and crude oil.

Molecular weight (M_w), specific heat of liquid (c_p), and the vapour pressure parameters for the above n-alkanes were then used to represent the respective product mixtures. For gasolines, Eqn. [A.1] was then used to calculated vapour pressure. For all other product mixtures, the following equation was used (Reid *et al.* 1987):

$$\ln (P_v) = (VPa) - (VPb)/T + (VPc) \ln(T) + (VPd)\, P_v/T^2 \qquad [A.2]$$

(6) The explosive yield factor (Y_f) for vapours and gases produced by all of hydrocarbon products considered was taken to be 0.03 (FEMA/DOT/EPA 1989).

(5) The kinematic viscosity (V_s) of all liquid hydrocarbon product mixtures considered was taken from Fingas *et al.* (1979).

References

FEMA/DOT/EPA. 1989. Handbook of Chemical Hazard Analysis Procedures, U.S. Federal Emergency Management Agency, U.S. Department of Transportation, U.S. Environmental Protection Agency, Washington, D.C.

Appendix A

Fingas, M.F., Duval, W.S., and Stevenson, G.B. 1979. The Basics of Oil Spill Clean-UP, Environmental Emergency Branch, Environmental Protection Service, Environment Canada, Ottawa.

IARC 1989. Occupational Exposures in Petroleum Refining; Crude Oil and Major Petroleum Fuels, Vol. 45 of IARC Monograph on the Evaluation of Carcinogenic Risk to Humans, International Agency for Research on Cancer, Lyon, France.

Reid, R. C., Prausnitz, J. M. and Poling, B. E. 1987. The Properties of Gases and Liquids, McGraw-Hill, New York, New York.

Weiss, G. ed. 1987. Hazardous Chemical Data Book, Noyes Data Corp., Park Ridge, New Jersey.

APPENDIX B

PRODUCT RELEASE AND HAZARD ZONE CHARACTERIZATION MODELS

B.1 Introduction

This Appendix describes the analytical models that are used to characterize product release and the associated acute release hazards resulting from failure of a gas or liquid pipeline. The models presented address the following:

- the release of gas and liquid products (*i.e.*, release rate and release volume);
- the evaporation of liquid pools (*i.e.*, evaporation rate);
- the dispersion of gas and liquid vapour (*i.e.*, volume concentration distribution);
- the heat intensity associated with fire hazards (*i.e.*, jet fire, pool fire and flash fire); and
- the overpressure associated with explosion hazards (*i.e.*, vapour cloud explosion).

The models described in this appendix have been adapted from widely recognized models existing in the public domain. Primary reference sources include: 'Handbook of Chemical Hazard Analysis Procedures' (FEMA/DOT/EPA 1989);'Guidelines for Use of Vapour Cloud Dispersion Models' (Hanna and Drivas 1987); 'Techniques for Assessing Industrial Hazards' (Technica 1988); 'Loss Prevention in the Process Industries' (Lees 1980); and Brzustowski's work on hydrocarbon flares (Brzustowski 1971, 1973, and 1976).

Each of the following sections provides the technical basis for a particular model, including a detailed description of the associated equations and any major assumptions. The sections are organised as follows:

Section B.2 Release of Gas

Section B.3 Release of Liquid

Section B.4 Evaporation of Liquid

Section B.5 Jet Fire

Section B.6 Pool Fire

Section B.7 Dispersion of Neutral Buoyancy Gas

Section B.8 Dispersion of Dense Gas

Appendix B

Section B.9 Vapour Cloud Fire

Section B.10 Vapour Cloud Explosion

B.2 Release of Gas

B.2.1 Overview

- *Scenario description.* Discharge of gas from a pressurized pipeline.
- *Output.* Release rate and release volume where the release rate is an effective steady-state release rate for use in assessing the severity of acute hazards such as fires and explosions.
- *Sources.* The model for release rate is based on the steady-flow of perfect gases (FEMA/DOT/EPA 1989, Hanna and Drivas 1987, and Lees 1980). Both choked and non-choked flow conditions are considered.

B.2.2 Assumptions

- The product is idealized as a perfect gas.
- Pipeline failures are classified as leaks or ruptures. For leaks the orifice is assumed to be a circular hole of variable diameter (hole diameter << pipe diameter). For ruptures the orifice is assumed to be a circular hole with a diameter equal to the inside diameter of the pipe.
- The maximum initial release rate is estimated assuming frictionless gas flow through the pipeline at operating pressure. Note, however, that frictional effects at the orifice are taken into account by multiplying the release rate by a friction factor of 0.62 which is commonly used for circular holes with sharp edges (Lees 1980).
- For leaks associated with small hole sizes it is conservatively assumed that the initial maximum release rate is sustained. However, for large hole sizes associated with large leaks and ruptures, it is recognized that the initial release rate will decrease rapidly with time due to frictional effects and dropping effective line pressure. This time dependent release rate for large hole sizes is approximated by a reduced effective steady-state release rate that is intended to serve as a representative release rate for use in characterizing the severity of acute release hazards (*i.e.,* fires and explosions). The effective release rate is assumed to be a fractional multiple of the maximum initial release rate. The value of the fractional multiplier is further assumed to vary linearly with the ratio of effective hole diameter to line diameter. For a hole size ratio of 1.0 (*i.e.,* full bore rupture) the multiplier is 1/3 and as the hole size ratio approaches zero (*i.e.,* for pin holes) the multiplier approaches 1.0. Based on a review of published information on time dependent release rates and steady-state approximations for gas pipelines (e.g., HSE 1994) it is considered that the chosen rate multiplier of 1/3 will provide a reasonable estimate of the effective release rate for acute hazard scenarios.
- Product release is assumed to be driven by a positive pressure differential. Under certain circumstances however (*e.g.* release from a low pressure pipeline in deep water), the pressure differential will be negative and other effects such as product buoyancy need to be considered

in estimating release rate. These effects are addressed in an approximate fashion by assuming a minimum release velocity equal to the normal product flow velocity. For a full bore rupture scenario this implies a release rate equal to the product flow rate.

- The outside area surrounding the orifice is assumed to be filled with escaping gas, therefore, sonic velocity for discharge into both air and water is established in the medium of a perfect gas.
- The variation in internal pressure due to hydrostatic pressure is not considered for gas pipelines because the associated effect is negligible.
- The volume of gas release is jointly controlled by the release rate, the product flow rate, the block valve spacing, and the emergency response time (*e.g.*, time to close valves or time to plug leaks).

B.2.3 Model Description

Maximum release rate from a pressurized gas pipeline can be estimated using the following equations (FEMA/DOT/EPA 1989, Hanna and Drivas 1987, and Lees 1980):

(1) Choked flow conditions (sonic velocity)

$$(\dot{m}_{RG})_{max} = C_d A_h \left[\gamma P_1 \rho \left(\frac{2}{1+\gamma} \right)^{\frac{\gamma+1}{\gamma-1}} \right]^{1/2} \qquad [B.2.1]$$

for $\frac{P_2}{P_1} \leq \left(\frac{2}{1+\gamma} \right)^{\frac{\gamma}{\gamma-1}}$

(2) Non-choked flow condition

$$(\dot{m}_{RG})_{max} = C_d A_h \left\{ \frac{2\gamma P_1 \rho}{\gamma - 1} \left[\left(\frac{P_2}{P_1} \right)^{\frac{2}{\gamma}} - \left(\frac{P_2}{P_1} \right)^{\frac{\gamma+1}{\gamma}} \right] \right\}^{1/2} \qquad [B.2.2]$$

for $1 > \frac{P_2}{P_1} \geq \left(\frac{2}{1+\gamma} \right)^{\frac{\gamma}{\gamma-1}}$

When internal pressure P_1 is less than external pressure P_2 (*e.g.*, for low pressure lines in deep water), Equation [B.2.2] is not applicable. In this case, the discharge velocity is assumed to be equal to the pipeline flow velocity under normal operating conditions. For a full bore rupture (hole size equal to pipe diameter) this assumption leads to a release rate equal to the flow rate.

Appendix B

Variables and constants in Equations [B.2.1] and [B.2.2] include:

$\dot{m}_{RG}$ = mass release rate of gas (kg/s);

C_d = 0.62, friction factor (Lees 1980);

A_h = area of the hole (m^2);

γ = specific heat ratio of the product;

P_1 = $P_0 + P_a$, internal pressure (Pa);

P_2 = $P_a + \rho_w g H_0$, external pressure (Pa);

P_0 = pipeline operating pressure (Pa);

P_a = atmospheric pressure (Pa);

ρ_w = 1000 kg/m^3, density of water;

g = 9.8 m/s^2, acceleration due to gravity;

H_0 = water depth at the release location (m);

ρ = $(P_0 + P_a)\, M_w / R\, T_1$, density of a perfect gas (kg/m^3); [B.2.3]

M_w = molecular weight (kg/mol);

R = 8.413 Pa-m^3/mol-°K, gas constant; and

T_1 = product flow temperature (°K).

B.2.4 Calculation Algorithm

1. Calculate gas density (Equation [B.2.3]).
2. Calculate the equivalent steady release rate using:

$$\dot{m}_{RG} = \alpha\, (\dot{m}_{RG})_{max} \geq \dot{m}_0\, A_h / A_0 \qquad [B.2.4]$$

where the maximum release rate, $(\dot{m}_{RG})_{max}$, is defined in Equations [B.2.1] and [B.2.2]. The ratio between the effective steady-state release rate and the instantaneous maximum release rate, α, is defined as a linear function of effective hole area:

Appendix B

$$\alpha = 1 - 2A_h / 3A_0 \geq 1/3 \qquad [B.2.5]$$

in which A_0 is the cross-sectional area of the pipe. It is noted that [B.2.4] assumes that the release velocity is always greater than pipeline flow velocity associated with flow rate $\dot{m}_0$.

3. Calculate weight of lost product.

$$M_R = M_0 + \dot{m}_0 t_1 \qquad \text{for ruptures} \qquad [B.2.6a]$$

and

$$M_R = \dot{m}_{RG} t_2 \qquad \text{for leaks} \qquad [B.2.6b]$$

where M_R = total weight of released product (kg);

M_0 = weight of product between block valves (kg);

$\dot{m}_0$ = pipeline flow rate for normal operation (kg/s);

t_1 = min $\{t_{dtect}, \rho V_{dtect} / \dot{m}_{RG}\} + t_{close}$, time between failure and valve closure (s);

t_2 = min $\{t_{dtect}, \rho V_{dtect} / \dot{m}_{RG}\} + t_{stop}$, time between failure and leak stoppage (s);

V_{dtect} = detectable release volume (m^3);

t_{dtect} = time to leak detection (s);

t_{close} = time to block valve closure (s); and

t_{stop} = time to leak stoppage (s).

4. Calculate total release volume at standard conditions.

$$V_R = M_R / \rho_s \qquad [B.2.7]$$

where V_R = total release volume (m^3); and

ρ_s = product density at standard temperature (60°F) and pressure (atmospheric pressure).

Appendix B

B.3 Release of Liquid Product

B.3.1 Overview

- *Scenario description.* Discharge of liquid product from a pressurized pipeline.
- *Output.* Release rate and release volume where the release rate is an effective steady-state release rate for use in assessing the severity of acute hazards such as fires and explosions.
- *Sources.* Release rate for liquid discharge is calculated using the Bernoulli equation for steady flow of incompressible fluids. The equations for the flashing and aerosol fraction of HVP liquids are based on work by Lees (1980) and Hanna and Drivas (1987). The Fauske-Cude method for two-phase critical flow (Technica 1988) is used for two-phase discharge of HVP products.

B.3.2 Assumptions

- The liquid product is idealized as an incompressible fluid.
- Pipeline failures are classified as leaks or ruptures. For leaks the orifice is assumed to be a circular hole of variable diameter (hole diameter << pipe diameter). For ruptures the orifice is assumed to be a circular hole with a diameter equal to the inside diameter of the pipe.
- Flow in pipeline is assumed to be turbulent flow in liquid phase.
- Friction at the orifice is taken into account by multiplying the release rate with a friction factor of 0.62 which is commonly used for circular holes with sharp edges (Lees 1980).
- Release rate is driven by a pressure differential and therefore depends on the effective internal line pressure. For leaks associated with small hole sizes the effective internal pressure is equal to the operating pressure. However, for large hole sizes associated with large leaks and ruptures, it is recognized that for incompressible fluids the effective internal pressure will approach the product vapour pressure. This hole size dependent driving pressure is approximated by an effective internal pressure that is assumed to vary linearly with release rate. For release rates greater than or equal to the flow rate the effective internal pressure is set equal to the product vapour pressure. For release rates approaching zero the effective pressure approaches the line operating pressure. (Note that the above implies an iterative calculation process.)
- Product release is assumed to be driven by a positive pressure differential. Under certain circumstances, however (*e.g.* release from a low pressure pipeline in deep water), the pressure differential will be negative and other effects such as product buoyancy need to be considered in estimating release rate. These effects are addressed in an approximate fashion by assuming a minimum release velocity equal to the pipe flow velocity. For full bore rupture scenarios this implies a release rate equal to the product flow rate.
- If product is released into air and the pipeline operating temperature exceeds the product boiling point, a fraction of liquid will be assumed to immediately flash to vapour and an

equal amount of liquid will be assumed to become an aerosol and evaporate rapidly into the air.

- The volume of gas release is jointly controlled by the release rate, the product flow rate, the line elevation profile and block valve spacing, and the emergency response time (*e.g.*, time to close valves or time to plug leaks).

B.3.3 Model Description

1. Liquid release.

Release rate in liquid phase can be calculated by the Bernoulli equation based on momentum conservation (FEMA/DOT/EPA 1989, Hanna and Drivas 1987, and Lees 1980):

$$\dot{m}_R = C_d A_h [\, 2\, \rho_l (P_1 - P_2)\,]^{1/2} \qquad [B.3.1]$$

where ρ_l is the density of liquid (kg/m^3).

It is noted that Equation [B.3.1] is not applicable when the internal pressure P_1 is less than the external pressure P_2. In this case, the discharge velocity is set equal to the pipeline flow velocity under normal operating conditions (as long as the block valves remain open) by adopting the following assumption

$$\dot{m}_R \geq \dot{m}_0\, A_h / A_0 \qquad [B.3.2]$$

For a rupture with hole size equal to pipe diameter, this leads to a release rate equal to the nominal product flow rate.

2. Two-phase release. The adopted method was proposed by Fauske and Cude (Technica 1988) which assumes the critical pressure at the orifice to be 55% of internal pressure, or

$$P_c = 0.55\, P_1 \qquad [B.3.3]$$

The flow rate under the choked flow condition is calculated by

$$\dot{m}_R = C_d A_h [\, 0.9\, \rho_m P_1]^{1/2} \qquad [B.3.4]$$

in which ρ_m is the mean density of two-phase mixture

$$\rho_m = [\, F_{vap}/\rho_v + (1 - F_{vap})/\, \rho_l\,]^{-1} \qquad [B.3.5]$$

and ρ_v is the density of vapour (kg/m^3). The vapour fraction that flashes at critical condition is defined as

$$F_{vap} = (T_1 - T_{bc})\, c_p / H_{vap} \qquad [B.3.6]$$

where T_{bc} = boiling point at the critical pressure (°K);

c_p = specific heat of liquid (J/kg °K); and

H_{vap} = heat required to evaporate the liquid (J/kg).

3. Effect of hydrostatic pressure. For a pipeline with a varying elevation profile, the equivalent hydrostatic pressure, after the friction losses are accounted for, is given by

$$P_h = \rho_l\, g\, H_1 \qquad [B.3.7]$$

The equivalent liquid height

$$H_1 = H_{10} / (1 + f\, L / D) \qquad [B.3.8]$$

in which H_{10} is the liquid height and f is the friction factor

$$f = 1.14 - 2 \lg (\varepsilon/D + 21.25/Re^{0.9}) \qquad [B.3.9]$$

The dominant factor affecting f is the viscosity of liquid which has a broad range of variability for different hydrocarbon products.

The term of $(1 + f\, L / D)^{-1}$ in Equation [B.3.8] reflects the loss of pressure due to friction. It is based on Darcy's formula for pipe flow (Perry 1984) that pressure loss due to friction

$$P_f = f\, u^2\, \rho_l\, L / 2\, D \qquad [B.3.10]$$

Since most liquid pipelines operate under turbulent flow condition, f is usually calculated for turbulent flow by equations such as whose developed by Colebrook. Equation [B.3.9] is a simplified form of Colebrook's equation proposed by Jain (1976).

Variables in Equations [B.3.7] to [B.3.10] include:

H_0 = elevation difference between the crest and the failure location (m);

L = pipeline distance between the crest and the failure location (m);

D = pipeline diameter (m);

Appendix B

P_f = pressure loss due to friction (Pa);

u = pipe flow velocity after failure (m/s);

u_0 = pipe flow velocity for normal operation (m/s);

ε = pipe wall roughness ($\varepsilon = 0.05$ mm for steel pipes, see Perry 1984);

Re = $u_0 D / V_s$, Reynolds number; and

V_s = kinematic viscosity (m^2/s).

B.3.4 Calculation Algorithm

B.3.4.1 Release Rate of LVP Product

1. Calculate effective hydrostatic pressure using Equations [B.3.6] to [B.3.8].

2. Determine total effective internal pressure P_1 by

$$P_1 = P_i + P_h \qquad [B.3.11]$$

and

$$P_i = P_0 + P_a - (P_0 + P_a - P_{v0})\ \dot{m}_R / \dot{m}_0 \geq P_{v0} \qquad [B.3.12]$$

where P_{v0} is the product vapour pressure at pipeline operating temperature (T_1).

3. Calculate liquid release rate by iteratively solving [B.3.11] and [B.3.1]

B.3.4.2 Release Rate of HVP Product

1. Release of HVP liquid can be classified into three categories dependent on internal pressure (P_1) and vapour pressure (P_{v0}).

a. Liquid phase (when $P_c \geq P_{v0}$).

The calculation is essentially the same as that for LVP product. When P_c approaches, the release rate ($\dot{m}_1$) reaches its maximum which is noted as $\dot{m}_{c1}$.

b. Two-phase choked flow (when $P_c < P_{v0}$ and $\dot{m}_R > \dot{m}_{c1}$).

Appendix B

The release rate can be calculated following Equations [B.3.3] to [B.3.6]. Its consists of a vapour portion ($\dot{m}_g = F_{vap}\ \dot{m}_R$) and a liquid portion ($\dot{m}_l = (1 - F_{vap})\ \dot{m}_R$).

c. Transition zone between *a* and *b* (when $P_c < P_{v0}$ and $\dot{m}_R \leq \dot{m}_{c1}$).

When the liquid is above the boiling temperature but the flashing portion is not sufficient to form a choked flow (*e.g.* less than 1%), the release rate is assumed to remain at the maximum liquid release rate of $\dot{m}_{c1}$.

2. For HVP products released in air, a portion of the liquid flashes into vapour immediately. If the product temperature, which is taken to be equal to the pipeline temperature, exceeds the product boiling point (*i.e.*, $T_1 > T_b$), the total fraction (including flashing fraction and aerosol fraction) of vapour release is given by (Lees 1980, and Hanna and Drivas 1987):

$$\dot{m}_{RG} = 2\,(T_1 - T_b)\,c_p\,\dot{m}_l / H_{vap} + \dot{m}_g \qquad \text{[B.3.12]}$$

where $\dot{m}_{RG}$ = total vapour release rate (kg/s); and

T_b = normal boiling temperature of the liquid (°K).

Release rate for the liquid portion that does not flash is $\dot{m}_{RL} = \dot{m}_R - \dot{m}_{RG}$. The gas release rate ($\dot{m}_{RG}$) will be used for jet fire calculation, and the liquid release rate ($\dot{m}_{RL}$) will be used to evaluate evaporation and liquid pool fire consequences.

B.3.4.3 Release Volume

Calculate release volume according to the failure mode by

$$V_R = V_0 + \dot{m}_0\,t_1/\rho_l \qquad \text{for ruptures} \qquad \text{[B.3.13a]}$$

and

$$V_R = [\dot{m}_R\,t_1 + \dot{m}_{R2}\,(t_2 - t_1)]\,/\rho_l \qquad \text{for leaks} \qquad \text{[B.3.13b]}$$

where V_0 = volume of liquid between block valves that is available for release after valves closure (m^3); and

$\dot{m}_{R2}$ = release rate after block valve closure (kg/s).

The secondary release rate $\dot{m}_{R2}$ is calculated in a way similar to $\dot{m}_R$ as outlined above, except that the P_i in [B.3.11] always equals to the vapour pressure (P_{v0}) as the block valves are closed.

Appendix B

B.4 Evaporation of Liquid

B.4.1 Overview

- Scenario description: A spilled liquid evaporates either as a volatile liquid or as a cold boiling liquid, depending on the pool temperature and the boiling point of the liquid. LVP hydrocarbon liquids usually evaporate in a volatile manner while HVP liquids are more likely to behave as a cold boiling liquid.
- Output: Rate of evaporation.
- Sources: Models in the Handbook of Chemical Hazard Analysis Procedures (FEMA/DOT/EPA 1989) are used for pool spreading and evaporation of cold boiling liquids. The volatile evaporation model developed by the Engineering and Service Laboratory of U.S. Air Force (Kahler *et al.* 1989) is adopted for LVP liquids.

B.4.2 Assumptions

- Pool shape is circular and the size is assumed to be constant during evaporation.
- Variables such as ground slope and soil penetration that may affect pool size are not considered.
- Rate of evaporation is assumed to be constant.
- The total spill amount is assumed to evaporate (ground absorption is not modeled).

B.4.3 Model Description

1. Evaporation of a volatile liquid (Kahler *et al.* 1989)

$$f_V = 2.22\text{x}10^{-5}\, u_a^{0.75}\,(1+0.0043T_p^2)\,\frac{P_v\, M_w}{P_{vh}\, M_{wh}} \qquad \text{[B.4.1]}$$

where f_V = evaporation flux (kg/s/m^2);

u_a = wind speed (m/s);

P_{vh} = vapour pressure of hydrazine (Pa);

M_{wh} = molecular weight of hydrazine (kg/mol);

T_p = pool temperature (°C). It is assumed that T_p is the higher of ambient temperature and pipeline temperature and $T_p \geq 0$ °C.

Appendix B

Comparison with other models shows that this model gives an average to conservative evaporation rate (Hanna and Drivas 1987).

2. Evaporation of a cold boiling liquid (FEMA/DOT/EPA 1989)

$$f_V = 1.597 \times 10^{-6} (514.2 - T_b) M_w e^{-0.0043 T_b} \quad [B.4.2]$$

where T_b is the normal boiling point in degree Celsius.

3. Pool size from an instantaneous spill (FEMA/DOT/EPA 1989)

$$D_{max} = 1.798 \left[\frac{V_R^2 \rho}{f_V} \sqrt{\frac{g}{C_f}} \right]^{2/11} \quad [B.4.3]$$

where V_R = total release volume of liquid (m^3);

C_f = 0.5, ground friction coefficient.

4. Pool size from a continuous spill

$$D_{max} = 1.128 \sqrt{\frac{\dot{m}_{RL}}{f_V}} \quad [B.4.4]$$

in which the evaporation rate is assumed to be equal to the spill rate.

B.4.4 Calculation Algorithm

1. Calculate evaporation flux. First identify whether the liquid is volatile or cold boiling by comparing the pool temperature with the boiling point. The evaporation flux can then be calculated by using Eqn. [B.4.1] or [B.4.2].

2. Calculate pool size using Eqn. [B.4.3] or [B.4.4]. Identify the spill scenario as instantaneous or continuous by examining (FEMA/DOT/EPA 1989)

$$\tau = t_R f_V / \rho V_R^{1/3} \quad [B.4.5]$$

where t_R = min $\{ \frac{M_R}{m_R}, t_2 \}$

It is assumed to be an instantaneous spill if $\tau < 0.002$, or a continuous spill if $\tau \geq 0.002$.

3. Calculate evaporation rate by

Appendix B

$$\dot{m}_V = f_V \pi (D_{max}/2)^2 \qquad [B.4.6]$$

B.5 Jet Fire

B.5.1 Overview

- Scenario description: Gas or vapour emerging from a gas or HVP pipeline forms a jet at the puncture which becomes a jet flame when ignited.
- Output: The distribution of thermal radiation intensity.
- Sources: Dimensions of a jet fire were based on a model developed by Brzustowski (1976). Thermal radiation is calculated using a point source model.

B.5.2 Assumptions

- Centre of the flame is located halfway between the release point and the tip of flame.
- The total radiant heat of the fire is concentrated at the flame centre and radiates as a point source. (Note, this model is very approximate in the immediate vicinity of the jet fire however the validity of the model increases as the distance from the fire centre increases.)

B.5.3 Model Description

Equations for the dimensions of a jet fire are given by Brzustowski (1976). The non-dimensional curvilinear length of the flame is

$$\bar{S}_L = 2.04 \ \bar{C}_L^{-1.03} \qquad (\text{if } \bar{C}_L < 0.5) \qquad [B.5.1a]$$

or $$\bar{S}_L = 2.51 \ \bar{C}_L^{-0.625} \qquad (\text{if } \bar{C}_L \geq 0.5) \qquad [B.5.1b]$$

where

$$\bar{C}_L = C_{LFL} \frac{\dot{m}_{RG} \ M_w}{A_h \ \rho \ u_a \ M_{wa}} \qquad [B.5.2]$$

The term of ($\dot{m}_{RG}/A_h \rho$) gives the velocity of the released product u_j (m/s). M_{wa} is the molecular weight of air (about 29 g/mol), and C_{LFL} is the lower flammability limit.

The non-dimensional vertical and horizontal distances ($\bar{Z}_L$ and $\bar{X}_L$) corresponding to $\bar{S}_L$ can be calculated by

Appendix B

$$1.04\ \bar{\bar{X}}_L^{\,2} + 2.05\ \bar{\bar{X}}_L^{\,0.28} = \bar{\bar{S}}_L \qquad (\text{if } \bar{\bar{C}}_L \geq 0.5 \text{ and } \bar{\bar{S}}_L \leq 2.35) \qquad \text{[B.5.3a]}$$

or $$\bar{\bar{X}}_L = \bar{\bar{S}}_L - 1.65 \qquad (\text{if } \bar{\bar{C}}_L < 0.5 \text{ or } \bar{\bar{S}}_L > 2.35) \qquad \text{[B.5.3b]}$$

and $$\bar{\bar{Z}}_L = 2.05\ \bar{\bar{X}}_L^{\,0.28} \qquad \text{[B.5.4]}$$

They can be converted into vertical and downwind horizontal distances between the flame tip and the release source by

$$Z_L = k\ \bar{\bar{Z}}_L \qquad \text{[B.5.5]}$$

and $$X_L = k\ \bar{\bar{X}}_L \qquad \text{[B.5.6]}$$

where $$k = \frac{\dot{m}_{RG}\ d_h}{u_a\ A_h \sqrt{\rho\ \rho_a}} \qquad \text{[B.5.7]}$$

is the conversion factor (m) and d_h is the diameter of the hole (m).

B.5.4 Calculation Algorithm

1. Calculate the dimension of jet flame using Eqn. [B.5.1] to [B.5.7];

2. Calculate the total radiant power

$$P = \chi\ \dot{m}_{RG}\ H_c \qquad \text{[B.5.8]}$$

where H_c is the heat of combustion (J/kg) and χ is the fraction of radiant heat (Table B.1, Brzustowski 1971).

Product	Methane	Ethane	Propane	Butane	Pentane and higher
c	0.2	0.25	0.3	0.3	0.4

Table B.1 Fraction of Radiant Heat for Hydrocarbon Fires

3. Locate the radiant source at the centre of the flame and calculate the intensity of thermal radiation using a point source model

$$I_F = P / 4\ \pi\ r^2 \qquad \text{[B.5.9]}$$

where r is the distance from the assumed fire centre to the target (m), and I_F is heat intensity (W/m^2).

B.6 Pool Fire

B.6.1 Overview

- Scenario description: A pool of flammable hydrocarbon liquid is ignited and burns as a three dimensional radiant heat source.
- Output: Distribution of heat intensity.
- Sources: The pool fire model is adapted from the model given in the Handbook of Chemical Hazard Analysis Procedures (FEMA/DOT/EPA 1989), which includes calculations of pool size, burning rate and heat intensity.

B.6.2 Assumptions

- Pool size and burning rate are constant.
- Pool shape is assumed to be circular.
- Pool is ignited soon after release.
- Pool size is estimated as a continuous spill.
- Total spill volume will eventually be consumed in pool fire.

B.6.3 Model Description

Burning rate in a pool fire is given by (FEMA/DOT/EPA 1989)

$$\dot{m}_B = 1.543\text{x}10^{-3}\, A_p\, M_w\, e^{-0.0043Tb} \qquad [B.6.1]$$

in which $\dot{m}_B$ is the burning rate (kg/s), A_p is the pool area (m^2), M_w is the molecular weight (g/mol) and T_b is the boiling point in °F.

B.6.4 Calculation Algorithm

1. Calculate the burning flux (FEMA/DOT/EPA 1989).

$$f_B = 1.543\text{x}10^{-3}\, M_w\, e^{-0.0043Tb} \qquad [B.6.2]$$

Appendix B

2. Estimate pool size using the model for continuous spill.

$$D_{max} = 1.128 \sqrt{\frac{\dot{m}_{RL}}{f_B}} \qquad [B.6.3]$$

3. Calculate heat intensity using the model for a three dimensional fire (FEMA/DOT/EPA 1989).

$$I_F = E\,F\,\tau \qquad [B.6.4]$$

where the transmissivity τ is assumed to be unity. The surface emission power E (kW/m^2) and view factor F are defined as

$$E = 117 - 0.313\,T_b \qquad [B.6.5]$$

$$F = 1.143\,(D_{max}/2\,r)^{1.757} \qquad [B.6.6]$$

The boiling point T_b in Eqn. [B.6.5] is in degrees Fahrenheit.

B.7 Dispersion of Neutral Buoyancy Gas

B.7.1 Overview

- Scenario description: Gas or vapour discharged into the atmosphere disperses in the downwind direction. The dispersing gas forms a cloud which may burn or explode if ignited.
- Output: Concentration distribution at ground level.
- Sources: The standard Gaussian dispersion model for short duration release, as given in the Handbook of Chemical Hazard Analysis Procedures (FEMA/DOT/EPA 1989), is used for neutral buoyancy gases.

B.7.2 Assumptions

- The model considered is a plume model for continuous release.
- The plume moves downwind at average wind speed.
- Air mixing is assumed to occur in the cross wind directions.
- Initial momentum and buoyant rise are not considered.

Appendix B

B.7.3 Model Description

At a given location (ξ, η) in which ξ and η are the respective downwind and cross wind distances from the dispersion source, the maximum concentration at ground level is given by the Gaussian dispersion model (FEMA/DOT/EPA 1989)

$$C_{max} = 0.5\, C_c\, [\text{erf}\,(\frac{\xi}{\sqrt{2}\sigma_x}) - \text{erf}\,(\frac{\xi - u_a t_s}{\sqrt{2}\sigma_x})] \qquad \text{if } \xi \geq 0.5\, u_a\, t_s \qquad \text{[B.7.1a]}$$

$$C_{max} = C_c\, \text{erf}\,(\frac{u_a\, t_s}{2\sqrt{2}\sigma_x}) \qquad \text{if } \xi > 0.5\, u_a\, t_s \qquad \text{[B.7.1b]}$$

where $C_c = \dfrac{\dot{m}_s}{\pi\sigma_y\sigma_z u_a} \exp(-\eta^2/2\sigma_y^2)$ (kg/m^3); [B.7.2]

$\dot{m}_s$ = $\dot{m}_{RG} + \dot{m}_V$, supply rate of the dispersion source (kg/s);

t_s = duration of dispersion event = t_R

σ_x, σ_y, σ_z = dispersion coefficients in the downwind, crosswind, and vertical directions, respectively (m);

and erf() is the error function defined as $\text{erf}(x) = \dfrac{2}{\sqrt{\pi}} \int_0^x e^{-t^2} dt$.

For a given concentration, the Gaussian model defines the boundary of an area within which the gas concentration is higher than the given level. The shape of this area is approximately an ellipse with the downwind distance and maximum crosswind width as the major and minor axes.

B.7.4 Calculation Algorithm

1. For a given (ξ, η), calculate the values of σ_x, σ_y and σ_z.

2. Use Eqn. [B.7.1] and [B.7.2] to calculate the concentration level at (ξ, η).

Appendix B

B.8 Dispersion of Dense Gas

B.8.1 Overview

- Scenario description: Vapours discharged into the atmosphere and those evaporated from liquid pools disperse in the downwind direction. The dispersing vapour forms a cloud which may burn or explode if ignited.
- Output: Downwind and crosswind distances for a given concentration at ground level. These distances can be used to define the ellipse that encompasses the area where the concentration is higher than the given level.
- Sources: Equations for dense gas dispersion are adapted from the models given in the Handbook of Chemical Hazard Analysis Procedures (FEMA/DOT/EPA 1989).

B.8.2 Assumptions

- Dispersion is assumed to be affected by atmospheric stability but not wind speed.
- Crosswind cloud dispersion is estimated using empirical rules which characterize the shape of a dense gas vapour cloud.
- Buoyant rise and momentum rise are not considered.

B.8.3 Model Description

For a given volume concentration C in volume percent, the downwind distance D and the maximum crosswind width W can be estimated by the following equations.

1. For neutral or unstable weather,

$$D = 98\,(\dot{m}_s / M_w C)^{0.54} \quad \text{and} \quad W = 0.5\,D \quad \text{(continuous release)} \qquad \text{[B.8.1]}$$

$$D = 380\,(\dot{m}_s\, t_s / M_w C)^{0.24} \quad \text{and} \quad W = D \quad \text{(instantaneous release)} \qquad \text{[B.8.2]}$$

The boundary between the two release modes is

$$t_s = 0.0035\,(\dot{m}_s / M_w C)^{1.25} \qquad \text{[B.8.3]}$$

where $\dot{m}_s$ is in lb/min, t_s is in minutes, M_w is in g/mol, and D and W are in ft.

2. For stable weather,

$$D = 165\,(\dot{m}_s / M_w C)^{0.54} \quad \text{and} \quad W = 0.9\,D \quad \text{(continuous release)} \qquad \text{[B.8.4]}$$

Appendix B

$$D = 240\,(\dot{m}_s\, t_s / M_w\, C)^{0.27} \quad \text{and} \quad W = 1.4\,D \qquad \text{(instantaneous release)} \qquad [B.8.5]$$

The boundary between the two release modes is

$$t_s = 0.25\,(\dot{m}_s / M_w\, C) \qquad [B.8.6]$$

B.8.4 Calculation Algorithm

1. For a given concentration level C and dispersion duration t_s, determine whether it is an instantaneous release or a continuous release according to Eqn. [B.8.3] or [B.8.6].

2. For a given weather condition, use corresponding equations to calculate downwind distance D and maximum crosswind width W.

B.9 Vapour Cloud Fire

- Scenario description: Dispersion of gas or vapour forms a cloud of flammable gas. A delayed ignition causes the cloud (in the concentration range between the lower and upper flammability limits) to burn as a flash fire.

- Output: Shape and size of the burning area associated with the flash fire.

- Sources: The shape and size of the flammable vapour cloud is used to define the burning area associated with a vapour cloud fire. The extent of the flammable cloud is determined using the dispersion models given in Sec. 7 and 8 and the appropriate volume concentration levels. These models assume that contours of equal volume concentration can be approximated by an elliptical shape. The effective burning area of the cloud fire is therefore defined by two elliptically shaped volume concentration contours corresponding to the upper and lower flammability limits.

B.10 Vapour Cloud Explosion

B.10.1 Overview

- Scenario description: Dispersion of gas or vapour forms a cloud of flammable gas. A delayed ignition of the vapour cloud may cause an explosion under certain circumstances.

- Output: Distribution of overpressure from vapour cloud explosion.

- Sources: Vapour cloud explosion model given in the Handbook of Chemical Hazard Analysis Procedures (FEMA/DOT/EPA 1989).

Appendix B

B.10.2 Assumptions

- Only the flammable portion of total release volume will contribute to a vapour cloud explosion.
- Overpressure from the explosion is calculated based on an equivalent amount of TNT.
- Confinement and weather conditions are not considered.

B.10.3 Model Description

Equation for overpressure (FEMA/DOT/EPA 1989, Lees 1980)

$$P_E = \exp(9.097 - (25.13 \ln(r/M_{TNT}^{1/3}) - 5.267)^{1/2}) \quad \leq 14.7 \text{ psi} \qquad \text{[B.10.1]}$$

where P_E is the overpressure in psi, r is the distance (ft), and M_{TNT} is the equivalent mass of TNT (lb) given by (FEMA/DOT/EPA 1989)

$$M_{TNT} = Y_f M_C H_c / 1155 \qquad \text{[B.10.2]}$$

In Eqn. [B.10.2], Y_f is the yield factor (0.03 for hydrocarbon products), H_c is the heat of combustion (kcal/kg) and M_C is the total mass of the flammable cloud (lb).

B.10.4 Calculation Algorithm

1. Calculate total mass of the flammable cloud M_C by

$$M_C = \dot{m}_s L_1 / u_a \qquad \text{[B.10.3]}$$

where $L_1 = \min \{\xi_{LFL}, u_a t_s\}$ and ξ_{LFL} is the dispersion distance for lower flammability limit.

2. Calculate explosive overpressure for a given distance by Eqn. [B.10.1] and [B.10.2].

References

Brzustowski, T. A. 1971. Predicting Radiant Heating from Flares, ESSO Engineering Research and Development Report EE15ER.71.

Brzustowski, T. A. 1973. "A new criterion for the length of a gaseous turbulent diffusion flame", Combustion Science and Technology, 6, 313-319.

Brzustowski, T. A. 1976. "Flaring in the energy industry", Progress in Energy and Combustion Science, 2, 129-141.

Appendix B

FEMA/DOT/EPA 1989. Handbook of Chemical Hazard Analysis Procedures, U.S. Federal Emergency Management Agency, U.S. Department of Transportation, U.S. Environmental Protection Agency, Washington, DC.

Hanna, S. R. and Drivas, P. J. 1987. Guidelines for Use of Vapor Cloud Dispersion Models, Center for Chemical Process Safety, American Institute of Chemical Engineers.

Jain, A. K. 1976. "An Accurate Explicit Equation for Friction Factor," J. Hydraulics Div., ASCE, Vol. 102, No. HY5.

Kahler, J. P., Curry, R. G. and Kandler, R. A. 1989. Calculating Toxic Corridors, AWS/TR-80/003, First completed in 1980, Revised in 1989, Air Weather Service, Scott AFB, Illinois.

Lees, P. L. 1980. Loss Prevention in the Process Industries, Butterworth Group, London, U.K.

Perry, R. H., Green, D. W. and Maloney, J. O. 1984. Perry's Chemical Engineering Handbook, sixth edition, McGraw-Hill, New York, New York.

Technica 1988. Techniques for Assessing Industrial Hazards—A Manual, World Bank Technical Paper No. 55, The World Bank, Washington D. C.

APPENDIX C

CONDITIONAL EVENT PROBABILITIES FOR ACUTE RELEASE HAZARDS

C.1 Overview

This Appendix describes the basis for the conditional event probabilities given in Table 7.1 which are associated with the branches in the acute release hazard event trees shown in Figures 7.3.

C.2 Liquid Product Pipelines

Representative release event and hazard frequency models were developed for use in risk assessments of Liquefied Petroleum Product (LPG) installations by the UK Health and Safety Executive (HSE) based on historical incident data review and release modelling. Key findings relevant to the modelling of liquid product pipeline release incidents, as reported by Crossthwaite *et al.* (1988), includes the following:

- The probability of immediate ignition is taken to be 0.05 for all failure modes.
- The probability of delayed ignition of a large vapour cloud (associated with vessel rupture) passing over industrial land is taken to be ~1 and 0.9 for unstable and stable weather conditions, respectively.
- For a large cloud passing over urban land the delayed ignition probabilities are 80% of the values applicable to industrial land uses.
- For a large cloud passing over rural land the delayed ignition probabilities are 4% of the values applicable to industrial land uses.
- For limited releases involving holes in piping systems (as opposed to vessel ruptures) the delayed ignition probabilities associated with a relatively high density of surrounding ignition sources are taken to be 0.8, 0.45, and 0.24 for release rates associated with hole diameters of 50 mm, 25 mm, and 13 mm respectively.
- The ratio of vapour cloud fire to vapour cloud explosion is taken to be 3:1 during unstable weather conditions and 10:1 during stable weather condition.

The above information can be used to develop a set of conditional event probabilities for liquid product pipelines if the following assumptions are made:

- The delayed ignition probabilities given for piping systems with holes apply to vapour clouds passing over urban land during unstable weather conditions.

- The three hole sizes associated with piping system releases correspond to rupture, large leak, and small leak failure modes.
- The ignition probabilities given for large vapour clouds are taken to apply to pipeline rupture events and the corresponding probabilities for large and small leaks are obtained by prorating the rupture probabilities using the values given for piping system releases.

The resulting conditional event probabilities are given in Table C.1. It is noted that the conditional probabilities developed from the HSE data are most applicable to high vapour pressure (HVP) liquid products that form a heavier than air vapour under atmospheric conditions (*e.g.*, propane and butane). The probabilities given will therefore be conservative for HVP liquid products that form a buoyant vapour under atmospheric conditions (*e.g.*, ethane). The probabilities given in Table C.1 are also conservative for low vapour pressure (LVP) liquid products because they produce significantly less vapour than HVP products for a given mode of pipeline failure and thereby form smaller vapour clouds which have a lower probability of interacting with distributed ignition sources.

C.3 Natural Gas Pipelines

Historical incident data compiled by the European Gas Pipeline Incident Data Group for gas transmission pipelines suggests that the immediate ignition probability (P_i) is highly dependent on the mode of failure. Incident data from the operating period covering 1970 to 1992 indicates the following (EGIG 1993):

Failure Mode (hole size)	Immediate Ignition Probability
pinhole / crack (^{2} 20 mm)	0.027
significant hole (20 mm to line dia.)	0.019
rupture (line dia. ^{2} 400 mm)	0.099
rupture (line dia. > 400 mm)	0.235

A world-wide review of pipeline failure incident data carried out by British Gas suggests ignition probabilities in the range of 0.1 for leaks and 0.5 for ruptures (Fearnehough 1985).

Based on the above, representative values of the probability of immediate ignition will be taken to be 0.03, 0.10, and 0.25 for small leaks, large leaks and ruptures, respectively.

No specific historical information regarding the delayed ignition probability of natural gas was found in the literature. It is noted, however, that due to the buoyant nature of natural gas, which tends to rise quickly thereby minimizing its potential interaction with ground based ignition sources, the ignition probabilities will in general be much lower than for the dense, ground hugging vapour clouds associated with liquid product releases. Based on the above and in the

absence of specific incident data it will be assumed that the delayed ignition probabilities for natural gas releases are 0.5 times the values calculated for liquid product releases.

No specific historical information regarding the delayed explosion probability of natural gas was found in the literature. In the absence of relevant historical data the ratio of vapour cloud fires to vapour cloud explosions for natural gas will be assumed to be the same as for liquid products.

The conditional event probabilities for natural gas pipeline releases based on the above are given in Table C.1.

References

Crossthwaite, P. J., Fitzpatrick, R. D. and Hurst, N. W. 1988. "Risk assessment for the siting of developments near liquefied petroleum gas installations", Symposium Series No. 110, Institute of Chemical Engineers, 373-400.

Fearnehough, G. D. 1985. "The control of risk in gas transmission pipelines", Symposium Series No. 93, Institute of Chemical Engineers, 25-44.

EGIG 1993. Gas pipeline incidents, Report 1970-1992, European Gas Pipeline Incident Data Group.

Probability of Immediate Ignition		
small leak	large leak	rupture
0.05	0.05	0.05

Probability of Delayed Ignition - small leak		
weather	unstable	stable
urban	0.24	0.22
rural	0.012	0.011
industrial	0.30	0.27

Probability of Delayed Ignition - large leak		
weather	unstable	stable
urban	0.45	0.41
rural	0.02	0.02
industrial	0.56	0.51

Probability of Delayed Ignition - rupture		
weather	unstable	stable
urban	0.8	0.72
rural	0.04	0.036
industrial	1	0.9

Probability of Explosive Conditions		
weather	unstable	stable
urban	0.33	0.1
rural	0.33	0.1
industrial	0.33	0.1

Liquid Products

Probability of Immediate Ignition		
small leak	large leak	rupture
0.03	0.1	0.25

Probability of Delayed Ignition - small leak		
weather	unstable	stable
urban	0.12	0.11
rural	0.006	0.0054
industrial	0.15	0.14

Probability of Delayed Ignition - large leak		
weather	unstable	stable
urban	0.23	0.20
rural	0.011	0.010
industrial	0.28	0.25

Probability of Delayed Ignition - rupture		
weather	unstable	stable
urban	0.4	0.36
rural	0.02	0.018
industrial	0.5	0.45

Probability of Explosive Conditions		
weather	unstable	stable
urban	0.33	0.1
rural	0.33	0.1
industrial	0.33	0.1

Natural Gas

Table C.1 Conditional event probabilities for acute release hazards

APPENDIX D

HAZARD TOLERANCE THRESHOLDS

D.1 Overview

This document summarizes the acute hazard tolerance thresholds that have been established based on a review of relevant literature. Thresholds are required for the calculation of the Number of Fatalities node parameter (node 6) and the Offshore Damage Cost node parameter (node 9.4).

D.2 Thresholds for Human Fatality

Hazard	Exposure	Parameter	Units	Lower Bound Tolerance Threshold	Upper Bound Tolerance Threshold
jet / pool fire	on deck	heat intensity	kW/m^2	6.30	37.5
jet / pool fire	below deck	heat intensity	kW/m^2	15.7	37.5
asphyxiating vapour cloud	on or below deck	volume concentration	ratio	0.306	0.713
vapour cloud fire	on deck	fraction of C_{LFL} (1)		0.5	1.0
vapour cloud fire	below deck	fraction of C_{LFL} (1)		N/A	N/A
vapour cloud explosion	on or below deck	blast pressure	kPa	15.9	69.0

(1) Lower flammability limit of the product

The rationale behind each of the adopted threshold values is given in the following:

Appendix D

1. Threshold for jet / pool fire

- For below deck exposure, the lower bound fatality threshold is based on the maximum allowable heat intensity on structures providing shelter from radiant heat as defined in 'Recommended Design Flare Radiation Levels Excluding Solar Radiation' (API 521). The corresponding heat intensity is 15.7 kW/m^2; at or below which it is assumed that people below deck will be protected indefinitely and escape would not be necessary. A heat intensity of 37.5 kW/m^2 is cited in a study by the World Bank (1985) as being sufficient to damage process equipment which could potentially eliminate shielding.

- For on deck exposure the threshold relates to the probability of reaching safe shelter. There is variation in the lower limits of the on deck or outdoor exposure threshold reported in literature. A threshold of 10 kW/m^2 is proposed by the SFPE (1988) based on a 1% chance of fatality for an assumed exposure time of 40 seconds (FEMA/DOT/EPA (1989) cites 10 kW/m^2 for fatality and 5 kW/m^2 for injury). The chosen level of 6.3 kW/m^2 is cited by Jones and Fearnehough (1986) as the level at which a receptor only needs to travel a short distance in order to escape.

- The literature review did not produce a directly citable upper bound for the on deck exposure threshold, however, it can be assumed that fatalities associated with on deck exposure will result from either:

  a.) a heat intensity so high that an individual sustains fatal injuries before reaching shelter; or

  b.) a heat intensity so high that the potential shelter is destroyed.

  The recognized threshold value associated with scenario *b* (*i.e.*, 37.5 kW/m^2) was found to be lower than the value associated with *a* since the time to reach shelter, associated with a reasonable evacuation distance and travel speed, is typically less than the time required to sustain a dosage of thermal radiation sufficient to cause a 99% chance of fatality (as summarized by Lees 1980).

2. Threshold for vapour cloud fire

- Models for vapour cloud or flash fire often equate the extent of the flammable cloud to the burning area. The extent of the flammable cloud can be determined using dispersion models. The models adopted in this program assume that contours of equal vapour concentration can be approximated by an elliptical shape. The effective burning area is therefore taken to be an ellipse corresponding to the vapour concentration contour associated with the lower flammability limit, C_{LFL}.

- Flash fires burn quickly and secondary ignition within the flash fire zone is unlikely (Craven 1976). People below deck are therefore assumed to be safe. Note, this assumption has also been adopted in work reported by DnV Technica Ltd. (1988).

- For on deck exposure it is assumed that all people within the C_{LFL} concentration contour will fail to survive the flash fire event (Pape 1989). Acknowledging that fire may spread beyond the C_{LFL} contour, FEMA/DOT/EDA (1989) assumes that a plume has the potential to burn out to the boundaries of the area bound by a concentration contour that is associated with

approximately one-half of the C_{LFL}. The C_{LFL} and one-half C_{LFL} vapour concentration levels are adopted herein as upper and lower bound thresholds for on deck exposure to flash fires.

3. Threshold for vapour cloud explosion

- Less (1980) reports that blast overpressure levels of 15.5 psi (107 kPa) and 29.0 psi (200kPa) are respectively associated with a 1% and 99% chance of fatality due to direct blast effects (*i.e.*, lung hemorrhaging of people outdoors, ignoring projectiles and whole body translation). Lees also reports a 1.0 psi (6.9kPa) to 8.0 psi (55 kPa) range for slight to serious injuries due to flying glass and other 'missiles'.

- Indoor fatalities are usually assumed to be associated with crushing and/or projectile injuries. In this regard, Lees (1980) sites 2.3 psi (15.9 kPa) as the lower limit for serious structural damage and 10 psi (69.0 kPa) for probable total building destruction. These building damage thresholds are therefore adopted as lower and upper thresholds for below deck exposure.

- In developing thresholds for on deck exposure it is recognized that close proximity to structural element (and the associated potential for projectiles) will significantly undermine the direct exposure threshold values cited by Lees. This is conservatively acknowledged by adopting the below deck threshold values cited above for on deck exposure as well.

4. Threshold for asphyxiation

- Most references list methane, ethane, propane and butane as simple asphyxiants (Lees 1980, Matheson 1971). The legal limits for oxygen concentration in working environments are between 16% to 19%. It is however generally considered that oxygen deficiency symptoms become evident when blood hemoglobin becomes 90% saturated, which occurs at the oxygen concentration level of 14.5% (NIOSH 1980). The lower limit on asphyxiating vapour concentration of 30.6% adopted herein corresponds to this 14.5% oxygen concentration.

- An oxygen concentration of 6% or less, which corresponds to an asphyxiating vapour concentration of 71.3% or more, will cause death in 6 to 8 minutes (FEMA/DOT/EPA 1989). This concentration is adopted as the upper limit.

Appendix D

D.3 Thresholds for Offshore Property Damage

Hazard	Parameter	Units	Property Damage Thresholds	
			Lower Bound	Upper Bound
jet / pool fire	heat intensity	kW/m^2	15.7	37.5
vapour cloud fire	fraction of C_{LFL}(1)		N/A	N/A
vapour cloud explosion	blast pressure	kPa	15.9	69.0

(1) Lower flammability limit.

The basis for the threshold values tabulated above is as follows:

1. Thresholds for jet / pool fire and vapour cloud fire

- The upper bound threshold for structures or vessels exposed to thermal radiation is based on the heat intensity cited in a study by the World Bank (1985) as being sufficient to damage process equipment. The lower bound threshold is set at the maximum heat intensity allowed on structures that are intended to provide shelter (API 521). No significant damage is assumed for vapour cloud fires due to the lack of secondary ignition potential (see thresholds for fatality).

2. Threshold for vapour cloud explosion

- The overpressure thresholds for vapour cloud explosions are based on work cited by Lees (1980). An overpressure of 2.3 psi (15.9 kPa) is associated with the lower limit of serious structural damage, and 10 psi (69.0 kPa) is associated with probable total building destruction.

References

Crossthwaite, P. J., Fitzpatrick, R. D. and Hurst, N. W. 1988. Risk Assessment for the Siting of Developments Near Liquefied Petroleum Gas Installations. Institute of Chemical Engineers, Symposium Series No. 110, 373-400.

DnV Technica Ltd. 1988. Techniques for Assessing Industrial Hazards.

Fearnehough, G. D. 1985. The Control of Risk in Gas Transmission Pipeline. Institute of Chemical Engineers, Symposium Series No. 93, 25-44.

Appendix D

FEMA/DOT/EPA 1989. Handbook of Chemical Hazard Analysis Procedures, U.S. Federal Emergency Management Agency, U.S. Department of Transportation, U.S. Environmental Protection Agency, Washington, DC.

Jones, D. A. and Fearnehough, G. D. 1986. Natural Gas Transmission by Pipelines. Fifth International Symposium on Loss Prevention and Safety.

Lees 1980. Loss Prevention in the Process Industries.

Matheson 1971. Matheson Gas Data Book, Matheson Gas Products.

NIOSH 1980. Working in Confined Spaces, Criteria for a recommended standard, Notional Institute for Occupational Safety and Health, U.S. Department for Health, Education, and Welfare, Washington, D.C. (MED: RC962.3 N277 1980)

SFPE 1988. SFPE Handbook of Fire Protection Engineering, P. J. DiNenno *et al.* ed., Society of Fire Protection Engineers, Boston, Massachusetts.

Pape 1989. HSE Assessment for Consultation Distances for Major Hazard Installations. Safety Cases, F. P. Lees and M. L. Ang ed., Butterworths, Sevenoaks, U.K.

World Bank 1985. Manual of Industrial Hazard Assessment Techniques. Office of Environmental and Scientific Affairs, World Bank, Washington, D.C.

APPENDIX E

THE UTILITY FUNCTION

E.1 Introduction

This Appendix contains the mathematical descriptions of the utility functions selected for the project. Utility theory defines different functional forms that can represent different attitudes toward risk and tradeoffs between attributes. The attitudes and trends that are considered applicable for the present problem are discussed in Section 13.2 of the main report. The functional forms corresponding to these attitudes are given in this Appendix. In each case, the function contains some constants that can be determined from the decision maker's response to questions regarding simple choices involving uncertain options or tradeoffs between attributes. The information required to define and verify these constants is given in each case. In addition, the Appendix gives examples that demonstrate the application of utility functions in evaluating different choices.

E.2 Single Attribute Utility Functions

E.2.1 Cost

As discussed in the main report, the utility function for cost is required to be: 1) monotonically decreasing; 2) risk averse; and 3) increasingly risk averse. A function that satisfies the above conditions is given as follows (Keeney and Raiffa 1976):

$$u(c) = k_{c1} + k_{c2} \ln(k_{c3} - c) , \quad c < k_{c3} \qquad [E.1]$$

where k_{c1}, k_{c2}, k_{c3} are constants. To evaluate these three constants, three points on the utility function must be given. The first two points are defined by scaling the function between two arbitrary values. Utility is usually scaled in the range of 0 to 1.0, where a zero utility is assigned to the worst possible outcome (*i.e.*, maximum possible cost, denoted c_0) and a utility of 1.0 is assigned to the best possible outcome (*i.e.*, the minimum possible cost, denoted c_*). Note that the subscripts 0 and * are consistently used to denote the worst and best possible values of an attribute, respectively. These two conditions lead to:

$$u(c_0) = k_{c1} + k_{c2} \ln(k_{c3} - c_0) = 0 \qquad [E.2a]$$

and

$$u(c_*) = k_{c1} + k_{c2} \ln(k_{c3} - c_*) = 1.0 \qquad [E.2b]$$

Appendix E

The third condition can be determined by asking the decision maker to specify the certain cost that would be equivalent to a 50-50 chance at paying c_0 or c_*. This is called the certainty equivalent of that lottery and is denoted c_{ce}. By definition, c_{ce} must be greater than $(c_0+c_*)/2$ for a risk averse function. Because the utility associated with the certainty equivalent is equal to the expected utility of the lottery, a third point on the utility function can be defined as:

$$k_{c1} + k_{c2} \ln(k_{c3} - c_{ce}) = 0.5[k_{c1} + k_{c2} \ln(k_{c3} - c_0)] + 0.5[k_{c1} + k_{c2} \ln(k_{c3} - c_*)] \quad \text{[E.2c]}$$

Solving Equations [E.2] gives

$$k_{c3} = (c_0 c_* + c_{ce}^{\ 2}) / (c_0 + c_* - 2c_{ce}) \ , \quad k_{c3} > c_0 \quad \text{[E.3a]}$$

$$k_{c2} = 1 / \ln\left[(k_{c3} - c_*) / (k_{c3} - c_0)\right] \quad \text{[E.3b]}$$

$$k_{c1} = 1 - k_{c2} \ln(k_{c3} - c_*) \quad \text{[E.3c]}$$

After defining the utility function, it can be checked by calculating the certainty equivalents of a number of lotteries and confirming that they are consistent with the decision maker's preferences.

As an example, consider a case in which c_* = \$2 million and c_0 = \$12 million. Also assume that the certainty equivalent of a 50-50 lottery at \$2 million or \$12 million is \$9 million. Equations [E.3] can be used to calculate k_{c1} = -0.478, k_{c2} = 0.59, and k_{c3} = 14.25. The utility function is then given by

$$u(c) = -0.478 + 0.59 \ln(14.25 - c) \ , \ 2 < c < 12 \quad \text{[E.4]}$$

This function is plotted in Figure 13.6 of the main report. Confirmation of the appropriateness of the function can be achieved by calculating the certainty equivalents of some arbitrary lotteries and verifying that they are consistent with the decision maker's preferences. For example, the certainty equivalent of a lottery l_1 defined as a 50-50 chance at c = \$2 million or c = \$7 million is \$4.83 million. This is calculated by finding the expected utility of the lottery using Equation [E.4] and then finding the fixed cost that has the same utility value using the inverse of Equation [E.4]. Similarly, the certainty equivalent of a lottery l_2 defined as a 50-50 chance at c = \$7 million or c = \$12 million is \$10.21 million. If these values are consistent with the decision maker's preferences, then the utility function is adequate. Otherwise, the value of c_{ce} can be redefined, the utility function re-evaluated and the confirmation process repeated.

It is also worth noting that the lotteries l_1 and l_2 have the same range of \$5 million, but l_1 has a reference value of \$4.5 million and l_2 a reference value of \$9.5 million (see Section 13.2.2.1 for the definitions of reference value and range). The risk premiums for these lotteries are \$0.33 million for l_1 and \$0.71 million for l_2 (see Section 13.2.2.1 for definition of risk premium). It can therefore be seen that the risk premium increases with the reference value for lotteries having the same range, confirming that this utility function is increasingly risk averse.

Appendix E

E.2.2 Number of Fatalities

Based on the discussion in Section 13.2.2.3 it was decided that a risk neutral (linear) utility function should be used for the number of fatalities. This utility function is given by:

$$u(n) = 1 - n / n_0 \qquad [E.5]$$

where n_0 is the maximum possible (highest) number of fatalities. Equation [E.5] assumes that the minimum number of fatalities n_* is 0. It can be verified that this equation satisfies the scaling conditions $u(n_0) = 0$ and $u(n_*) = 1.0$. If n_0 is equal to 10 for example Equation [E.5] gives

$$u(n) = 1 - n / 10 \ , \ 0 < n < 10 \qquad [E.6]$$

E.2.3 Equivalent Spill Volume

A risk prone utility function was selected for the equivalent spill volume. The function used is as follows:

$$u(v) = k_{v1} + k_{v2}\, v^{k_{v3}} \ , \quad 0 < k_{v3} < 1 \qquad [E.7]$$

where k_{v1}, k_{v2}, k_{v3} are constants. As in the case of cost, these constants can be evaluated from the following conditions:

$$u(v_0) = k_{c1} + k_{c2}\, v_0^{\,k_{c3}} = 0 \qquad [E.8a]$$

$$u(v_*) = k_{c1} + k_{c2} v_*^{\,k3} = 1.0 \qquad [E.8b]$$

and

$$k_{c1} + k_{c2}\, v_{ce}^{\,k_{c3}} = 0.5[k_{c1} + k_{c2}\, v_0^{\,k_{c3}}] + 0.5[k_{c1} + k_{c2}\, v_*^{\,k_{c3}}] \qquad [E.8c]$$

where v_* is the minimum spill volume, v_0 is the maximum spill volume, and v_{ce} is the certainty equivalent of a 50-50 lottery at a spill volume of v_0 or v_*. Solving Equations [E.8] and assuming that $v_* = 0$, leads to

$$k_{v3} = \ln(0.5) / \ln(v_{ce} / v_0) \ , \quad 0 < k_{v3} < 1 \qquad [E.9a]$$

$$k_{c2} = -1 / v_0^{\,k_{v3}} \qquad [E.9b]$$

$$k_{v1} = 1 \qquad [E.9c]$$

Consider for example a case in which $v_* = 0$ and $v_0 = 1000$ m^3. Also assume that the certainty equivalent v_{ce} of a 50-50 lottery at 0 or 1000 m^3 is 100 m^3. Equations [E.9] can be used to calculate $k_{v1} = 1$, $k_{v2} = -0.125$, and $k_{v3} = 0.3$. The utility function is then given by

$$u(v) = 1 - 0.125 v^{0.3} \quad 0 < v < 1000 \qquad [E.10]$$

This function is plotted in Figure 13.7 of the main report. As in the case of cost, the appropriateness of the function can be confirmed by calculating the certainty equivalents of some additional lotteries. For example, the certainty equivalent of a lottery l_1 defined as a 50-50 chance at v= 0 million or v = 500 m^3 is 50 m^3. Similarly, the certainty equivalent of a lottery l_2 defined as a 50-50 chance at v= 500 m^3 or v = 1000 m^3 is 720 m^3. If these values are consistent with the decision maker's preferences, then the utility function is adequate. It is noted that this function is decreasingly risk prone as can be verified by calculating the risk premiums for lotteries l_1 and l_2. These values are -200 m^3 and -30 m^3.

E.3 Multi-attribute Utility Function

Based on the preferential and utility independence trends explained in Section 13.2.3.2, it can be shown that a multiplicative utility function is appropriate (see Theorem 6.2 in Keeney and Raiffa 1976). This form is given by:

$$u(c,n,v) = [(k k_c\, u(c)+1)(k k_n\, u(n)+1)(k k_v\, u(v)+1) - 1]/k \qquad [E.11]$$

where $u(c)$, $u(n)$, $u(v)$ are the single attribute utility functions discussed in Section E.2, and k, k_c, k_n, k_v are constants. The utility function is scaled between 0 and 1 so that:

$$u(c_0, n_0, v_0) = 0 \qquad [E.12a]$$

$$u(c_*, n_*, v_*) = 1 \qquad [E.12b]$$

The constants k_c, k_n, and k_v are given by:

$$k_c = u(c_*, n_0, v_0)\ ,\ 0 < k_c < 1 \qquad [E.13a]$$

$$k_n = u(c_0, n_*, v_0)\ ,\ 0 < k_n < 1 \qquad [E.13b]$$

$$k_v = u(c_0, n_0, v_*)\ ,\ 0 < k_v < 1 \qquad [E.13c]$$

These values can be assessed directly by the decision maker. Recall that the subscripts 0, * represent the worst and best possible values of each attribute, respectively. Equations [E.12] define the scale of the utility function: a utility of 0 corresponds to an outcome that consists of the worst values of all attributes, and a utility of 1 corresponds to an outcome consisting of the best values of all attributes. The constants in Equations [E.13] represent the utility value, on that scale of 0 to 1, associated with an outcome consisting of the best value of one attribute and the worst values of the other two attributes. To determine k_c, for instance, the decision maker must assign a utility value between 0 and 1 to an outcome consisting of the best consequences in $c = c_*$ combined with the worst consequences in n and v (*i.e.*, $n = n_0$ and $v = v_0$). The relative magnitude of the utility increases attached to improvements in single attributes reflect the tradeoffs between these attributes. For example if the decision maker assigns a utility value of 0.2 to a cost saving of \$10 million and a utility value of 0.4 to a reduction in the number of fatalities of 10, it can be concluded that saving 5 lives in twice as desirable as saving \$20 million, indicating that the value of a human life is approximately \$2 million.

Appendix E

Once k_c, k_n, and k_v are determined, k can be obtained by substituting $c = c_*$, $n = n_*$ and $v = v_*$ in Equation [E.11], and observing that $u(c_*) = u(n_*) = u(v_*) = u(c_*,n_*,v_*) = 0$. This lead to a quadratic equation from which k can be calculated as:

$$k = \frac{-(k_c k_n + k_n k_v + k_v k_c) + \sqrt{(k_c k_n + k_n k_v + k_v k_c)^2 - 4 k_c k_n k_v (k_c + k_n + k_v - 1)}}{2 k_c k_n k_v} \qquad [E.14]$$

It is noted that if $k_c+k_n+k_v = 1$, then $k = 0$. This results in simplifying the utility function to a weighted sum of the three single attribute functions, and this means that there is no interaction between the three attributes. If $k_c+k_n+k_v < 1$, then $k > 1$. In this case it can be verified from the utility function that raising all attributes simultaneously from their worst to their best values has a more positive impact on the utility function than the sum of the impacts of raising each attribute to its best value individually. It is therefore said that the three attributes are *complimentary*, indicating that there is some added benefit in achieving good results simultaneously in more than one attribute. A typical example of this trend is that of the general who is fighting on both fronts. Winning on both fronts is a must, otherwise the war will be lost. On the other hand , if $k_c+k_n+k_v > 1$, then $k < 1$. In this case raising each attribute from its worst to its best value has a more positive impact on the utility function than raising all attributes from their worst to their best values simultaneously. In this case it is said that the attributes are *substitutive*. It indicates that there is some importance attached to achieving good results in any of the attributes. A typical example is a corporation that markets two products, and although it is desirable to do well in both, it is essential to do well at least in one in order to remain in business.

Once the utility function is defined, it can be used to calculate some equivalent combinations of the three attributes. As discussed for the single attribute utility functions, these values can be used for verification or modification of the constants defined by the decision maker (Equations[E.13]).

E.4 Example

An example can be developed by considering the three single attribute utility functions defined in the examples given in Sections E.2.1 to E.2.3 (Equations [E.4], [E.6] and [E.10]). For these functions, the scale for the multi-attribute utility function is defined by substituting the minimum and maximum values of the attributes in Equations [E.12], leading to:

$$u(\$12\,\text{million}, 10\,\text{fatalities}, 1000\,\text{m}^3) = 0 \qquad [E.15a]$$

$$u(\$2\,\text{million}, 0\,\text{fatalities}, 0\,\text{m}^3) = 1 \qquad [E.15b]$$

The constants k_c, k_n, and k_v are assessed subjectively based on Equations [E.13] as:

$$k_c = u(\$2\,\text{million}, 10\,\text{fatalities}, 1000\,\text{m}^3) = 0.2 \qquad [E.16a]$$

$$k_n = u(\$12\,\text{million}, 0\,\text{fatalities}, 1000\,\text{m}^3) = 0.8 \qquad [E.16a]$$